Predicting Climate Change Effects on Kokanee Habitat Suitability in Lake Sammamish, Washington

October 2013

King County

Department of Natural Resources and Parks
Water and Land Resources Division
Science and Technical Support Section
King Street Center, KSC-NR-0600
201 South Jackson Street, Suite 600
Seattle, WA 98104
206-296-6519 TTY Relay: 711
www.kingcounty.gov/environment/wlr/science-section.aspx

Predicting Climate Change Effects on Kokanee Habitat Suitability in Lake Sammamish, Washington

Prepared for:

U.S. Fish and Wildlife Service

Submitted by:

Curtis DeGasperi
King County Water and Land Resources Division
Department of Natural Resources and Parks

Funded by U.S. Fish and Wildlife Service

Cooperative Agreement No. 13410BJ034

King County
Department of
Natural Resources and Parks
Water and Land Resources Division

Acknowledgements

The author gratefully acknowledges the collaboration and contributions from Denise Hawkins (Project Officer, U.S. Fish and Wildlife Service), Brad Thompson (former Project Officer, U.S. Fish and Wildlife Service), Kirk Krueger (Research Scientist, Washington Department of Fish and Wildlife) and Guillaume Mauger (Postdoctoral Research Associate, University of Washington Climate Impacts Group). Hans Berge kindly reviewed and edited the background information on kokanee provided in the report.

Citation

King County. 2013. Predicting Climate Change Effects on Kokanee Habitat Suitability in Lake Sammamish, Washington. Prepared for U.S. Fish and Wildlife Service, Lacey, Washington. Prepared by Curtis DeGasperi, Water and Land Resources Division. Seattle, Washington.

Table of Contents

APPENDICES

Figures

Tables

EXECUTIVE SUMMARY

Currently, USFWS participates in a conservation supplementation effort in an attempt to rebuild the population of kokanee in Lake Sammamish and several habitat restoration efforts are planned or have been completed. However, the long term success of such restoration efforts remains unknown given expectations for the effects of climate change (primarily warming) on the suitability of lake habitat for kokanee.

Lake Sammamish becomes thermally stratified in summer with surface waters that become too warm for coldwater fish like kokanee while oxygen levels in the cold bottom waters become too low for these fish. Kokanee require suitable dissolved oxygen and temperature conditions to survive. It has been postulated that climate change (i.e., warming) could exacerbate the spatial and temporal extent of unsuitable dissolved oxygen and temperature conditions for kokanee in Lake Sammamish – the so-called temperature-dissolved oxygen squeeze. The potential effect of climate change on restoration efforts has yet to be considered, although recent research suggests that the potential success of salmon restoration efforts will be poorly characterized if climate change is not explicitly evaluated.

This report documents the ability of 2- and 3-dimensional (2-D and 3-D) lake temperature models developed as part of an earlier King County study to simulate observed lake temperatures over an 8 year period (1995-2002). The report also documents the application of these models to estimating the potential effect of climate change on lake habitat suitability for kokanee.

The 2-D and 3-D lake temperature models were generally consistent in their predictions of the response of Lake Sammamish to future warming of the local climate. Overall, the available habitat for kokanee is predicted to decline in response to warming. The declines are due to projected warming throughout the lake, but with a disproportionate amount of warming predicted to occur in the surface layer in summer. The decline in habitat volume also results from earlier onset of stratification and a delay in destratification, which results in an extension of the period that the lake is stratified during the summer. The earlier onset of stratification results in warmer surface waters in the spring than would have occurred historically. The lake is also predicted to become much more thermally stable (i.e., more strongly stratified) under future warmer conditions.

How earlier onset of stratification and stronger stratification will affect hypolimnetic oxygen concentrations was not addressed in this study, but it is likely that the estimates presented here may be optimistic if in fact earlier onset of stratification leads to earlier declines in hypolimnetic dissolved oxygen concentrations.

Base on the results of this study, a few recommendations are made with the intent to further refine the understanding of potential effects of climate change on Lake Sammamish kokanee habitat:

- Develop 1-dimensional model to facilitate continuous long-term climate change simulations to better capture long-term natural variability
- Incorporate effect of climate change on watershed inputs to the lake (starting with tributary temperatures and flows)

- Develop additional water quality modeling capability starting initially with a simple 1-dimensional model capable of reproducing seasonal variation in phytoplankton biomass, nutrients and dissolved oxygen
- Identify relationships between inter-annual variation in temperature, dissolved oxygen and numbers of kokanee using available observed data and current condition modeling results.

1.0. INTRODUCTION

King County entered into a cooperative agreement with U.S. Fish and Wildlife Service (USFWS) to conduct a study with the objective of estimating the change in the amount of suitable habitat for kokanee (*Oncorynchus nerka*) in Lake Sammamish, Washington expected this century due to climate change. The Lake Washington-Sammamish Watershed is one of only five watersheds in Washington with extant populations of native kokanee (Pfeifer 1995). Kokanee abundance in Lake Sammamish has declined dramatically since at least the 1970's (Berge and Higgins 2003; Jackson 2010), resulting in a petition for protection under the U.S. Endangered Species Act in 2007. Currently, USFWS participates in a conservation supplementation effort in an attempt to rebuild the population (Lake Sammamish Kokanee Work Group 2010) and several habitat restoration efforts are planned or have been completed.[1] These efforts appear to be paying off as kokanee have been spawning in greater numbers in recent years.[2]

However, the long term success of such restoration efforts remains unknown given expectations for the effects of climate change (primarily warming) on lake habitat suitability. Lake Sammamish becomes thermally stratified in summer with surface waters that become too warm for coldwater fish like kokanee while oxygen levels in the cold bottom waters become too low for these fish. Kokanee require suitable dissolved oxygen (DO) and temperature conditions to survive. Berge (2009) postulated that climate change (i.e., warming) could exacerbate the spatial and temporal extent of unsuitable DO and temperature conditions for kokanee in Lake Sammamish – the so-called temperature-DO squeeze. The potential effect of climate change on restoration efforts has yet to be considered, although at least one study suggests that the potential success of salmon restoration efforts will be poorly characterized if climate change is not explicitly evaluated (Battin et al. 2007).

This report documents the ability of 2- and 3-dimensional (2-D and 3-D) lake temperature models developed as part of an earlier King County study to simulate observed lake temperatures over an 8 year period (1995-2002). The report also documents the application of these models to estimating the potential effect of climate change on the suitability of lake habitat for kokanee.

1.1 Background

Climate change has been demonstrated to affect lake ecosystems in a variety of ways (De Stasio et al. 1996; Stefan et al. 1996; Schindler 1997; Livingstone 2003; Winder and Schindler 2004, Taner et al. 2011; Griffiths et al. 2011). Perhaps the best documented effect

[1] http://www.kingcounty.gov/environment/animalsAndPlants/salmon-and-trout/kokanee.aspx

http://www.kingcounty.gov/%20environment/animalsAndPlants/restoration-projects/kokanee-chinook-projects.aspx

[2] http://sammamishreview.com/2012/12/06/kokanee-salmon-make-their-return-in-greater-numbers

of climate change is that of increased air temperatures on the thermal behavior of lakes that in turn affects a number of physical, chemical and biological lake processes. Increasing air temperature generally results in more heat transfer to lake surfaces resulting in earlier onset of thermal stratification, increased resistance of the lake to thermal mixing during summer stratification (i.e., stronger stratification and increased water column stability) and delayed turnover of lakes in fall (e.g., Winder and Schindler 2004).

Although not addressed in this study, projected changes in the character of precipitation (particularly changes magnitude, timing and intensity) also have the potential to affect lake ecosystems (e.g., Taner et al. 2011). Potential effects include changes in the timing and/or magnitude of delivery of nutrients or changes in the lake hydrology (e.g., changes in the magnitude or seasonality of lake residence time).

Long physical, chemical and biological monitoring records of lakes can shed some light on potential effects of climate change by examining the response to natural climate variability and recent warming trends (e.g., Winder and Schindler 2004). Lake models that simulate lake temperature and vertical stratification in response to time varying climate inputs are necessary to evaluate the response to future climate when long term observations are not available and/or when future climate (i.e., air temperature) is expected to exceed the historically observed natural variability (Blenckner 2008). In this study, existing hydrodynamic models of Lake Sammamish are used to assess the effect of projected increases of air temperature based on downscaled global climate model simulations on kokanee habitat suitability.

As part of King County's Sammamish-Washington Analysis and Modeling Program (SWAMP), a 3-D hydrodynamic model of Lake Sammamish was developed (King County 2008) along with a suite of other models, including HSPF watershed models of the Sammamish basin (King County 2003) and a laterally-averaged 2-D model of the Sammamish River (King County 2009); the outlet of Lake Sammamish. In addition to the 3-D model of Lake Sammamish, a laterally-averaged 2-D model of the lake was also developed to troubleshoot the development of the 3-D model, which at that time had previously been applied to only one lake; nearby Lake Washington (Kim et al. 2006; Cerco et al. 2006).

The Lake Sammamish 3-D model is CH3D-Z (curvilinear hydrodynamics in three dimensions, Z-grid version) and the 2-D model is CE-QUAL-W2 Version 3.5. Both of these models were developed by the U.S. Army Corps of Engineers and have been used to assess a variety of hydrodynamic and water quality problems. For example, CH3D-Z has been used to simulate the hydrodynamics of Chesapeake Bay and provide the hydrodynamic input to the Chesapeake Bay water quality model (Cerco and Cole 1993) and CE-QUAL-W2 has been used in hundreds of lake and reservoir modeling studies (Cole and Wells 2006).[3]

[3] CE-QUAL-W2 application history: http://www.ce.pdx.edu/w2/

1.2 Study Area

The Lake Sammamish study area includes a number of small tributary basins draining to the eastern and western shores of the lake and Tibbetts and Issaquah Creek basins draining into the southern end of the lake (Figure 1). The lake discharge at the north end of the lake is controlled by a broad-crested weir, which defines the beginning of the Sammamish River.

The total basin drainage area covers approximately 230 km^2 (excluding the lake surface). Issaquah Creek is the largest single tributary basin at 145 km^2. Although the Issaquah Creek basin includes the urban center of the town of Issaquah, about 70 percent of the Issaquah basin is forested (albeit second and third growth) based on King County's 1995 land cover analysis. The Tibbetts Creek basin is also 70 percent forested. The southern area of the Lake Sammamish drainage is often referred to as the "Issaquah Alps" due to the high relief resulting from a westerly extension of the Cascade Mountains into the Puget Sound Lowlands. Elevations in the Issaquah Creek basin range from 8 m above mean sea level at the lake normal pool elevation to about 900 m at the top of Tiger Mountain in the Issaquah Creek basin.

Land cover in the east and west sub-basins is dominated by low- and medium-intensity development. The drainages on the western flank of the lake are more highly developed (20 percent forest cover remaining) due to the greater proximity to the urban center of Bellevue. The drainages on the east side of the lake have developed rapidly over the last 10 years with about 40 percent forest cover remaining. Due to the relatively large contribution of the Issaquah and Tibbetts Creek basins to the total drainage area, overall 68 percent of the Lake Sammamish drainage remains forested.

Welch et al. (1980) report that the lake itself has a surface area of 19.8 km^2, holds approximately 3.5×10^8 m^3 of water, and has a mean residence time of 1.8 yr. The lake has a maximum depth of about 32 m and a mean depth of 17.7 m (Welch et al. 1980). The lake is an elongated fiord-like trough about 13 km long oriented along a north-south axis reflecting its glacial provenance. The lake typically stratifies thermally beginning in April and de-stratifies in November. As the lake stratifies, the hypolimnion becomes progressively depleted of oxygen resulting in anaerobic bottom waters in late summer. During winter when the lake is oxygenated and relatively isothermal, temperatures typically do not go below 4 ^oC, although it has been reported that the lake surface was completely frozen in January 1950.[4]

The lake basin has undergone a fairly dramatic transformation beginning in the 1860s with the first European-American settlements along the lake shore. Hop farming and then logging, dairies and coal and clay mining were the primary endeavors of these settlers (Fish 1967). By 1940 a secondary wastewater treatment plant (WWTP) was built for the town of Issaquah with a capacity of 0.15 MGD (Lazoff 1980). By 1960, Issaquah Creek was receiving effluent from the Issaquah WWTP, a milk processing plant, a state fish hatchery (established in 1936) and runoff from sand and gravel operations.

[4] The Sammamish Heritage Society: http://www.iinet.com/~shs/sammamish1950.html; Lake Sammamish Living: http://www.lakesamm.com/professional1.shtml

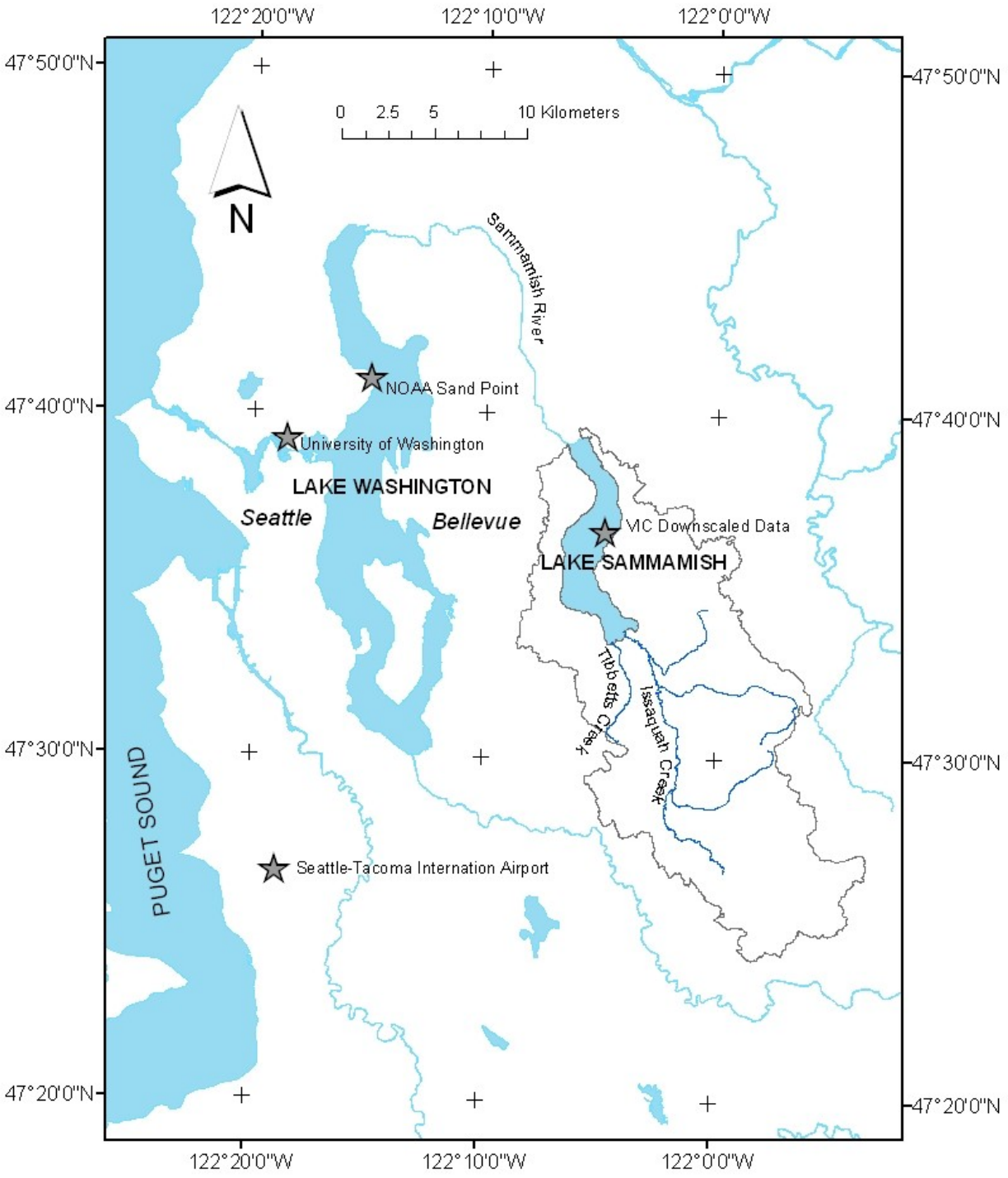

Figure 1. Map showing the Lake Sammamish study area, including an outline of the Lake Sammamish watershed.

Based on studies conducted by Isaac et al. (1966) on Lake Sammamish and similar studies related to an effort to divert secondary effluent from nearby Lake Washington (Edmondson 1968, 1969), wastewater from the Issaquah WWTP and the milk processing plant were completely diverted from Lake Sammamish by 1968. Lake Washington quickly recovered (Edmondson 1994), while the recovery of Lake Sammamish did not progress as quickly as expected based on flushing alone (Welch et al. 1975, Welch 1977). The delayed recovery of Lake Sammamish is well documented and has been attributed to sediment-nutrient interactions and the relatively smaller proportion of the total phosphorus load that was diverted (Birch et al. 1980; Welch 1985; Welch et al. 1980, 1986).

In spite of all the changes that have occurred since the 1860s, it appears that the lake has remained in a more or less mesotrophic state (Welch et al. 1980). The hypolimnion has also consistently become anaerobic from about August through October more as a result of the lake's morphometry than excessive primary production since the epilimnion-to-hypolimnion ratio is relatively high (about 1.0) (Welch 1977). As a point of comparison, the hypolimnion of nearby Lake Washington has an epilimnion-to-hypolimnion ratio of about 0.39.[5] Although Lake Washington has a similar level of primary production, it has a much larger hypolimnetic volume in which to absorb the respiration of the setting organic detritus delivered externally and produced within the lake and still have oxygen remaining in the hypolimnion before late summer turnover.

1.3 Study Goals and Objectives

As noted above, the objective of this project is to estimate the change in the amount of suitable habitat for kokanee in Lake Sammamish, Washington expected in this century due to climate change.

The overarching goal is to ensure that protection and restoration measures implemented to restore the long term viability of kokanee in Lake Sammamish will be effective enough to offset future limitations introduced as a result of a changing climate. This study focuses exclusively on the effect of increasing air temperatures on the thermal regime and amount of suitable cold water habit for kokanee in the lake.

[5] Lake Washington physical characteristics: http://green.kingcounty.gov/lakes/LakeWashington.aspx

2.0. MODELING APPROACH

In theory, modeling should be an iterative approach that involves initial conceptualization and implementation based on management information needs and available resources followed by testing and model refinement. However, the application of models as an aid in management decision making typically requires a more finite project timeline. Ideally, modeling and management decision making would be a coupled iterative process that allows for additional data collection, model testing, model refinement, and re-evaluation of model results and management decisions based on them. This project embraces this concept by using existing lake temperature models to conduct an initial assessment of the sensitivity of Lake Sammamish to future climate warming and an assessment of the implications of changes in the lake thermal regime on kokanee salmon habitat. Depending on the results of this study, further model development or development of additional models and analyses may be warranted.

2.1 Description of Models

The 2-D and 3-D models that were developed as part of an earlier King County study are described below. The models were developed and tested using routine temperature profiling data collected over an eight year period between 1995 and 2002. Although desirable, resources were not available to update and test the models with data collected since that time. Therefore, the climate change simulations are limited to evaluating the response of the lake to increasing air temperatures over this eight year period. Details regarding the simulation time period and the development of model inputs are provided in Section 2.2.

2.1.1 3-Dimensional Model

The 3-D model selected for this study was the Curvilinear Hydrodynamics in Three Dimensions – Z Plane (CH3D-Z) model, originally developed for Chesapeake Bay and later adapted for application to Lake Washington (Kim et al. 2006) and Lake Sammamish (King County 2008). CH3D-Z is capable of modeling horizontal and vertical circulation induced by surface heat exchange, tide, wind, density effects (salinity and temperature), freshwater inflows, turbulence, and the effect of the earth's rotation. As the name implies, the horizontal CH3D grid is curvilinear (i.e., boundary-fitted) to best represent deep channels and flow along irregular shorelines. A report describing the development of the Lake Washington CH3D-Z model and a user's manual for the Lake Washington application have been prepared by Johnson et al. (2003) and Johnson and Kim (2004), respectively.

A two-equation (k-ε) turbulence closure model is employed in CH3D-Z to represent vertical turbulent mixing. The eddy viscosity and eddy diffusivity turbulence terms are derived from the computation of kinetic energy (k) and energy dissipation (ε) due to the effects of surface wind shear, bottom shear, velocity gradient turbulence production, turbulent energy dissipation, and density stratification. Since vertical momentum is neglected to facilitate the solution of the finite difference equations (hydrostatic assumption), convective mixing is accounted for by checking the vertical density distribution after each

time step. At locations where the water column is unstable, the maximum vertical eddy coefficients are applied to simulate convective mixing in a diffusive manner.

An externally processed equilibrium temperature and heat exchange coefficient time series is used to simulate thermal heat exchange at the lake surface. The pre-processing of meteorological data (air temperature, dew point, wind speed and direction, cloud cover and solar radiation) into the model input file is documented in King County (2008).

In the current version of the model, surface evaporation rate is supplied in an input file to the model. Therefore, the evaporation rate used to model the mass transfer of water from the surface of the lake is uncoupled from the evaporative heat flux computed for the external equilibrium heat exchange input file. The daily evaporation rate used in the Lake Washington application (Johnson et al. 2003) was used in the Lake Sammamish application. It turns out that the decoupling of the effect of evaporation on the lake water balance is of some convenience for this application, because the effect of increasing air temperature on lake heat exchange is effectively decoupled from changes in lake volume (and water level) that might occur as lake surface evaporation increases as air temperature increases.

Daily rainfall on the lake surface is also provided in an input file, but the heat flux associated with rainfall is not currently considered in the model. Similarly, the current version of the model allows for a distributed inflow to the lake surface to account for un-gauged surface runoff along the lake shoreline, but the heat flux (and momentum) associated with the distributed inflow is not considered.

The horizontal resolution of the boundary-fitted model grid is illustrated in Figure 2. The grid surface contains 249 active cells with a maximum of 30 vertical layers. Each layer is 0.91 m thick except for the surface layer, which varies with water surface elevation. Overall, computations are performed on 4,283 grid cells using a 60 second time step. The model simulates an 8-year time span (currently developed and tested for the period 1995-2002) in a little over 6 hours on a 64-bit Windows PC equipped with two 2.66 GHz quad core processors. Model output was written to a self-describing binary file format (NetCDF) during runtime resulting in eight separate 531 MB files for each year model run; a total of 4.25 GB for an 8-year model run.

2.1.2 2-Dimensional Model

The 2-D model (longitudinal/vertical) selected for this study was CE-QUAL-W2, which evolved from LARM (Laterally Averaged Reservoir Model) developed by Edinger and Buchak (1975). The water quality algorithms were incorporated into the model by the Water Quality Modeling Group at the U.S. Army Engineer Waterways Experiment Station (WES) resulting in Version 1.0 of CE-QUAL-W2 (Environmental and Hydraulic Laboratory 1986), which has been maintained and continually improved by the U.S. Army Corps of Engineers. The current version of the Lake Sammamish model was developed using Version 3.5 of CE-QUAL-W2 (Cole and Wells 2006).

Lake surface heat exchange is computed internally during model execution based on the same meteorological inputs as in the 3-D model. In addition to an equilibrium temperature approach, the model also provides for what is known as a term-by-term heat exchange

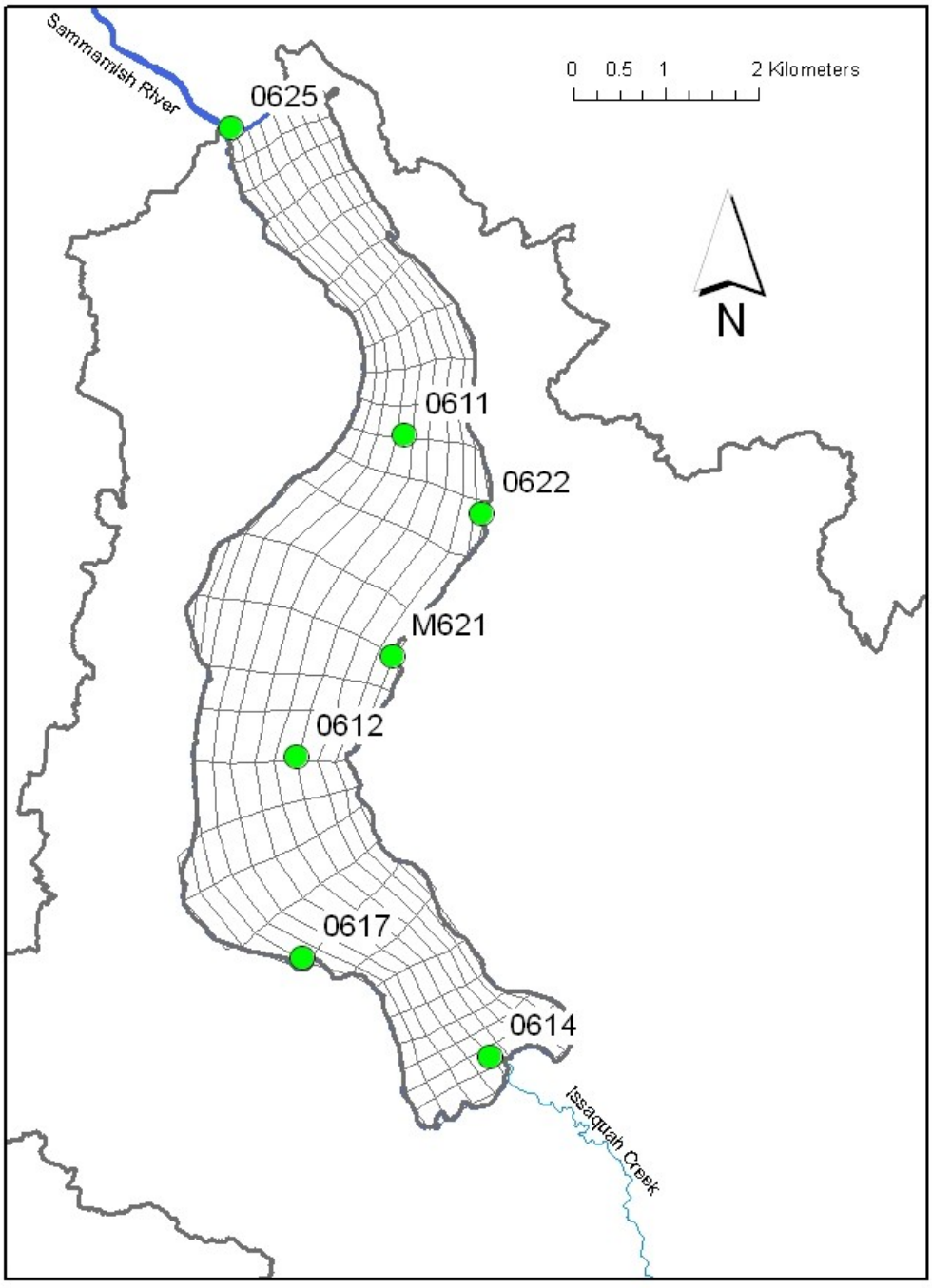

Figure 2. Map showing the Lake Sammamish CH3D-Z boundary-fitted model grid and locations of routine water quality profiling stations. Major inflow (Issaquah Creek) and the lake outflow (Sammamish River) also shown.

computational approach. This approach explicitly calculates the surface heat exchange components, including evaporative heat loss, short- and long-wave radiation, convection, conduction and back radiation (Cole and Wells 2006). The equilibrium temperature approach was used for this application.

The model also provides a switch that allows for inclusion of evaporative heat loss in the heat exchange computations, but excludes the evaporative loss of water from inclusion in the water balance. This can be useful in cases where the lake water balance is very sensitive to changes in evaporative losses, which would require revision of estimated ungauged inflows for every modification of the meteorological input file.

Since changes in precipitation and tributary flows (and their temperatures) were not investigated as part of this study, evaporative water losses were excluded from the computation of the water balance so that a single distributed inflow time series could be used for any particular meteorological input file. Sensitivity analyses conducted as part of this study, but not reported in detail here, indicated that the lake heat budget was relatively insensitive to changes in distributed tributary inflow. For example, turning off inflows and outflows as well as evaporative water loss had a minimal effect on lake temperature prediction skill. This is consistent with the relatively long residence time of the lake, which results in surface heat exchange and wind mixing as the dominant processes affecting the lake thermal regime. Livingstone (2003) noted the dominance of surface heat exchange as the driver of temperatures of Lake Zurich, a relatively large, deep lake in Switzerland.

The longitudinal resolution of the 2-D grid is illustrated in Figure 3. The lake is represented by 22 longitudinal segments and vertical resolution was defined using 0.91 m thick layers resulting in a close approximation of the 3-D model vertical layering scheme. The QUICKEST-ULTIMATE numerical transport solution scheme was used with the recommended time weighting factor (THETA) of 0.55. The vertical turbulence algorithm W2N was used with an implicit scheme and a maximum vertical eddy viscosity of 0.01 $m^2 s^{-1}$. The model time step was optimized and averaged about 100 seconds in each model run, which resulted in 8-year simulations that took approximately 30 minutes to run on a 64-bit Windows PC equipped with two 2.66 GHz quad core processors. Model output was written to a self-describing binary file format (NetCDF) during runtime resulting in an 841 MB file for each 8-year model run.

2.2 Development of Model Inputs

The models are forced with essentially the same hydrologic and meteorological data, with the exception of distributed flows (essentially net unaccounted flow) developed to balance the day-to-day changes in lake storage by matching daily changes in observed lake elevation. King County (2008) provides a detailed description of the development of the 1995-2002 flow (tributary inflows and outlet flow), inflow water temperature and meteorological time series inputs to the 3-D model, which were also used in the development of the 2-D model. Flow and temperature data were available for Issaquah Creek, the main tributary at the southern end of the lake. Data were also available for several small tributaries around the lake for all or portions of the simulation period.

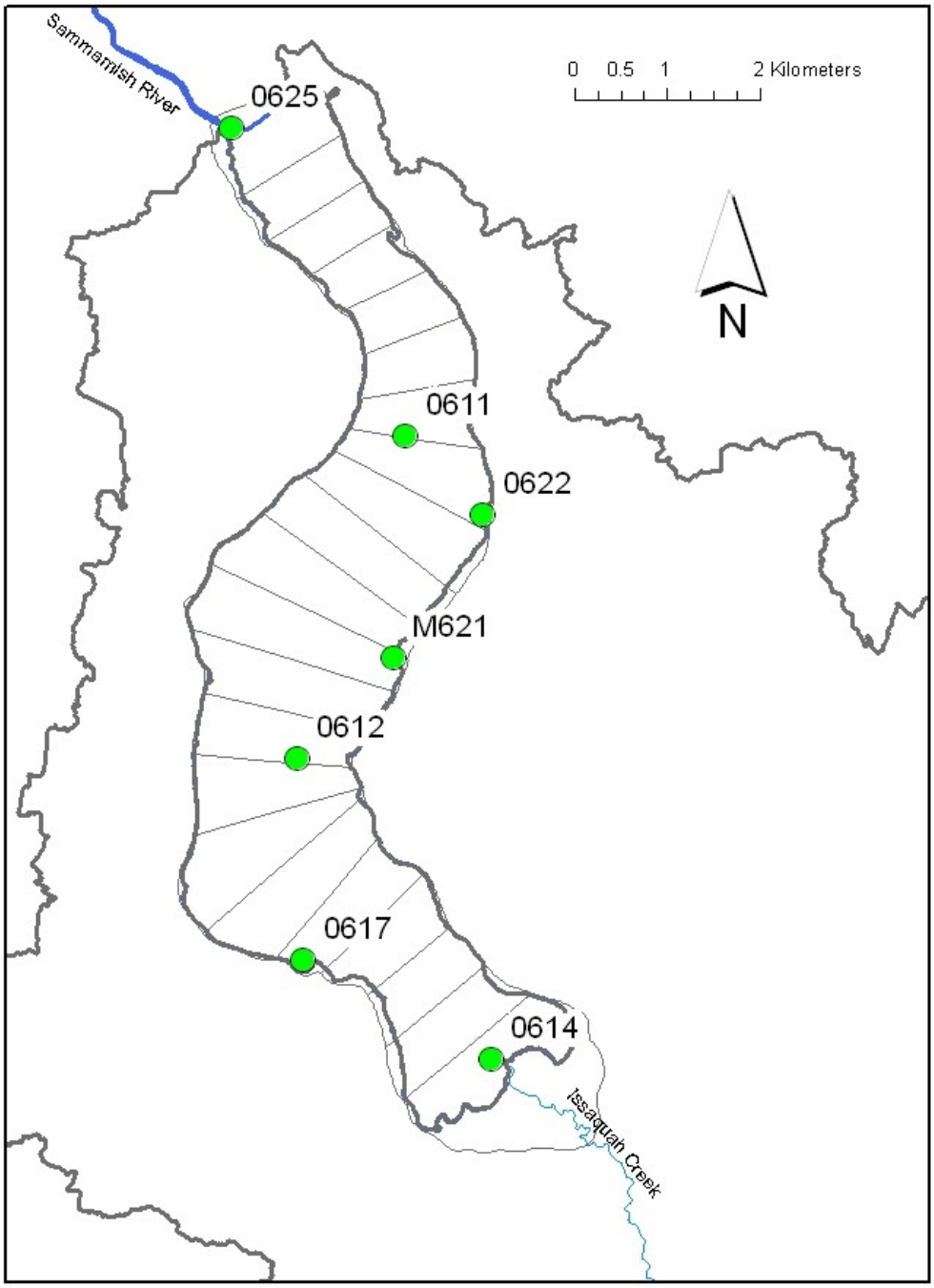

Figure 3. Map showing the longitudinal segmentation of the Lake Sammamish CE-QUAL-W2 grid and locations of routine water quality profiling stations. Major inflow (Issaquah Creek) and the lake outflow (Sammamish River) also shown.

With the exception of solar radiation data, meteorological data (air and dew point temperature, wind speed and direction, cloud cover) came from Sea-Tac International Airport, approximately 24 km southeast of the lake center (see Figure 1). Solar radiation data came primarily from one of two locations depending on the availability of data – University of Washington or National Oceanic and Atmospheric Administration, which were located in Seattle near the western shore of nearby Lake Washington (see Figure 1).

Because the rate of evaporation of water from the lake surface was provided as an external time series in the 3-D model, no changes in model inputs (other than changing the air and dew point temperature inputs) were necessary to run the climate change simulations. For this study, the effect of evaporation on the water budget in the 2-D model was turned off (EVC=OFF) and a distributed flow input time series was developed to balance the water budget to match daily changes in lake water surface elevation. This approach was preferred over other approaches that would have required the development of unique distributed flows for each climate change model run. The selected approach removes the effect of changes in inflows on lake water temperature so as to focus on the effect of changes in air and dew point temperature on lake thermal dynamics.

Climate change projections of meteorological conditions were provided by the University of Washington Climate Impacts Group (CIG) for five Global Climate Model (GCM) projections based on the A1B emissions scenario:[6]

- **Composite** - Composite average of 10 best climate models (see Littell et al. 2011)**.**
- **ECHAM5** - ECHAM5 Global Climate Model
- **HadGEM1** - HadGEM1 Global Climate Model
- **MIROC_3.2** - MIROC 3.2 'medres' Global Climate Model
- **PCM1** - PCM1 Global Climate Model

Note that the A1B emissions scenario is considered a “middle of the road” scenario, whereas the B1 family of scenarios is considered to be “optimistic” while the A2 scenarios are considered “pessimistic” with respect to controlling green house gas emissions.

These climate projections, including the historical (1949-2006) hourly time series used in the downscaling process were interpolated to a location representing the lake surface using the Variable Infiltration Capacity (VIC) model (version 4.1.2.g).[7] The Modified Delta Method was used to provide 58-year hourly time series representing two future 30-yr GCM simulation periods hereafter referred to as 2040s (2030-2059) and 2080s (2070-2099). The Modified Delta Method is described in detail in Littell et al. (2011). In general, this method allows for direct comparison of the historical 1995-2002 simulations to the equivalent period in simulations based on downscaled 2040s and 2080s meteorological data.

[6] Note that the A1B emissions scenario is considered a “middle of the road” scenario, whereas the B1 family of scenarios is considered to be “optimistic” while the A2 scenarios are considered “pessimistic” with respect to controlling green house gas emissions.

[7] For more information on VIC see:
http://www.hydro.washington.edu/Lettenmaier/Models/VIC/Documentation/Inputs.shtml

Differences among the 10 projections stem from differences in the future decades simulated (2040s/2080s) and the GCM from which projections were obtained (Composite, ECHAM5, HadGEM1, MIROC_3.2, PCM1). Variables provided by CIG in the downscaled meteorological output from VIC are summarized in Table 1 and include air temperature and relative humidity, which were the parameters used to modify the meteorological inputs to the lake models.

Table 1. Meteorological parameters represented in the downscaled GCM output provided by the Climate Impacts Group.

Parameter	Units
Date/Time	Pacific Standard Time
Incoming precipitation	mm
Air temperature	^{o}C
Near surface wind speed	m/s
Incoming longwave radiation	W m^{-2}
Net downward longwave flux	W m^{-2}
Incoming shortwave radiation	W m^{-2}
Net downward shortwave flux	W m^{-2}
Relative humidity	%
Near surface vapor pressure deficit	kPa

Historical wind data were also provided by CIG using the WRF regional climate model in which the model was run at 15 km resolution and forced by NCEP-NCAR Reanalysis data. Model results were output at 6-hourly averages for 10-m height u and v velocity components and wind speed. The four closest WRF grid points to the lake were then interpolated to hourly frequency.

Note that the 4 GCMs were selected by CIG to bracket the composite average projection based on relative differences in projected temperature and precipitation. For this effort, differences in warming are most relevant. Figure 4 illustrates that HadGEM1 resulted in the most warming and ECHAM5 and PCM1 tended to indicate the least warming. The Composite ensemble generally more closely matched the models that indicated less warming than the A1B HadGEM1 model; MIROC 3.2, PCM1 and ECHAM5. The average warming projected by the Composite ensemble was 1.9 and 3.5 ^{o}C in 2040 and 2080,

respectively. Projected warming by 2040 for the individual models ranged from 1.3 to 2.8 °C for the ECHAM5 and HadGEM1 models, respectively. Projected warming in 2080 ranged from 2.6 to 5.6 °C for the PCM1 and HadGEM1 models, respectively.

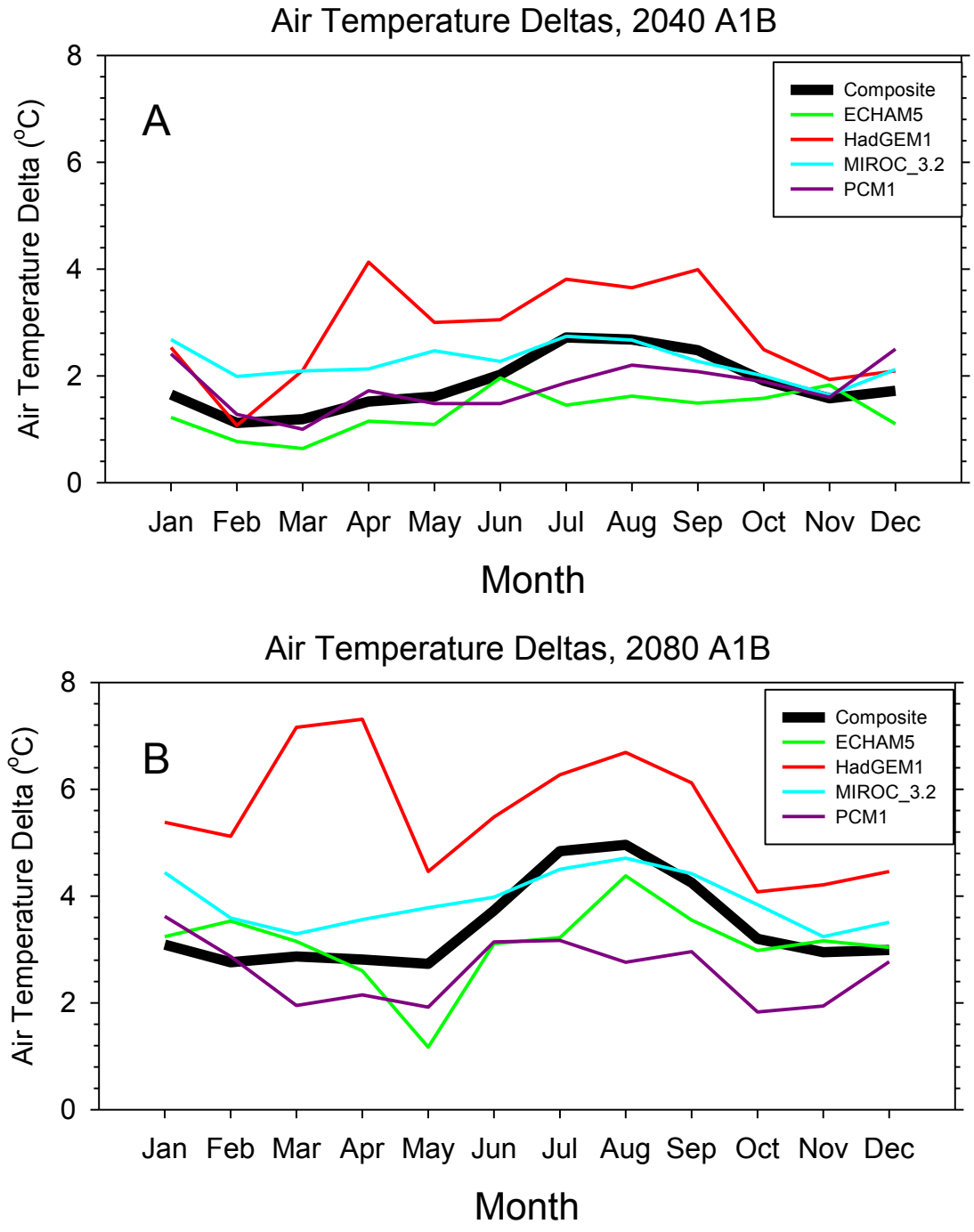

Figure 4. Plots of monthly deltas (future – historical) temperature for 2040s (A) and 2080s (B) for the five GCMs downscaled to Lake Sammamish.

Note: Data for figures provided by Guillaume Mauger, UW Climate Impacts Group

An eight year period, nominally representing the years 1995-2002, from the downscaled climate projections were used as the inputs for air temperature and dew point temperature for each model run. The monthly average air temperatures over the selected eight year period for the original forcing data from Sea-Tac and the historical and future climate change output are shown in Figure 5.

The observed (Sea-Tac) and historical downscaled data for Lake Sammamish were very similar with a difference in average air temperature of 0.4 °C, which was much smaller than the difference between these two sources of historical data compared to the 2040 and 2080 air temperature projections (see Figure 5). Although only representing 8 of the 58 years of downscaled data, the temperature increases projected during the eight year sample of output were almost identical to the entire 58 year period of downscaled data. The average warming projected by the Composite ensemble was 1.9 and 3.4 °C in 2040 and 2080, respectively. Projected warming by 2040 for the individual models ranged from 1.3 to 2.8 °C for the ECHAM5 and HadGEM1 models, respectively. Projected warming in 2080 ranged from 2.6 to 5.6 °C for the PCM1 and HadGEM1 models, respectively.

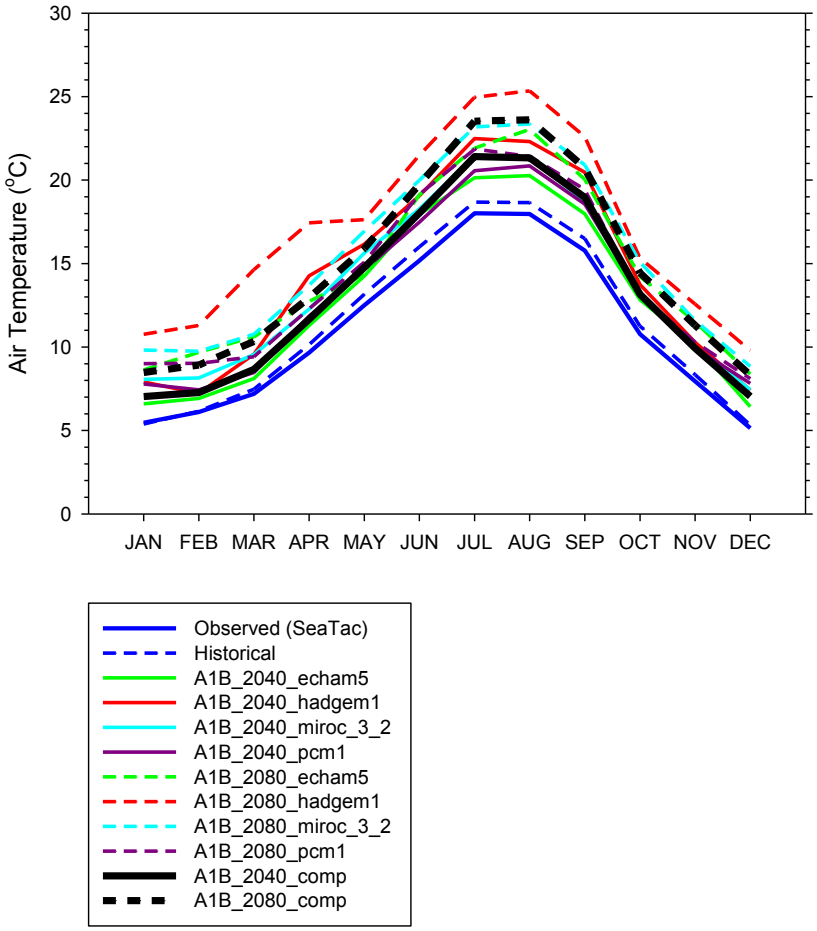

Figure 5. Plots of monthly deltas (future – historical) temperature for 2040s (A) and 2080s (B) for the five GCMs downscaled to Lake Sammamish.

2.3 Evaluation of Model Performance

Model performance was documented by comparing modeled lake temperatures to routine profiling observations made between 1995 and 2002 at seven stations distributed around the lake (see Figures 2 and 3). These stations were visited monthly during winter and twice monthly between spring (March/April) and fall (September/October) which allowed for approximately 4,500 point comparisons between models and observations. Comparisons included a suite of model performance metrics, including linear regression coefficient (r^2), bias, absolute mean error (AME), root mean square error (RMSE) and Nash-Sutcliffe model efficiency coefficient (NSE) (Table 2).

Formulas for calculating these model error statistics are provided below.

$$ME\,(Bias) = \frac{1}{N}\sum_{n=1}^{N} P_n - O_n \quad \text{(bias or mean error)}$$

$$\text{AME} = \frac{1}{N}\sum_{n=1}^{N} \left|P_n - O_n\right| \quad \text{(absolute mean error)}$$

$$\text{RMSE} = \sqrt{\frac{1}{N}\sum_{n=1}^{N} \left(P_n - O_n\right)^2} \quad \text{(root mean square error)}$$

$$SE(e) = \sqrt{\frac{1}{N}\sum_{n=1}^{N} \left(P_n - O_n\right)^2 - ME^2} \quad \text{(standard error)}$$

$$\text{REM} = \frac{\sum_{n=1}^{N} \left|P_n - O_n\right|}{\sum_{n=1}^{N} O_n} \; x\,100 \quad \text{(relative error of the mean, percent)}$$

$$\text{NSE} = 1 - \frac{\sum_{n=1}^{N} (P_n - O_n)^2}{\sum_{n=1}^{N} (O_n - \overline{O}_n)^2} \quad \text{(Nash - Sutcliffe model efficiency coefficient)}$$

Evaluations were performed on the model forced with the original meteorological input (Base) and with the gridded historical data provided by CIG (Historical). This provided an evaluation of the sensitivity of the model to the relatively small change in air and dew point temperature that resulted from changing the source of the contemporaneous meteorological input.

In general, these models performed better than half of the approximately 35 published temperature models surveyed by Arhonditsis and Brett (2004). These models also performed as well as or slightly better than the Lake Washington CH3D model with respect to bias and REM (Kim et al. 2006).

Table 2. Results of statistical analysis of output from original model setup using observed meteorological data (Base) and the same model forced with the historical gridded data representing the surface of the lake provided by the Climate Impacts Group.

	Regression r^2	Bias	AME	RMSE	SE	REM (%)	NSE
2-D Model (CE-QUAL-W2)							
Base	0.96	0.16	0.79	1.08	1.07	6.4	0.95
Historical	0.96	0.19	0.79	1.10	1.08	6.4	0.95
3-D Model (CH3D-Z)							
Base	0.95	-0.31	0.82	1.11	1.06	5.8	0.95
Historical	0.95	-0.25	0.81	1.09	1.06	5.8	0.95

Comparisons of modeled and observed temperature profiles for the central lake station (Station 0612) for the 2-D and 3-D model for 1995-2002 are provided in Appendix A and B, respectively.

2.4 Historical Context

For historical context with respect to kokanee and the Lake Sammamish ecosystem, the reader is referred to a number of reports and technical documents available on the King County web site.[8]A brief summary is provided below. A brief summary of the historical lake condition with respect to temperature and DO is also provided below for the 1995-2002 modeling period.

2.4.1 Lake Sammamish kokanee

Over 20 species of fish are found in Lake Sammamish, including species of trout (cutthroat and rainbow/steelhead), anadromous salmonids (coho, Chinook and sockeye) and kokanee. Kokanee is a form of sockeye salmon that spends its entire life in freshwater (i.e., it is non-anadromous) (Berge 2009). Native Lake Sammamish kokanee were more abundant historically with an "early run" and a "late run." The early run kokanee historically spawned almost exclusively in Issaquah Creek from August to September, but this run is considered to be extinct (Berge and Higgins 2003).

[8] King County Lake Sammamish kokanee website:
http://www.kingcounty.gov/environment/animalsAndPlants/salmon-and-trout/kokanee.aspx

The late run kokanee spawn in a number of smaller Lake Sammamish tributaries and along limited portions of the lake shoreline from the end of October through March. The total estimated number of late-run kokanee spawners has fluctuated considerably from one year to the next since the 1996 brood year with notable numbers of spawners observed in 2003 and 2012 (Figure 6). The average age of maturity for kokanee is 4 years, but in some cohorts there are more age-3 adults. On average, the returning adult kokanee represented on the spawning grounds resided in Lake Sammamish for three years prior to spawning. Therefore, kokanee spawning in late 2003 would have migrated from their natal tributary to Lake Sammamish as fry between March and May of 2000 and would have been produced from the 1999 brood year.

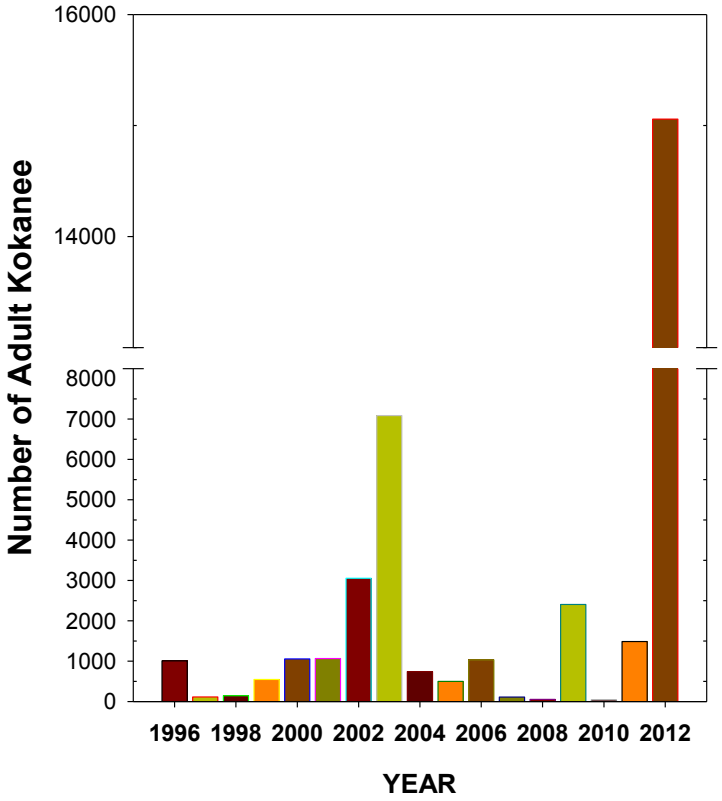

Figure 6. Area-under-the-curve escapement estimates of Lake Sammamish late-run kokanee using a 7 day stream life. Source: H. Berge, pers. comm.

Berge (2009) conducted an extensive study of the seasonal and diel distribution of fish in Lake Sammamish, with a focus on evaluating the implications of the temperature-DO "squeeze." The temperature-DO squeeze is the result of summer warming of the epilimnion and the associated depletion of hypolimnetic oxygen. Berge (2009) noted that the squeeze began in mid-July and persisted through September due to the combination of peak epilimnetic temperatures and hypoxic conditions in the hypolimnion. Berge (2009) estimated that the temperature-DO squeeze reduced the amount of favorable habitat (<17 ^{o}C and >4 mg DO/L) available for kokanee by 84 percent in late September. Both kokanee and cutthroat trout responded to the squeeze by favoring the cooler and better oxygenated

waters of the metalimnion where overlap occurs in food resources (primarily zooplankton) with other planktivorous salmon and trout and juvenile kokanee were at greater predation risk by piscivorous cutthroat trout. During thermal stratification, the density of zooplankton (an important food resource for kokanee) was 1.5 to 8 times higher in the warmer epilimnion than in the metalimnion, potentially affecting overall availability of food during this period.

Using visual predation and bioenergetics modeling, Berge (2009) found that kokanee growth efficiency was greatest during the spring and lowest for all size classes during the period of thermal stratification. Berge (2009) concluded that during thermal stratification temperature is a constraint to kokanee growth, making kokanee balance thermal stress with predation risk and that Lake Sammamish kokanee are not able to maximize growth during the thermally stratified period.

2.4.2 Temperature and dissolved oxygen

The air temperature during the period 1995-2002 varied seasonally with monthly average daily maximum temperatures peaking in late July or August (Figure 7). Monthly average minimum daily air temperatures typically occur in late January or early February. Monthly average maximum temperatures during summer were generally higher during the first four years of this period followed by four years with consistently lower summer maximum temperatures (see Figure 7).

The variability in the temperature-DO squeeze over the period 1995-2002 is illustrated in Figure 8 using color contour plots of temperature and DO measured at Station 0612 to illustrate how the epilimnion warms and the hypolimnion become anaerobic in the summer.[9]

The inter-annual variability in the temperature-DO squeeze is further illustrated in Figure 9 by plotting selected temperature and DO isopleths at the same central lake monitoring station. These temperature isopleths were selected based on suggested temperature thresholds provided by Kirk Krueger (Washington Department of Fish and Wildlife, pers. comm., email, May 28, 2013). The thresholds were

- >17 ^{o}C, salmonid avoidance
- 21.5 ^{o}C, salmonid thermal maximum
- 25.1 ^{o}C, salmonid lethal threshold

[9] Note that additional lake monitoring data, including data collected prior to 1995 and after 2002 have been collected as part of King County's long-term monitoring program (http://green.kingcounty.gov/lakes/LakeSammamish.aspx)

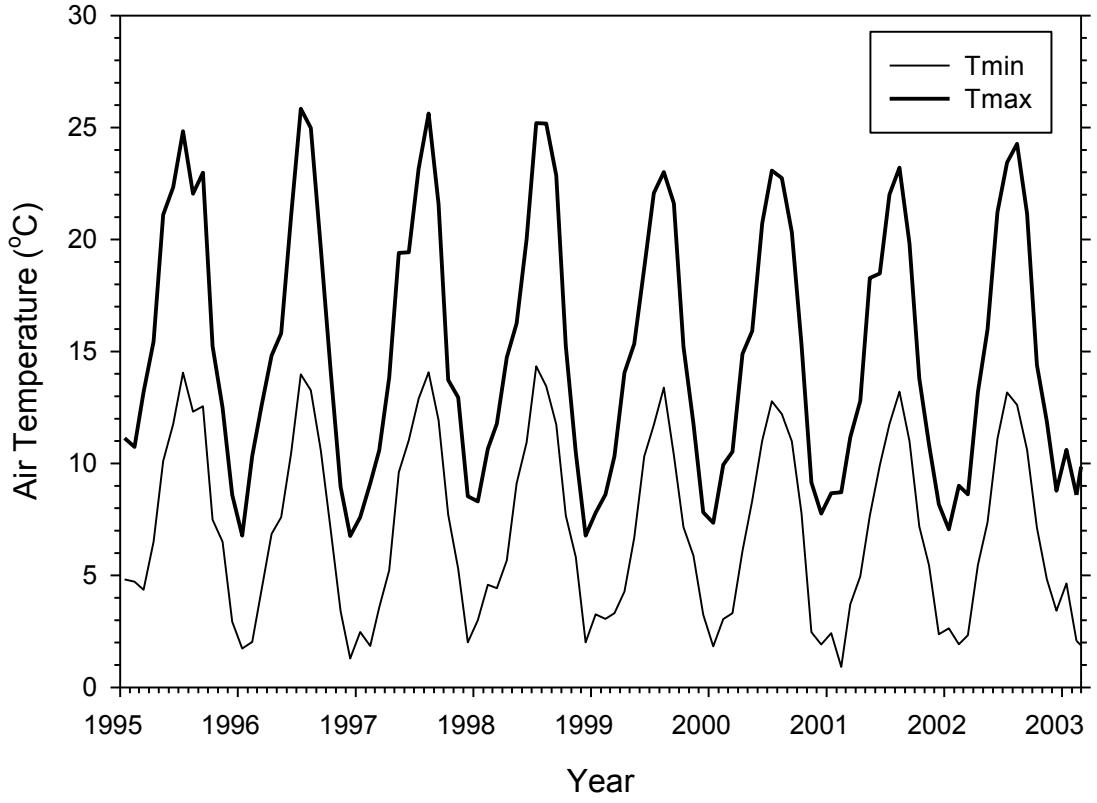

Figure 7. Time series of monthly average daily maximum and minimum air temperatures reported at Sea-Tac International Airport, 1995-2002.

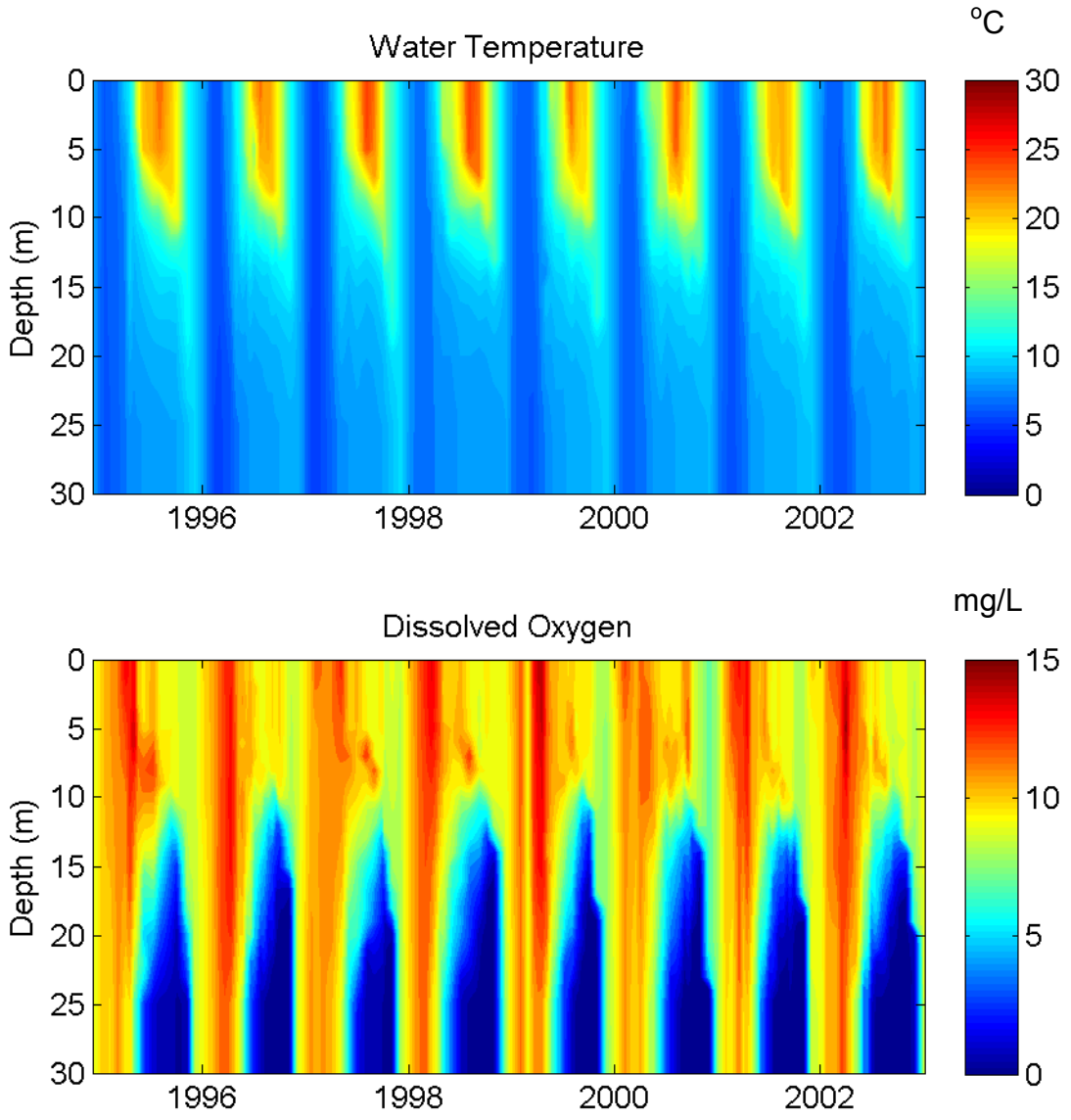

Figure 8. Color contour plots of Lake Sammamish water temperature (top) and dissolved oxygen (bottom) based on routine monthly winter and twice monthly spring-fall sampling at Station 0612 from 1995 to 2002.

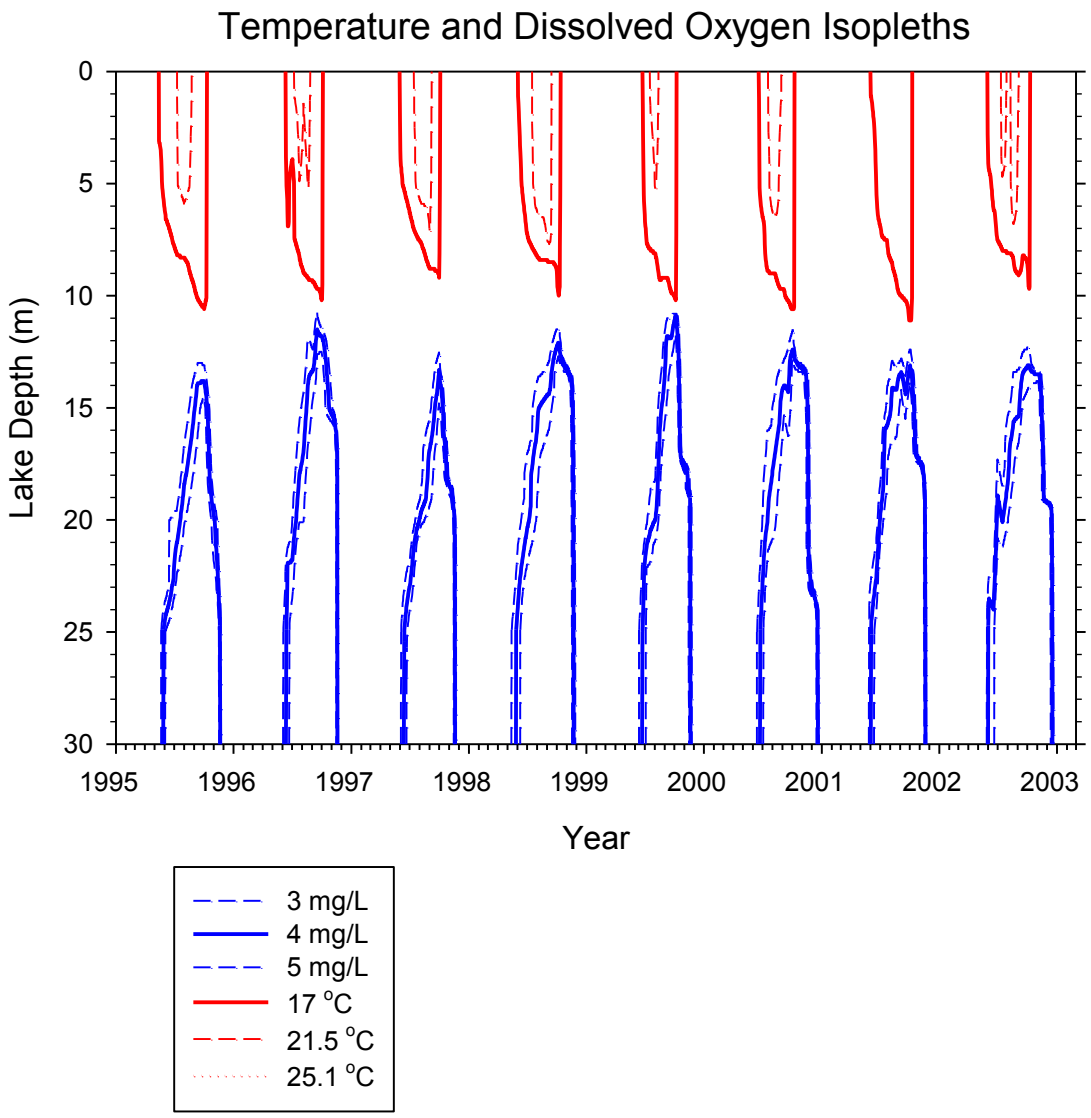

Figure 9. Isopleths of temperature and dissolved oxygen based on data from the central monitoring station in Lake Sammamish (0612), 1995-2002.

The DO isopleths chosen for display were based on Berge (2009). DO concentrations of 3, 4 and 5 mg/L represent a range of potential salmonid avoidance thresholds with 4 mg/L selected as the representative threshold for favorable salmonid habitat (Berge 2009). In general, each year as the lake stratifies; water with temperatures above 17 °C extends to about 10 m by September or October (Figure 9). As the lake stratifies the hypolimnetic oxygen concentrations decline and by late September or October hypolimnetic oxygen concentrations fall below 5 mg/L. Examination of Figure 9 illustrates the amount of inter-annual variability in the thermal character and hypolimnetic oxygen patterns in the lake.

To provide context for the temperature and DO isopleths, the depth-volume curve developed by Isaak et al. (1966) is shown in Figure 10. This curve illustrates that the top 10 m of the lake surface represents approximately half of the lake volume. The volume of the

lake below 12 m represents approximately 30 percent of the total lake volume. Therefore, the volume of optimal salmonid habitat in the lake by late summer is about 20 percent of the total volume of the lake and is isolated to a relatively narrow layer between 10 and 12 m depth.

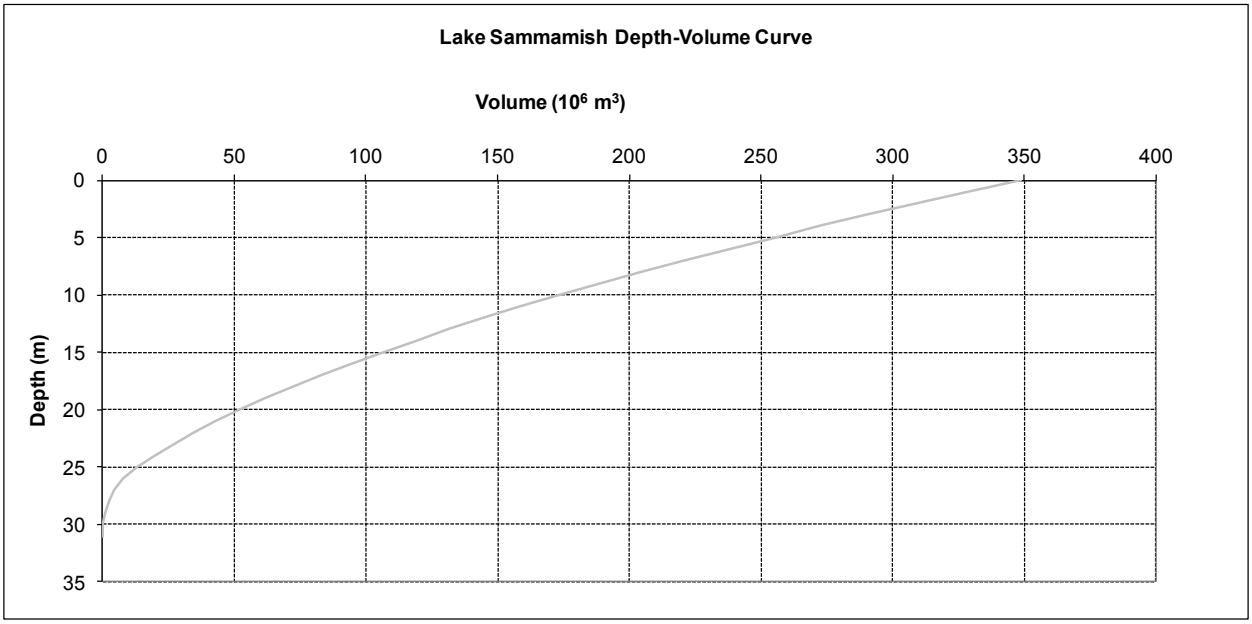

Figure 10. Lake Sammamish depth-volume relationship (Isaak et al. 1966).

2.5 Analysis/Synthesis of Results

The output from the 2-D and 3-D models were post-processed to calculate the volume of the lake each hour over the 8-year period with temperatures below the three thresholds described above – 17 °C (avoidance), 21.5 °C (thermal maximum) and 25.1 °C (lethal threshold). The evaluation was conducted by examining the temperature reported in each grid cell each hour and summing the grid volumes of the cells with temperatures below each of the three temperature thresholds. The hourly volumes were averaged into daily estimates of habitat volumes for the three thresholds.

An analysis of the observed DO data collected from the central long-term monitoring station (Station 0612) was conducted to estimate the daily volume of the lake with DO concentrations less than 4 mg/L. The daily volume of the lake for each model scenario and temperature threshold was subtracted from the volume of the lake with DO concentrations below 4 mg/L to provide an estimate of the daily habitat volume for each temperature threshold accounting for the DO squeeze. Following Berge (2009), the volume of the lake with temperatures below 17 °C and DO concentrations greater than 4 mg/L were characterized as "favorable" salmonid habitat.

Model output for the grid cell representing Station 0612 was exported and processed using Lake Analyzer (Read et al. 2011), a Matlab program designed for analyzing high resolution lake profiling data that is also well suited to analyzing lake temperature modeling output. This program calculates a number of metrics relevant to analyses of lake thermal regimes, including, but not limited to, thermocline depth and thermal (Schmidt) stability. Model output for the grid cell representing Station 0612 was also processed to determine the isotherms for the three temperature thresholds.

Daily time series plots of the results of the analyses described above (habitat volume response, response of threshold isotherms, thermocline depth and Schmidt stability) are presented in Appendices C through F for selected downscaled GCM (Composite, HadGEM1 and ECHAM5) and the historical meteorological data inputs as a baseline for comparison.

Summary metrics were also tabulated for each model run, including the mean July-September daily habitat volume (i.e., the daily habitat volume between July and September in each of the eight years of each model simulation was averaged), the mean July-September thermocline depth, the mean date of the onset of stratification, the mean date of lake destratification, the mean duration of stratification and the mean annual maximum Schmidt stability. The date of the onset of stratification and the date of lake destratification was determined using the same threshold Schmidt stability value as used by Winder and Schindler (2004) in their analysis of observed warming of Lake Washington – 50 g cm cm^{-2}.

Plots of the annual average July-September habitat volume over the eight year simulations were also created to evaluate the inter-annual variability and change over time using output from the 2-D and 3-D model runs based historical and the 2040 and 2080 A1B Composite input data. Monthly average plots of the same response variables (habitat volume, isotherm depths, thermocline depth and Schmidt stability were also developed for all of the model runs.

3.0. RESULTS AND DISCUSSION

3.1 Habitat Volume Response

The 2-D and 3-D models predicted generally similar responses with respect to suitable habitat volume for the three temperature thresholds (see Figure 11 through Figure 16 and figures in Appendix C). The models did not predict much habitat reduction based on the 17 ^{o}C avoidance threshold. Greater reductions in habitat volume were predicted for the avoidance (21.5 ^{o}C) and lethality (25.1 ^{o}C) thresholds. The amount of reduction in suitable habitat depended on the GCM model and temperature threshold, but generally the models predicted greater reductions in 2080 vs 2040.

The 2-D and 3-D model average July-September habitat volume results with respect to the three temperature thresholds are summarized in Table 3 and Table 4, respectively. These results better illustrate the small change predicted in what Berge (2009) described as "favorable habitat" for kokanee (temperatures less than 17 ^{o}C and DO concentrations greater than 4 mg/L). The 2-D model predicts a decrease of no more than 1 percent by 2040 and between 1 and 4 percent by 2080 (Table 3 and Figure 11). The 3-D model predicts a somewhat larger decrease in favorable habitat, ranging from 3 to 4 percent in 2040 to 5 to 10 percent in 2080 (Table 4 and Figure 12). Largest decreases are predicted to occur in May and October as a result of the lake stratifying earlier and remaining stratified longer (see Figure 11and Figure 12).

Much larger changes in habitat volume are predicted by the 2-D and 3-D models based on the 21.5 ^{o}C avoidance threshold (see Table 3 and Table 4). The decrease predicted by the 2-D model ranged from 12 to 19 percent in 2040 to 17 to 24 percent in 2080 (Table 3 and Figure 13). The decrease predicted by the 3-D model ranged from 9 to 20 percent in 2040 to 17 to 33 percent in 2080 (Table 4 and Figure 14). Habitat loss is predicted to occur from June to September, with the largest losses predicted to occur in September (see Figure 13 and Figure 14)

The reduction in habitat volume based on the lethality threshold of 25.1 ^{o}C is somewhat equivocal between the two models due to somewhat greater epilimnetic warming predicted by the 2-D model in the 2080s (see Figure 15 and Figure 16). The decrease predicted by the 2-D model by the 2040s ranged from 2 to 10 percent and by the 2080s the predicted reductions ranged from 6 to 27 percent (Table 3 and Figure 15). The reduction in habitat volume predicted by the 3-D model ranged from none to a 2 percent change in the 2040s and 1 to 13 percent by the 2080s (Table 4 and Figure 16). Habitat loss based on the 25.1 oC lethality threshold is predicted to occur between June to September, with greatest losses predicted in August (Figure 15 and Figure 16)

To illustrate the inter-annual variation in model-predicted habitat volume, the annual average July-September habitat volume (1995-2002) for each temperature threshold was plotted for the Historical, A1B 2040 Composite and A1B 2080 Composite model runs for the 2-D and 3-D models (see Figure 17 and Figure 18, respectively). These figures

compliment the tabular information summarized above showing generally that both models predict a relative small reduction in favorable habitat volume, larger reductions in habitat volume based on the avoidance temperature of 21.5 ^{o}C and equivocal reductions in habitat volume based on the 25.1 ^{o}C lethal temperature threshold.

Table 3. Average July-September salmonid habitat volumes (shown as percent of total lake volume) predicted by the 2-D Lake Sammamish model for each of the three temperature thresholds.

Scenario	Favorable habitat volume			Less than Avoidance threshold			Less than Lethal threshold		
	Hist	2040	2080	Hist	2040	2080	Hist	2040	2080
Composite	28	28	27	56	41	35	75	71	57
ECHAM5	28	28	26	56	44	36	75	73	62
HadGEM1	28	27	24	56	37	32	75	66	48
MIROC 3.2	28	27	26	56	40	34	75	70	57
PCM1	28	27	27	56	43	39	75	72	69

*Favorable Habitat Volume = volume <17^{o} C; Avoidance threshold = 21.5^{o} C; Lethal threshold = 25.1^{o} C

Table 4. Average July-September habitat volumes (shown as percent of total lake volume) predicted by the 3-D Lake Sammamish model for each of the three temperature thresholds.

Scenario	Favorable habitat volume			Less than Avoidance threshold			Less than Lethal threshold		
	Hist	2040	2080	Hist	2040	2080	Hist	2040	2080
Composite	30	27	25	67	52	42	74	73	69
ECHAM5	30	27	25	67	58	44	74	74	71
HadGEM1	30	25	20	67	47	34	74	72	61
MIROC 3.2	30	26	24	67	51	41	74	73	69
PCM1	30	27	25	67	56	50	74	73	73

*Favorable Habitat Volume = volume <17^{o} C; Avoidance threshold = 21.5^{o} C; Lethal threshold = 25.1^{o} C

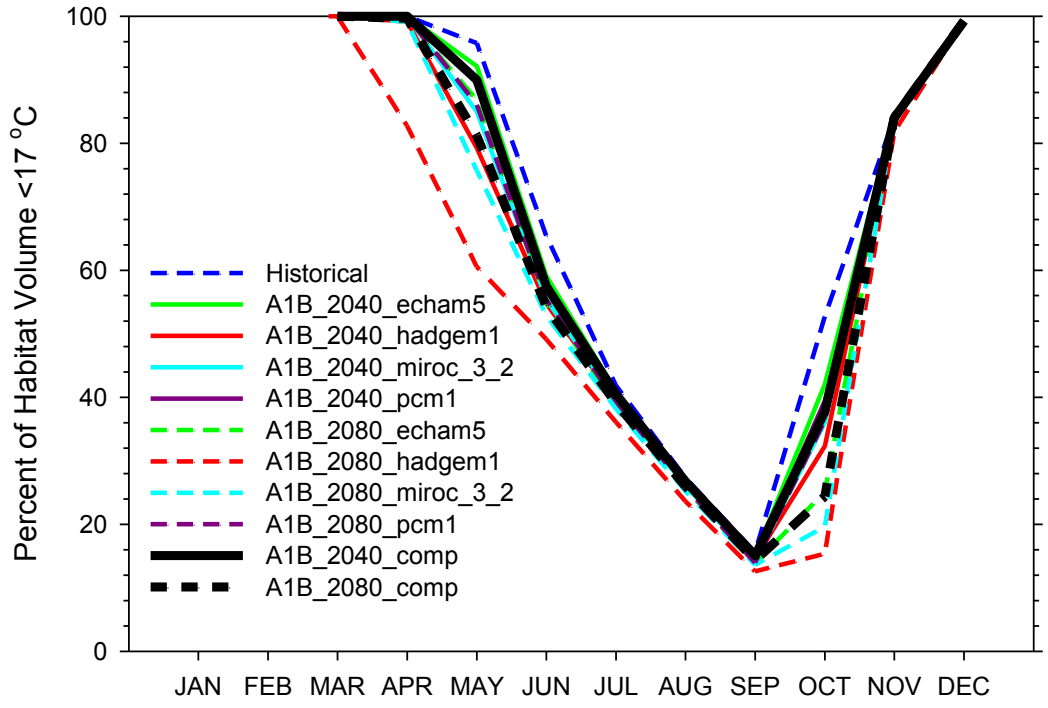

Figure 11. Monthly average salmonid habitat volume based on the eight years of output from the 2-D Lake Sammamish model using a 17 °C temperature threshold.

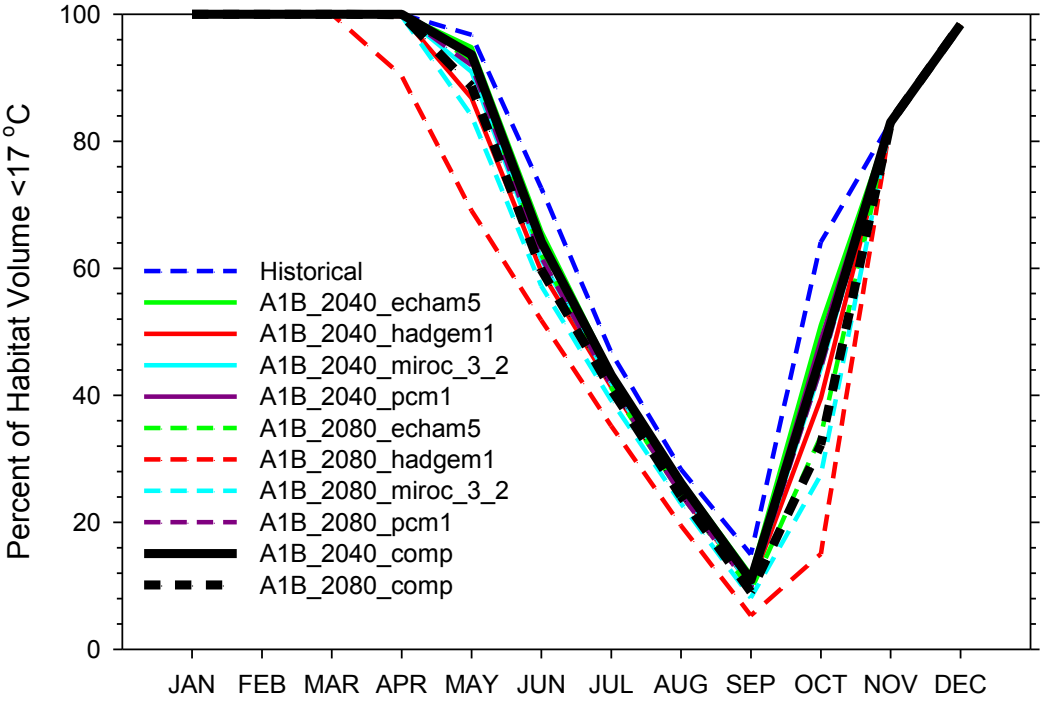

Figure 12. Monthly average salmonid habitat volume based on the eight years of output from the 3-D Lake Sammamish model and a 17 °C temperature threshold.

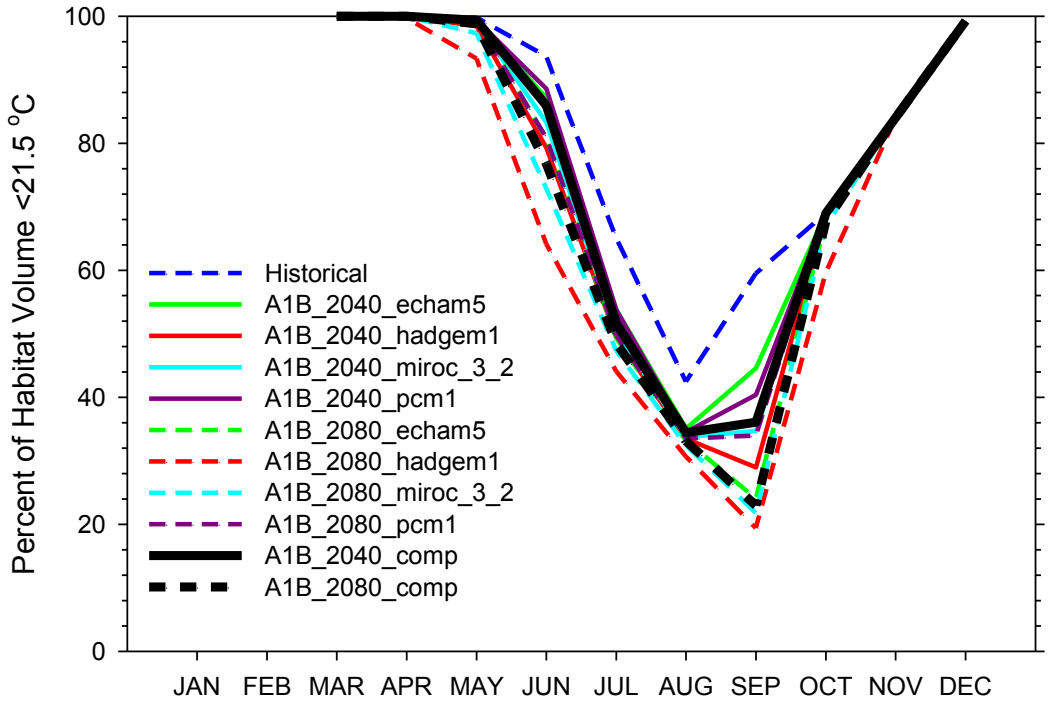

Figure 13. Monthly average salmonid habitat volume based on the eight years of output from the 2-D Lake Sammamish model and a 21.5 °C temperature threshold.

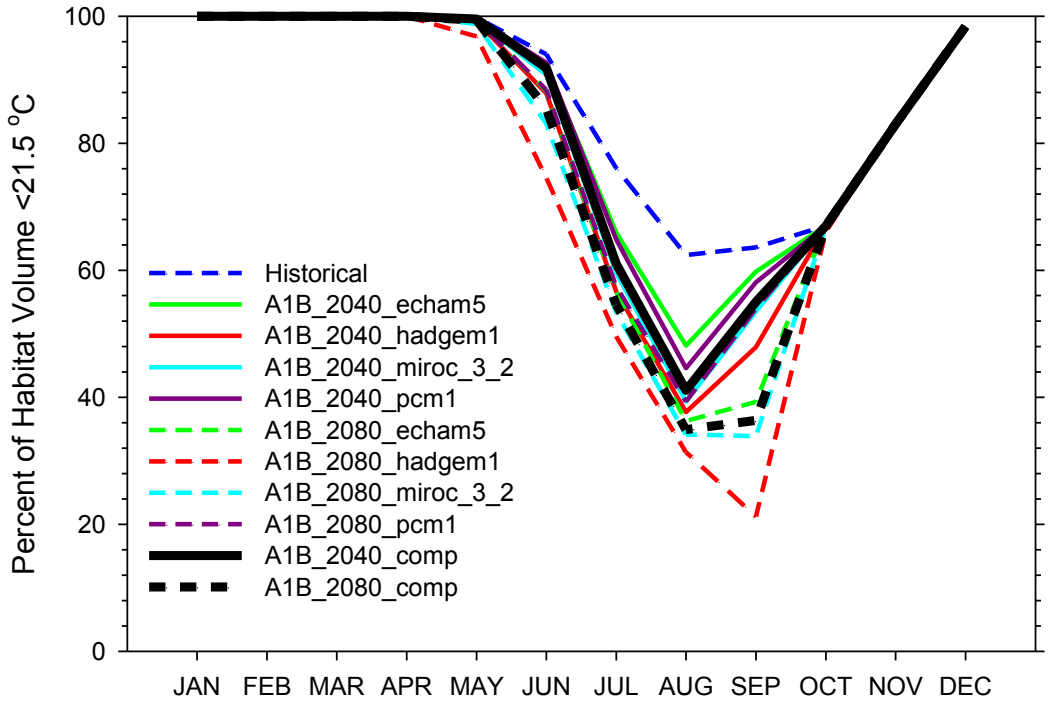

Figure 14. Monthly average salmonid habitat volume based on the eight years of output from the 3-D Lake Sammamish model and a 21.5 °C temperature threshold.

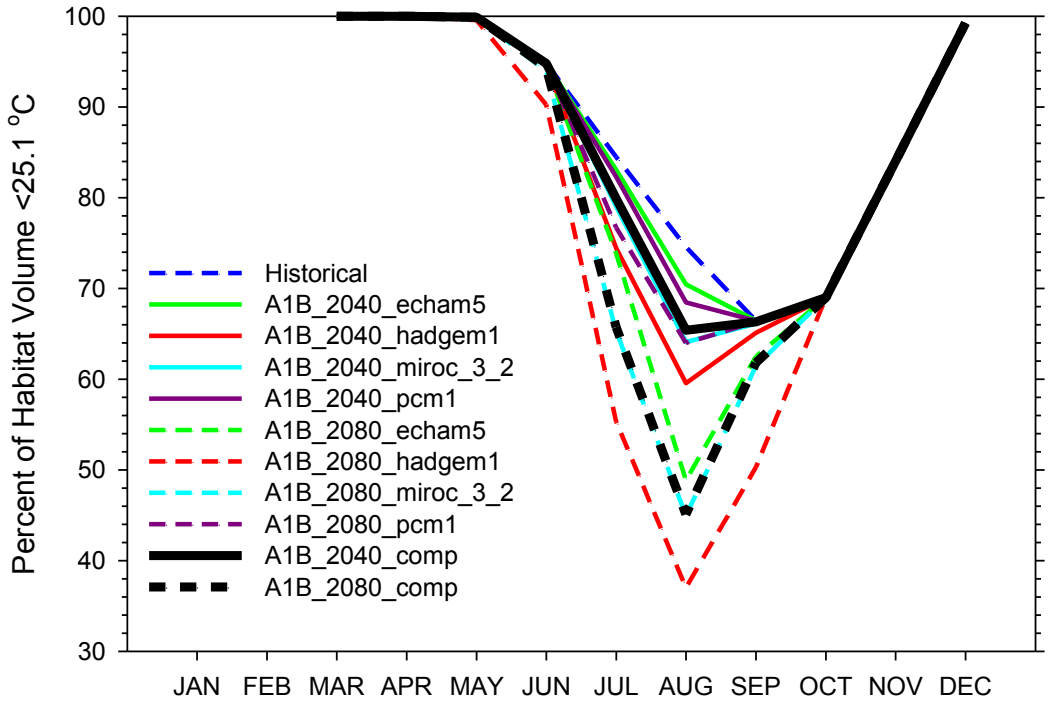

Figure 15. Monthly average salmonid habitat volume based on eight years of output from the 2-D Lake Sammamish model and a 25.1 °C temperature threshold.

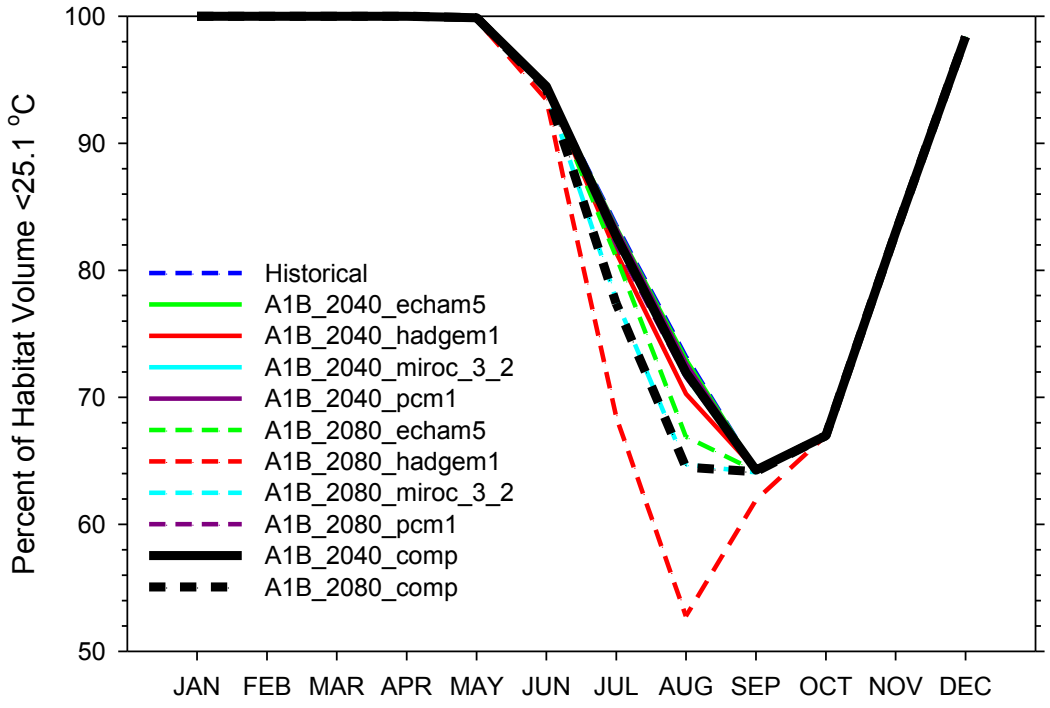

Figure 16. Monthly average salmonid habitat volume based on the eight years of output from the 3-D Lake Sammamish model and a 25.1 °C temperature threshold.

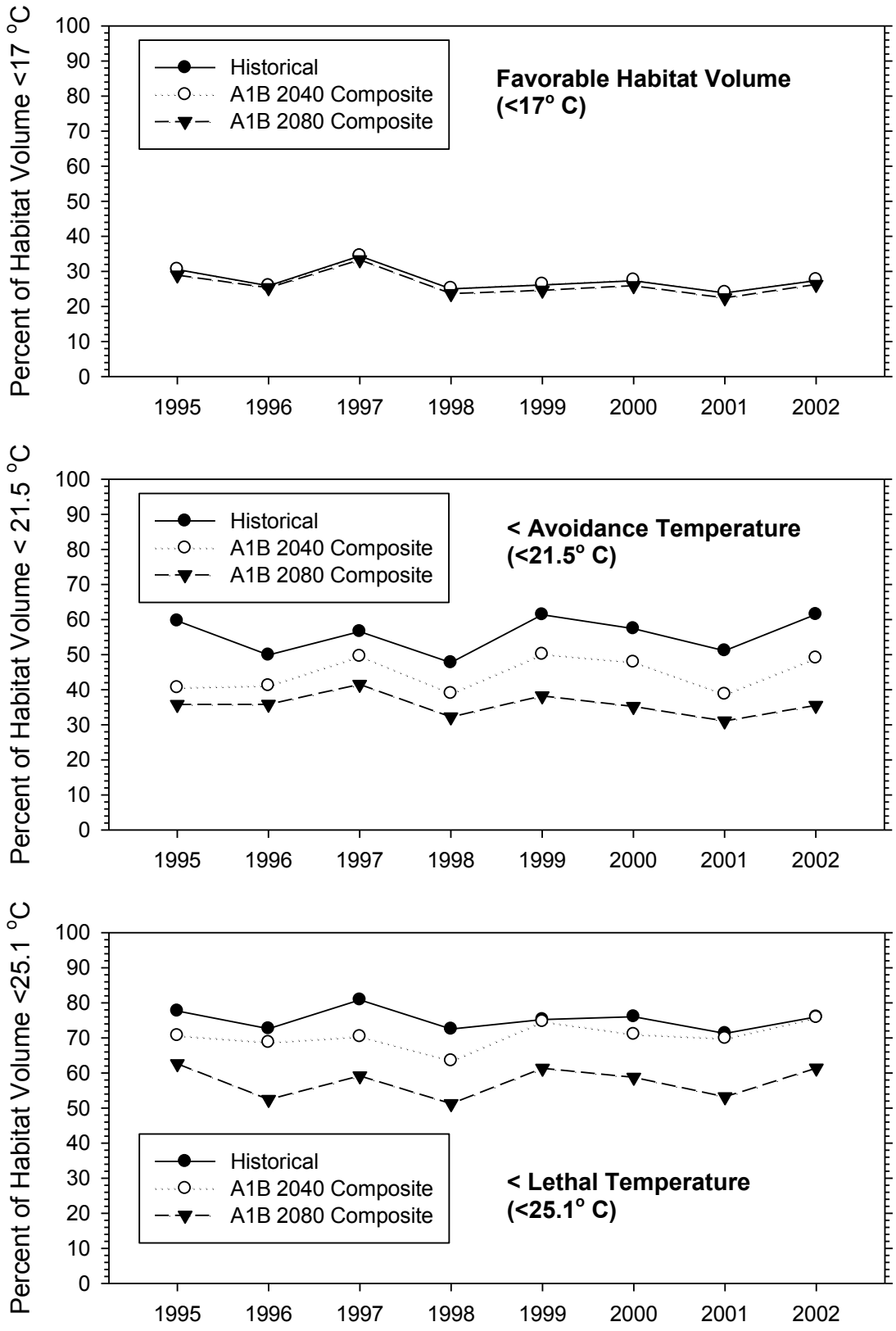

Figure 17. Annual average Jul-Sep salmonid habitat volume (in percent) based on output from the 2-D Lake Sammamish model for each of the three temperature thresholds.

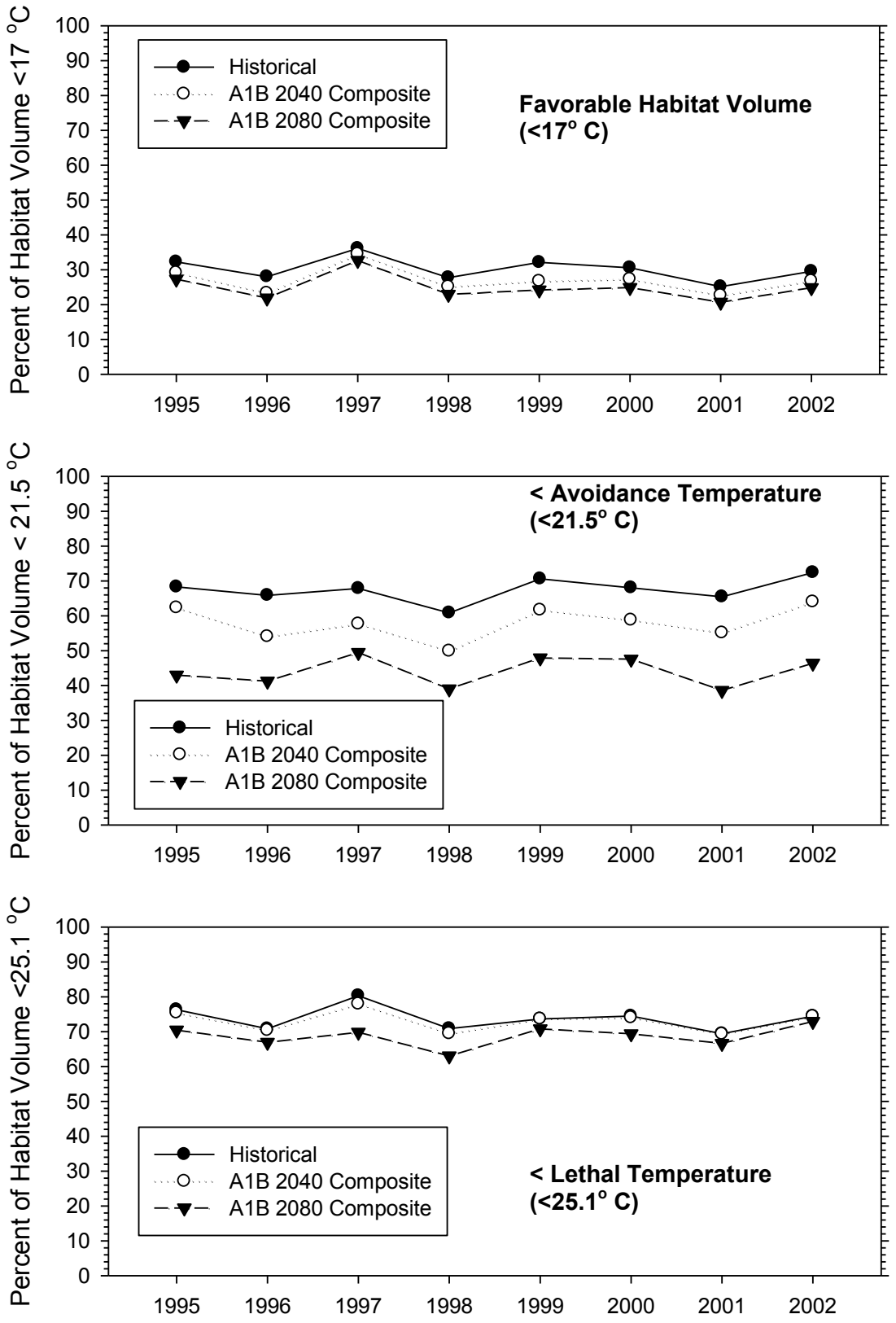

Figure 18. Annual average Jul-Sep salmonid habitat volume (in percent) based on output from the 3-D Lake Sammamish model for each of the three temperature thresholds.

3.2 Response of Threshold Isotherms

The 2-D and 3-D models predicted similar responses in the position of the three temperature thresholds plotted as isotherms (see Figure 19 through Figure 24 and figures in Appendix D). The predicted threshold isotherm responses were consistent with changes in habitat volume noted above. Note that the most significant shift in the position of the threshold isotherms occurs in the spring due to the predicted earlier onset of stratification (see section on lake stability below).

The 2-D and 3-D models were generally consistent in their prediction of the response of the 17 ^{o}C isotherm to warming (see Figure 19 and Figure 20). Generally, the 17 ^{o}C isotherm deepens in May and October and a smaller response in September, which is consistent with the response of favorable habitat volume to warming. The response of the 21.5 ^{o}C isotherm was also consistent with the associated habitat volume response with deepening of the 21.5 ^{o}C isotherm predicted from June to September (Figure 21 and Figure 22). The response of the 25.1 ^{o}C isotherm was equivocal between the two models, with more frequent occurrence and longer periods of elevated surface temperatures and more significant deepening of the 25.1 ^{o}C isotherm predicted in response to future warming by the 2-D model (Figure 23 and Figure 24).

Another way of illustrating the effect of a warming climate on lake istotherms is to look at a contour plot of the differences in temperature between any particular climate change scenario model run and the historical model simulation. Figure 25 presents three separate color contour plots of predicted lake temperature from 1995 to 2002 based on the 3-D model forced with Historical air temperature, A1B 2040 Composite air temperature and A1B 2080 Composite air temperature. Comparison of the three panels in Figure 25 illustrate that the model predicts much less warming in the hypolimnion with most of the warming occurring in the epilimnion. The epilimnion generally becomes warmer and warming extends over a longer period during the summer.

Figure 26 presents two color contour plot panels representing the difference between the 2040 and Historical (panel A) and between 2080 and Historical (panel B) temperature results to better illustrate the qualitative comparisons provided in Figure 25. Figure 26 indicates that the hypolimnion warms 1 ^{o}C or less by 2040 and no more than 2 ^{o}C by 2080. Warming in the epilimnion is predicted to be much more significant – up to 2 ^{o}C or more in 2040 with less warming occurring earlier and later in the year and as much as 4 ^{o}C warming by 2080 with less warming (on the order of 2.5 ^{o}C) occurring before and after the maximum summer water temperature increases.

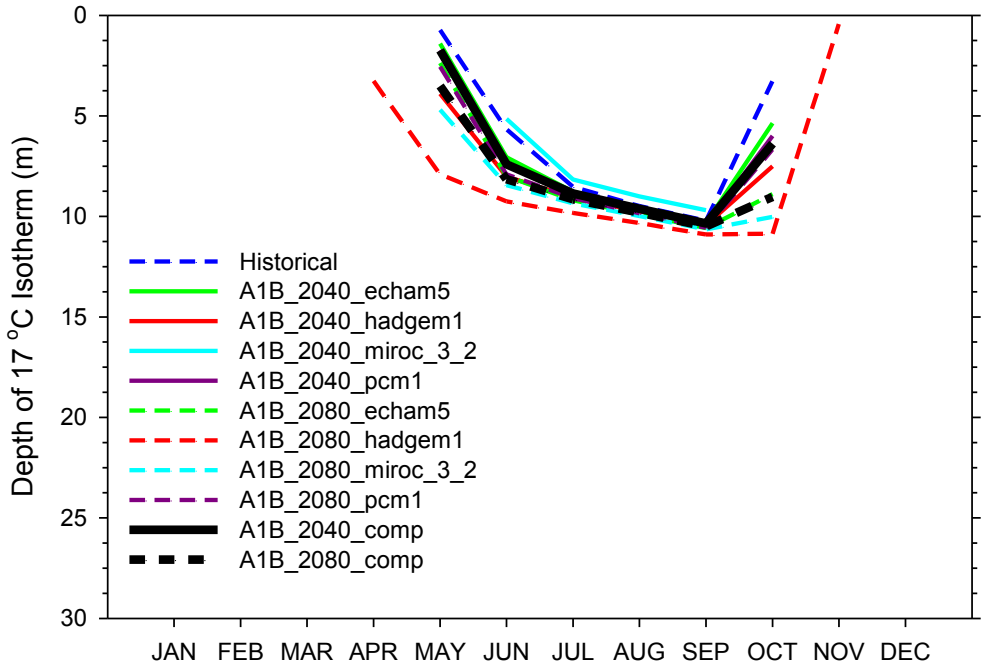

Figure 19. Monthly average 17 °C isotherms based on the eight years of output from the 2-D Lake Sammamish model.

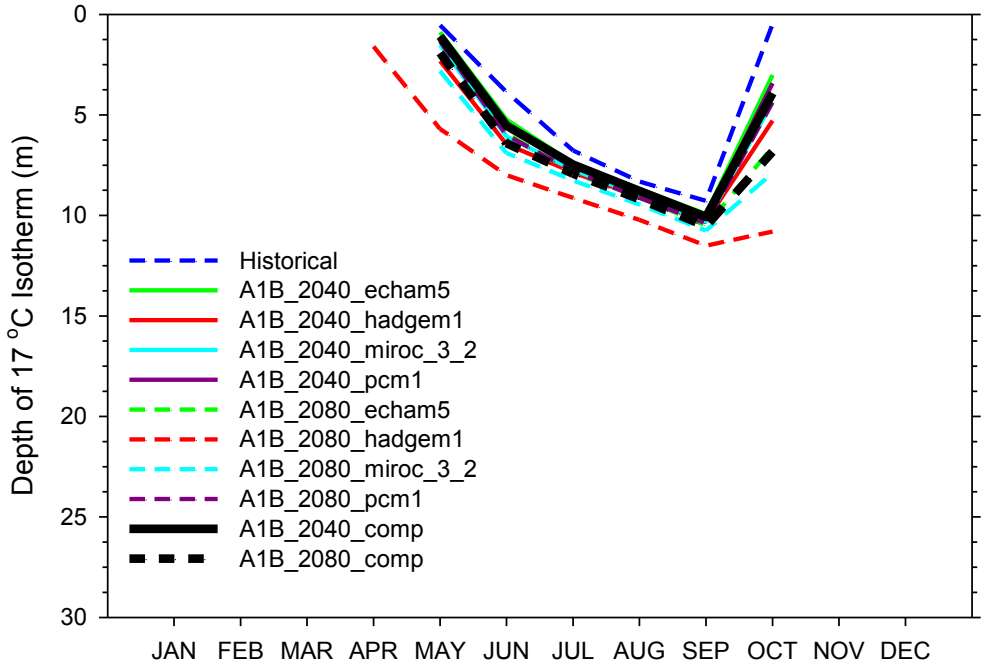

Figure 20. Monthly average 17 °C isotherms based on the eight years of output from the 3-D Lake Sammamish model.

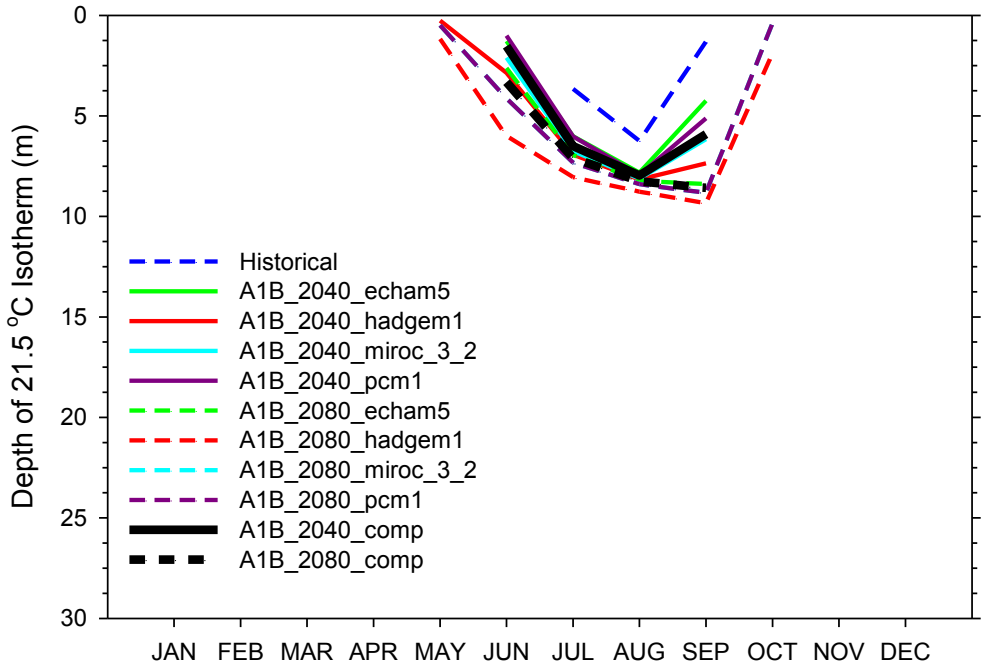

Figure 21. Monthly average 21.5 °C isotherms based on the eight years of output from the 2-D Lake Sammamish model.

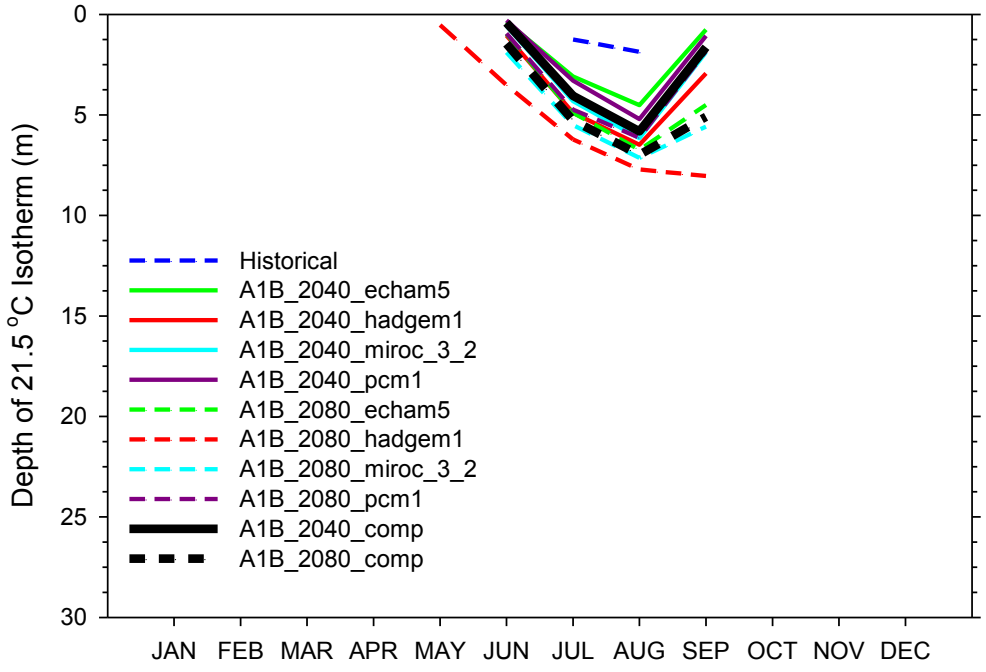

Figure 22. Monthly average 21.5 °C isotherms based on the eight years of output from the 3-D Lake Sammamish model.

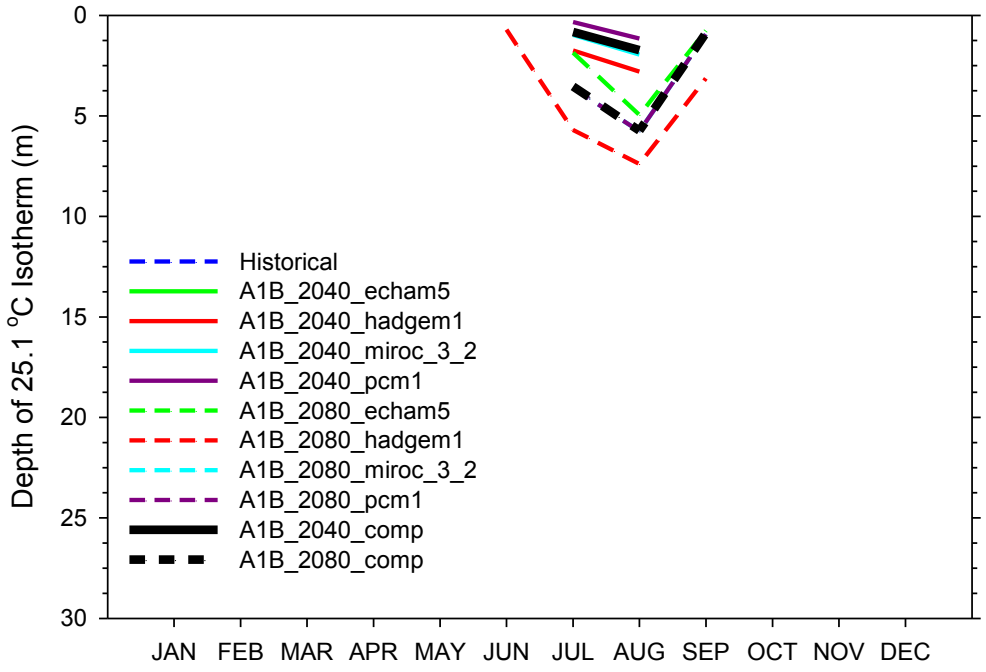

Figure 23. Monthly average 25.1 °C isotherms based on the eight years of output from the 2-D Lake Sammamish model.

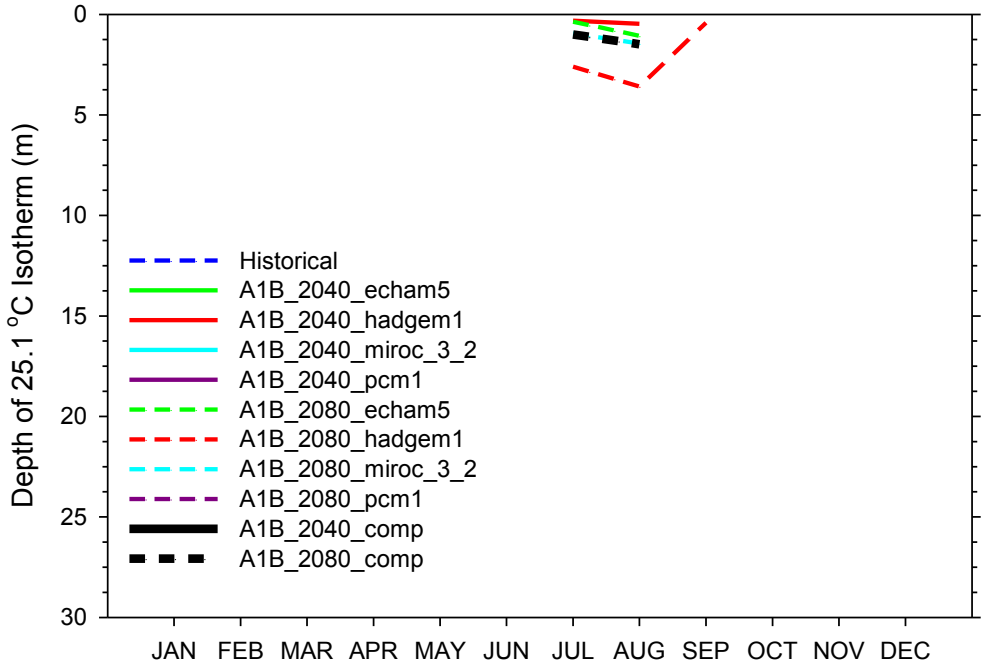

Figure 24. Monthly average 25.1 °C isotherms based on the eight years of output from the 3-D Lake Sammamish model.

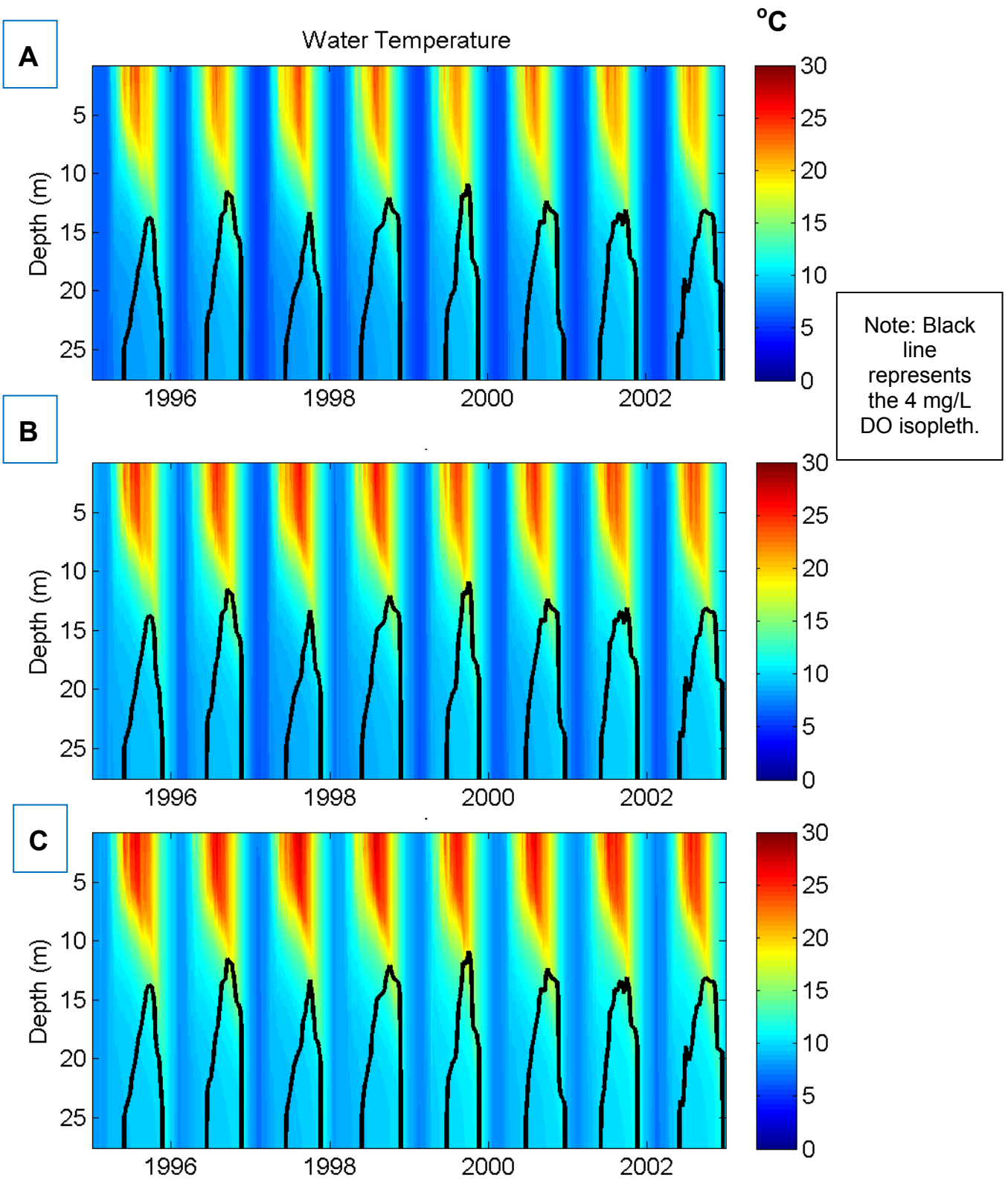

Figure 25. Color contour depth vs time (1995-2002) plots of lake temperature at the central lake station (0612) based on the 3-D model: (A) is the historical model run, (B) is the A1B Composite 2040 model run and (C) is the A1B Composite 2080 model run.

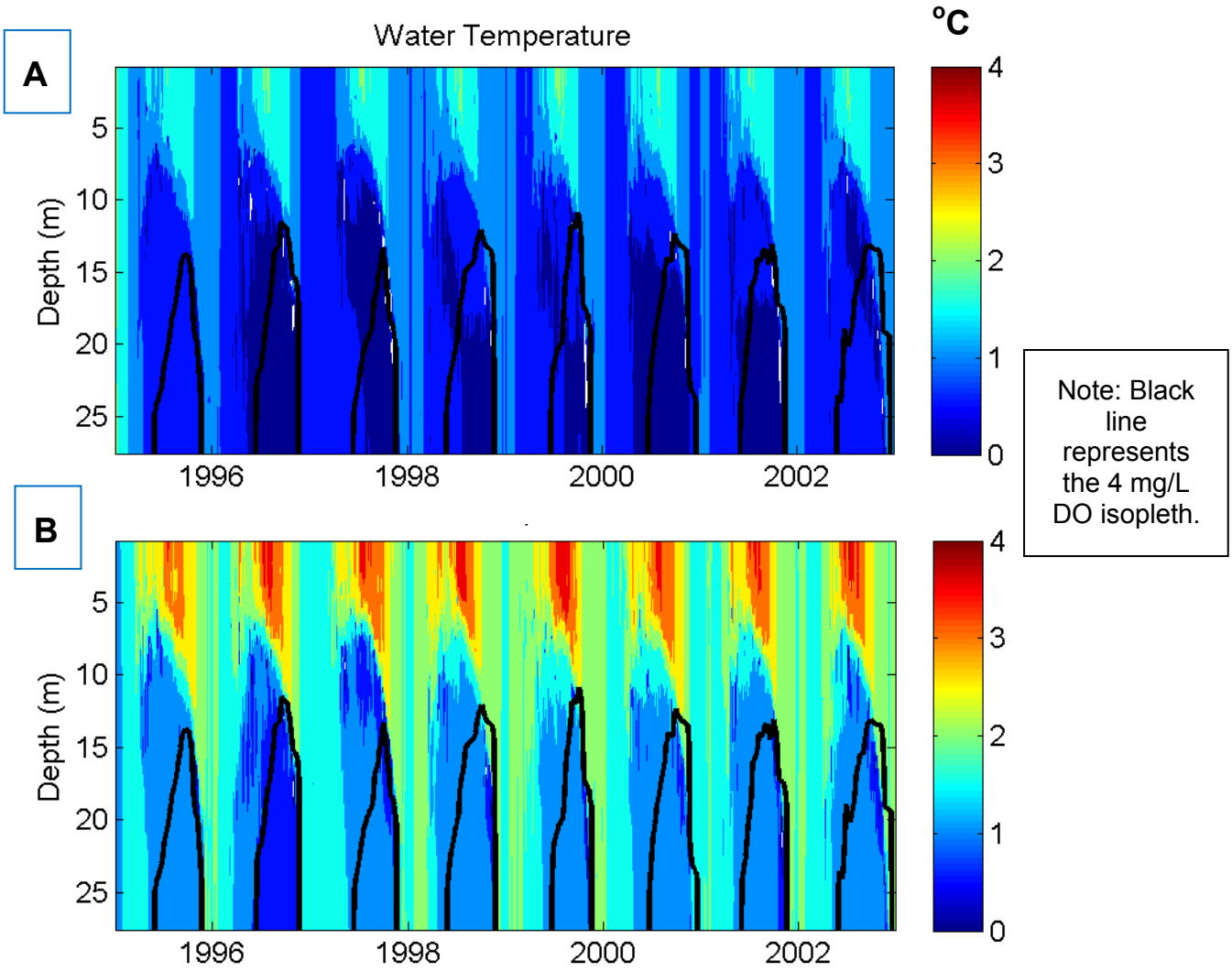

Figure 26. Color contour depth vs time (1995-2002) plots of the difference between climate model scenario and historical lake temperatures at the central lake station (0612) based on the 3-D model: (A) is the difference between A1B Composite 2040 and Historical and (B) is the difference between A1B Composite 2080 and Historical.

Note: Visually, panel A above represents the difference between panel B and A in Figure 25 and panel B above represents the difference between panel C and A in Figure 25.

3.3 Thermocline Depth

The 2-D and 3-D models predicted similar responses in the position of the depth of the thermocline (see Figure 27 and Figure 28 and figures in Appendix E). Note that the depth of the thermocline in summer doesn't shift substantially in response to warming, although thermoclines become established earlier in the spring under the warmer conditions predicted in the future.

To better illustrate the predicted response in the position of the depth of the thermocline during the critical July-September period for kokanee growth, the mean July-September thermocline depth was calculated for each model and climate scenario. In general, the thermocline depth is predicted to decline (i.e., to become shallower) in response to increasing air temperature (see Table 5and Table 6). Note that this conclusion is contingent on there being no significant changes in wind over the lake. Although there is a relatively high level of confidence that local air temperatures will increase in the future, there is much less certainty in projected changes in other climate variables like local wind speed and direction.

In general, expected decrease in the depth of the thermocline based on the 2-D model ranged from 0.18 to 0.6 m by 2040 and 0.26 to 0.55 m by 2080 (Table 5). The reductions predicted by the 3-D model were slightly smaller; 0.05 to 0.24 m by 2040 and 0.03 to 0.37 m by 2080. Because the routine lake profiling does not always sample temperature at meter intervals through the thermocline, changes of this magnitude would be difficult to detect.

Table 5. Average Jul-Sep thermocline depths predicted by the 2-D Lake Sammamish model at the central lake station (0612).

	Hist	2040	2080	Hist-2040	Hist-2080
Scenario	Depth (m)			Delta (m)	
Composite	9.41	9.06	8.86	-0.36	-0.55
ECHAM5	9.41	9.19	8.94	-0.22	-0.47
HadGEM1	9.41	9.09	9.12	-0.32	-0.29
MIROC 3.2	9.41	9.17	9.01	-0.25	-0.40
PCM1	9.41	9.23	9.15	-0.18	-0.26

Table 6. Average Jul-Sep thermocline depths predicted by the 3-D Lake Sammamish model at the central lake station (0612).

	Hist	2040	2080	Hist-2040	Hist-2080
Scenario	Depth (m)			Delta (m)	
Composite	8.65	8.41	8.28	-0.24	-0.37
ECHAM5	8.65	8.60	8.31	-0.05	-0.34
HadGEM1	8.65	8.48	8.45	-0.17	-0.20
MIROC 3.2	8.65	8.53	8.43	-0.12	-0.23
PCM1	8.65	8.51	8.62	-0.14	-0.03

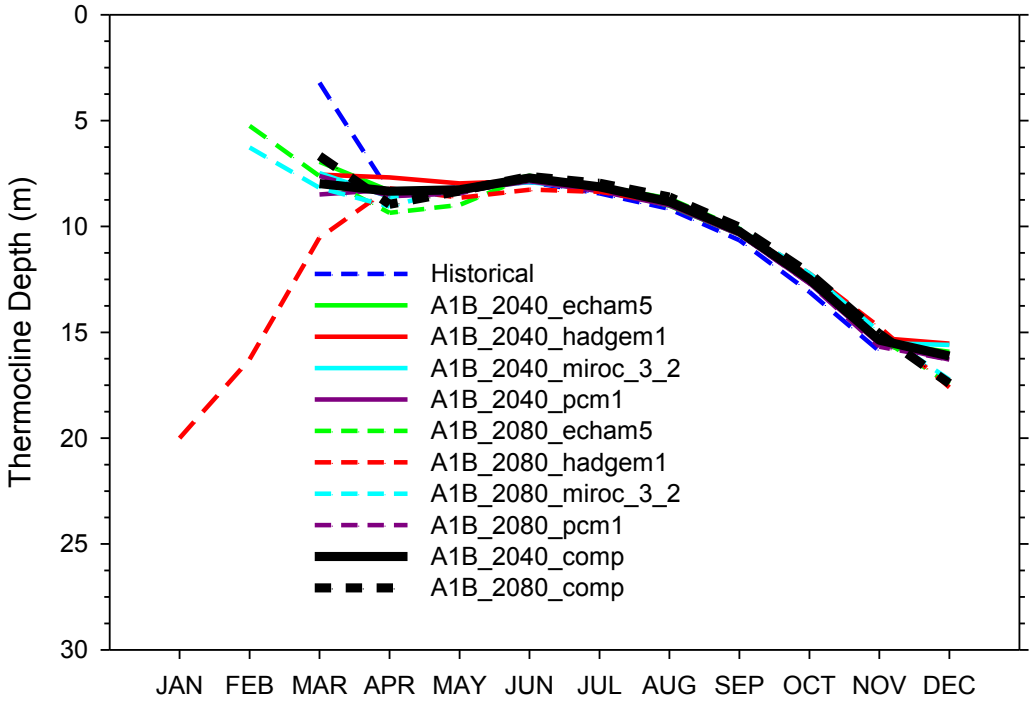

Figure 27. Monthly average thermocline depths based on the eight years of output from the 2-D Lake Sammamish model.

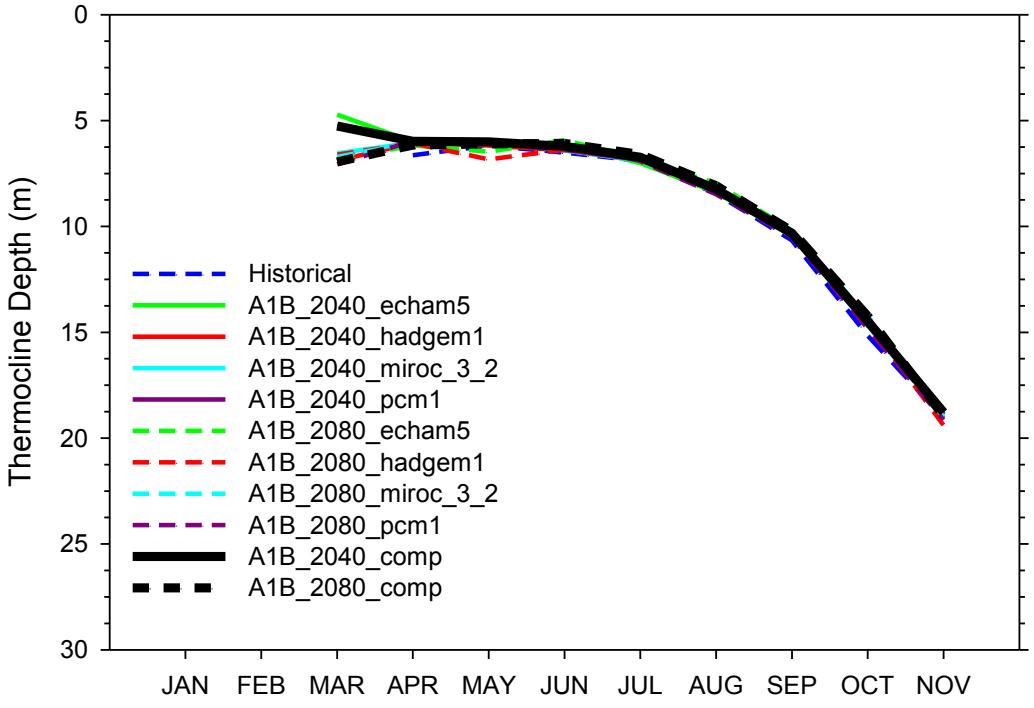

Figure 28. Monthly averaged thermocline depths based on the eight years of output from the 3-D Lake Sammamish model.

3.4 Schmidt Stability

The 2-D and 3-D models predicted similar responses in Schmidt stability, although the 2-D model predicts somewhat higher stability for any comparable 3-D model run (see Figure 29 and Figure 30 and figures in Appendix F). The models consistently predict that earlier stratification is expected with warming along with smaller extensions of the late summer stratification period (see Table 7 and Table 8). Note that the figures illustrating the monthly average Schmidt Stability for each model scenario include a vertical line representing the stability threshold of 50 J m^{-2} used to identify the onset and end of stratification (Figure 29 and Figure 30).

Based on the 2-D model, the onset of stratification is predicted to advance 7 days on average by 2040 and 23 days by 2080 (Table 7). The 3-D model on average predicted slightly smaller advances of 6 and 16 days by 2040 and 2080, respectively (Table 8). The average date of destratfication was predicted to occur later; the 2-D model predicted an average delay of 10 and 16 days and the 3-D model predicted a smaller delay of 6 and 9 days by 2040 and 2080, respectively. The earlier onset and delayed end of the stratification period translated into a predicted extension of the stratified period in the future. The 2-D model predicted an average extension of 17 and 39 days by 2040 and 2080, respectively (Table 7). The 3-D model predicted an average extension of 12 and 25 day by 2040 and 2080, respectively.

Earlier stratification of Lake Washington in response to warming over the last few decades has been documented by Winder and Schindler (2004) who estimated that the timing of stratification advanced by more than 20 days over the period 1962 to 2002. The shift in the timing of thermal stratification was shown to have cascading effects on the lake ecosystem. The spring diatom bloom occurred earlier in conjunction with the timing of stratification, but the timing of the appearance of *Daphnia* that depends on the spring diatom bloom as a food resource did not shift resulting in a long-term decline in the *Daphnia* population, with potential consequences for upper trophic levels (Winder and Schindler 2004).

A similar shift in the timing of stratification likely occurred over the same time period in Lake Sammamish, but reliable lake temperature records over that period are not available for Lake Sammamish – reliable routine lake temperature profiling did not begin until 1993. Lake Sammamish also does not have the long-term detailed records of phytoplankton and zooplankton biomass with which to evaluate retrospectively how climate change has already affected Lake Sammamish.

In addition to the relatively straightforward effect of decreasing oxygen solubility with increasing temperatures, there is also a potential for increasing lake stability and longer duration of stratification to affect the duration and magnitude of hypoxia in the hypolimnion of Lake Sammamish during the summer. A recent study of historical lake temperature and DO data collected on Lake Zurich suggested that recent climate warming resulted in a decrease in hypolimnetic oxygen and an increase in soluble reactive phosphorus released from anoxic bottom sediments (North et al. 2013).

Table 7. Comparison of historical and climate model scenario average (2040 and 2080) stratification metrics derived from Schmidt stability calculated from the 2-D Lake Sammamish model output from the central lake station (0612).

Metric	Historical	2040	2080
Onset date of stratification	8-Apr (98)	31-Mar (91)	15-Mar (75)
Date of destratification	17-Nov (321)	26-Nov (331)	2-Dec (337)
Duration of stratification (days)	223	240	262
Maximum Schmidt stability (J m^{-2})	1,187	1,394	1,573

Table 8. Comparison of historical and climate model scenario average (2040 and 2080) stratification metrics derived from Schmidt stability calculated from the 3-D Lake Sammamish model output from the central lake station (0612).

Metric	Historical	2040	2080
Onset date of stratification	11-Apr (102)	6-Apr (96)	27-Mar (86)
Date of destratification	10-Nov (315)	16-Nov (321)	20-Nov (324)
Duration of stratification (days)	213	225	238
Maximum Schmidt stability (J m^{-2})	1,025	1,201	1,344

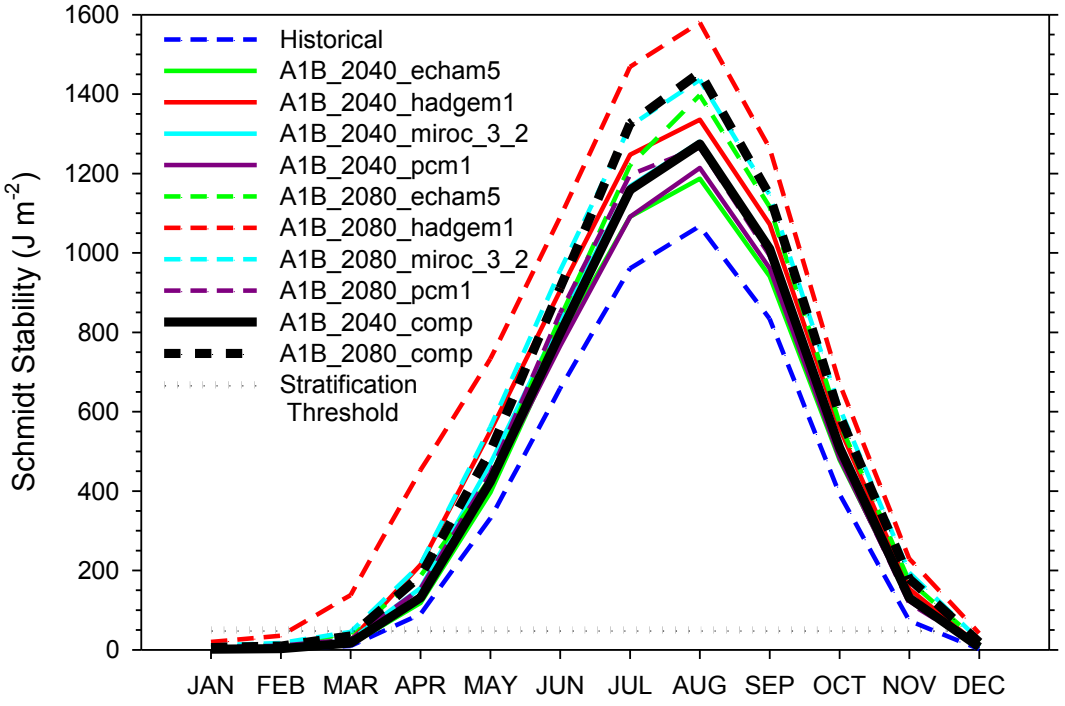

Figure 29. Monthly average Schmidt stability based on the eight years of output from the 2-D Lake Sammamish model.

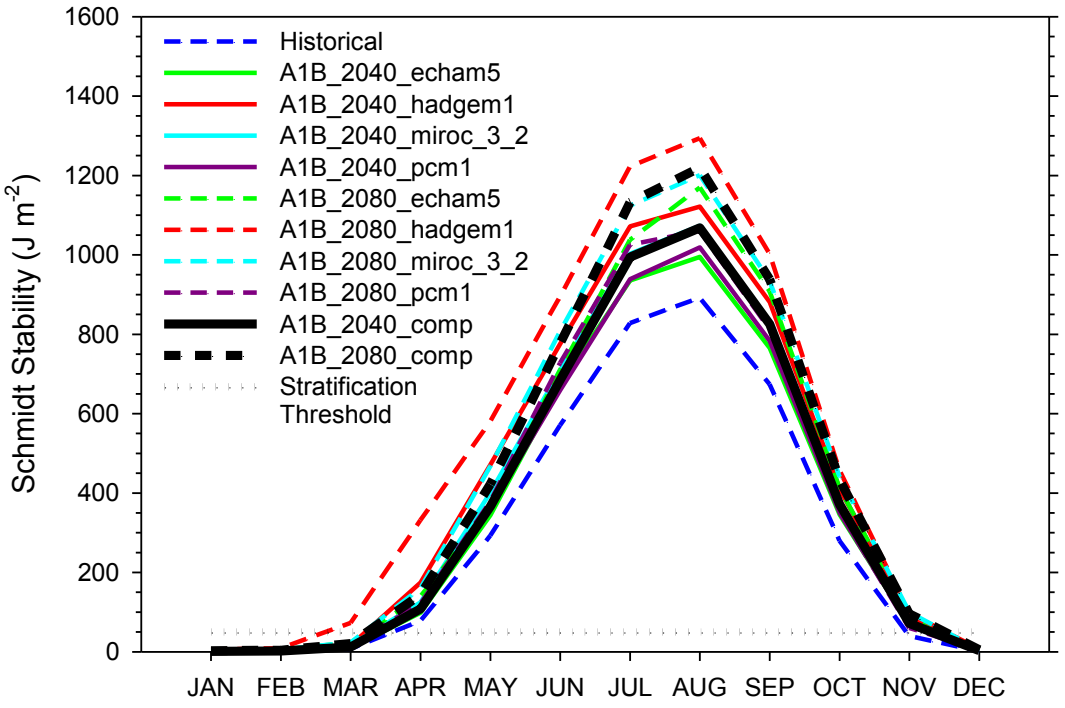

Figure 30. Monthly average Schmidt stability based on the eight years of output from the 3-D Lake Sammamish model.

4.0. CONCLUSIONS AND RECOMMENDATIONS

The 2-D and 3-D lake temperature models were generally consistent in their predictions in the response of Lake Sammamish to future warming of the local climate. Overall, the available habitat for kokanee is predicted to decline in response to warming. The declines are due to projected warming throughout the lake, but with a disproportionate amount of warming predicted to occur in the surface layer in summer. The decline in habitat volume also results from earlier onset of stratification and a delay in destratification, which results in an extension of the period that the lake is stratified during the summer. The earlier onset of stratification results in warmer surface waters in the spring than would have occurred historically. The lake is also predicted to become much more thermally stable (i.e., more strongly stratified) under future warmer conditions.

How increased lake stability and extension of the period of stratification will affect hypolimnetic oxygen concentrations was not addressed in this study, but it is likely that the estimates presented here may be optimistic if in fact increasing lake stability and an extended period of stratification leads to earlier declines in hypolimnetic DO concentrations.

Based on the results of this study, a few recommendations are made with the intent to further refine the understanding of potential effects of climate change on Lake Sammamish kokanee habitat:

- Develop 1-dimensional model to facilitate continuous long-term climate change simulations to better capture long-term natural variability
- Incorporate effect of climate change on watershed inputs to the lake (starting with tributary temperatures and flows)
- Develop additional water quality modeling capability starting initially with a simple 1-dimensional model capable of reproducing seasonal variation in phytoplankton biomass, nutrients and DO
- Identify relationships between inter-annual variation in temperature, dissolved oxygen and numbers of kokanee using available observed data and current condition modeling results.

5.0. REFERENCES

Arhonditsis, G.B. and M.T. Brett. 2004. Evaluation of the current state of mechanistic aquatic biogeochemical modeling. *Marine Ecology Progress Series* 271:13-26

Battin, J., M.W. Wiley, M.H. Ruckelshaus, R.N. Palmer, E. Korb, K.K. Bartz and H. Imaki. 2007. Projected impacts of climate change on salmon habitat restoration. *Proceedings of the National Academy of Sciences of the United States of America*. 104:6720-6725.

Berge, H. B. 2009. Effects of a temperature-oxygen squeeze on distribution, feeding, growth, and survival of kokanee (Oncorhynchus nerka) in Lake Sammamish, Washington. Master's Thesis, School of Aquatic and Fisheries Sciences, University of Washington. 84 p.

Berge, H. B. and K. Higgins. 2003. The current status of Kokanee in the greater Lake Washington watershed. King County Department of Natural Resources and Parks, Water and Land resources Division, Seattle, WA.

Birch, P.B., R.S. Barnes, and D.E. Spyridakis. 1980. Recent sedimentation and its relationship with primary productivity in four western Washington lakes. *Limnology and Oceanography* 25:240-247.

Blenckner, T. 2008. Models as tools for understanding past, recent and future changes in large lakes. Hydrobiologia 599:177-182.

Cerco, C.F. and T.M. Cole. 1993. Three-dimensional eutrophication model of Chesapeake Bay. *Journal of Environmental Engineering* 119:1006-1025.

Cerco, C.F., M.R. Noel and S.-C. Kim. 2006. Three-dimensional management model for Lake Washington, Part II: Eutrophication modeling and skill assessment. *Lake and Reservoir Management* 22:115-131.

Cole, T.M. and S.A. Wells. 2006. CE-QUAL-W2: A two-dimensional laterally averaged, hydrodynamic and water quality model, version 3.5. Instruction Report EL-06-1, U.S. Army Engineering and Research Development Center, Vicksburg, MS.

De Stasio, B.T., D.K. Hill, J.M. Kleinhans, N.P. Nibbelink and J.J. Magnuson. 1996. Potential effects of global climate change on small north-temperate lakes: Physics, fish, and plankton. *Limnology and Oceanography* 41:1136-1149.

Edinger, J.E. and E.M. Buchak. 1975. A hydrodynamic, two-dimensional reservoir model: The computational basis. Prepared for U.S. Army Corps of Engineer Division, Ohio River, Cincinnati, OH.

Edmondson, W.T. 1968. Water quality management and lake eutrophication: the Lake Washington case. pp. 139-178. In: Water Resources Management and Public Policy. T.H. Campbell and R.O. Sylvester, eds. University of Washington Press, Seattle, WA.

Edmondson, W.T. 1969. Eutrophication in North America. pp. 129-149. In: Eutrophication: Causes, consequences, correctives. Nat. Acad. Sci./Nat. Res. Council. Publication 1700.

Edmondson, W.T. 1994. Sixty years of Lake Washington: A Curriculum Vitae. *Lake and Reservoir Management* 10:75-84.

Environmental and Hydraulic Laboratory. 1986. CE-QUAL-W2: A numerical two-dimensional laterally-averaged model of hydrodynamics and water quality: User's manual. Instruction Report E-86-S. U.S. Army Engineer Waterways Experiment Station, Vicksburg, MS.

Fish, E.R. 1967. The Past at Present. Kingsport Press, Inc., Kingsport, TN.

Griffiths, J.R. Griffiths, D.E. Schindler, L.S. Balistrieri and G.T. Ruggerone. 2011. Effects of simultaneous climate change and geomorphic evolution on thermal characteristics of a shallow Alaskan lake. *Limnology and Oceanography* 56:193-205.

Isaac, G.W., R.I. Matsuda, and J.R. Welker. 1966. A limnological investigation of water quality conditions in Lake Sammamish. Water Quality Series No. 2, Municipality of Metropolitan Seattle, Seattle, WA.

Jackson, C. 2010. Lake Sammamish late-run kokanee spawning ground survey summary and escapement estimate. Washington Department of Fish and Wildlife, Fish Management Division, Region 2, Fish Program.

Jackson, C. 2010. Lake Sammamish Late-Run Kokanee Spawning Ground Survey Summary and Escapement Estiamte. Washington Department of Fish and Wildlife, Fish Management Division-Region 2 Fish Program, Olympia, WA.

Johnson, B.H., and S.-C. Kim. 2004. User's Guide for CH3D-Z with Lake Washington as an Example. Prepared for King County Department of Natural Resources and Parks, Seattle, WA. U.S. Army Corps of Engineers, Engineer Research and Development Center, Vicksburg, MS.

Johnson, B.H., S.-C. Kim, and G.H. Nail. 2003. A Three-Dimensional Hydrodynamic and Temperature Model of Lake Washington. Prepared for King County Department of Natural Resources and Parks, Seattle, WA. U.S. Army Corps of Engineers, Engineer Research and Development Center, Vicksburg, MS.

Kim, S.-C., C.F. Cerco and B.H. Johnson. 2006. Three-dimensional management model for Lake Washington, Part I: Introduction and hydrodynamic modeling. *Lake and Reservoir Management* 22:103-114.

King County. 2003. King County Watershed Modeling Services – Green River Water Quality Assessment, and Sammamish-Washington Analysis and Modeling Program Watershed Modeling Calibration Report. In Progress. Prepared by Aqua Terra Consultants in conjunction with King County Water and Land Resources Division, Seattle, WA. http://www.kingcounty.gov/environment/watersheds/green-river/watershed-quality-assessment.aspx (see documents below Modeling heading)

King County. 2008. Development of a 3-dimensional hydrodynamic model of Lake Sammamish. Prepared by Curtis DeGasperi, Water and Land Resources Division. Seattle, Washington. http://www.kingcounty.gov/environment/waterandland/lakes/lakes-of-king-county/sammamish/3D-hydrodynamic-model-lake-sammamish.aspx

King County. 2009. Development of a laterally averaged 2-dimensional water quality model of the Sammamish River. Prepared by Curtis DeGasperi, Water and Land Resources Division. Seattle, Washington. http://green.kingcounty.gov/WLR/Waterres/StreamsData/reports/Sammamish-river-report.aspx

Lake Sammamish Kokanee Work Group. 2010. Conservation Supplementation Plan for Lake Sammamish Late-run (Winter-run) Kokanee.

Lazoff, S. 1980. Deposition of diatoms and biogenic silica as indicators of Lake Sammamish productivity. M.S. thesis. University of Washington, Seattle, WA.

Littell, J.S., M.M. Elsner, G. S. Mauger, E. Lutz, A.F. Hamlet, and E. Salathé. 2011. Regional Climate and Hydrologic Change in the Northern US Rockies and Pacific Northwest: Internally Consistent Projections of Future Climate for Resource Management. Project report: April 17, 2011. Latest version online at: http://cses.washington.edu/picea/USFS/pub/Littell_etal_2010/

Livingstone, D.M. 2003. Impact of secular climate change on the thermal structure of a large temperature center European lake. *Climatic Change* 57:205-225.

North, R.P., R.L. North, D.M. Livingstone, O. Köster and R. Kipfer. 2013. Long-term changes in hypoxia and soluble reactive phosphorus in the hypolimnion of a large temperate lake: consequences of a climate regime shift. *Global Change Biology* doi: 10.1111/gcb.12371.

Pfeifer, B. 1995. Decision document for the management and restoration of indigenous Kokanee of the Lake Sammamish/Sammamish River basins with special emphasis on the Issaquah Creek stock. Washington Department of Fish and Wildlife, Inland Fisheries Division, Mill Creek.

Read, J.S., D.P. Hamilton, I.D. Jones, K. Muraoka, L. Winslow, R. Kroiss, C.H. Wu and E. Gaiser. 2011. Derivation of lake mixing and stratification indices from high-resolution lake buoy data. *Environmental Modeling & Software* 26:1325-1336.

Schindler, D.W. 1997. Widespread effects of climatic warming on freshwater ecosystems in North America. *Hydrological Processes* 11:1043-1067.

Stefan, H.G., M. Hondzo, X. Fang, J.G. Eaton and J.H. McCormick. 1996. Simulated long-term temperature and dissolved oxygen characteristics of lakes in the north-central United States and associated fish habitat limits. *Limnology and Oceanography* 41:1124-1135.

Taner, M.Ü., J.N. Carleton and M. Wellman. 2011. Integrated model projections of climate change impacts on a North American lake. *Ecological Modelling* 222:3380-3393.

Welch, E.B. 1977. Nutrient diversion: Resulting lake trophic state and phosphorus dynamics. EPA-600/3-77-003. Corvallis Environmental Research Laboratory, Office of Research and Development, U.S. Environmental Protection Agency, Corvallis, OR.

Welch, E.B. 1985. The eventual recovery of Lake Sammamish following phosphorus diversion. J. Water Pollut. Control Fed. 57:977-978.

Welch, E.B., C.A. Rock, R.C. Howe, and M.A. Perkins. 1980. Lake Sammamish response to wastewater diversion and increasing urban runoff. *Water Research* 14:821-828.

Welch, E.B., D.E. Spyridakis, J.I. Shuster, and R.R. Horner. 1986. Declining lake sediment phosphorus release and oxygen deficit following wastewater diversion. J. Water Pollut. Control Fed. 58:92-96.

Welch, E.B., T. Weiderholm, D.E. Spyridakis, and C.A. Rock. 1975. Nutrient loading and trophic state of Lake Sammamish, Washington. Prepared for Organization for Economic, Co-operation and Development (OECD) North America Project. Department of Civil Engineering, University of Washington, Seattle, WA.

Winder, M. and D.E. Schindler. 2004. Climatic effects on the phenology of lake processes. *Global Change Biology* 10:1844-1856.

Appendix A

2-D Model Calibration Figures for Station 0612

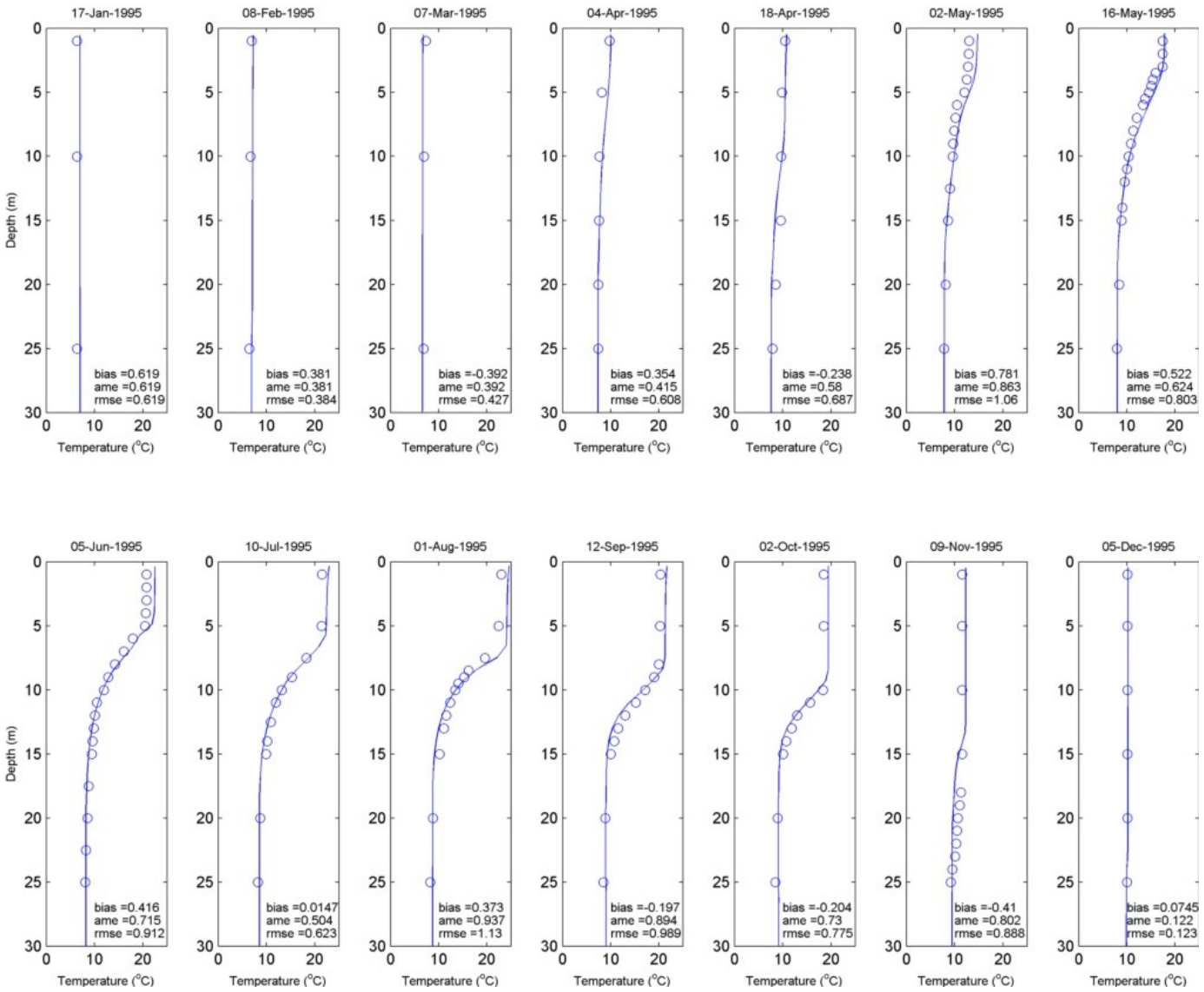

Figure 31. 2-D model (solid lines) vs. observed (open circles) temperature profiles – Station 0612, 1995.

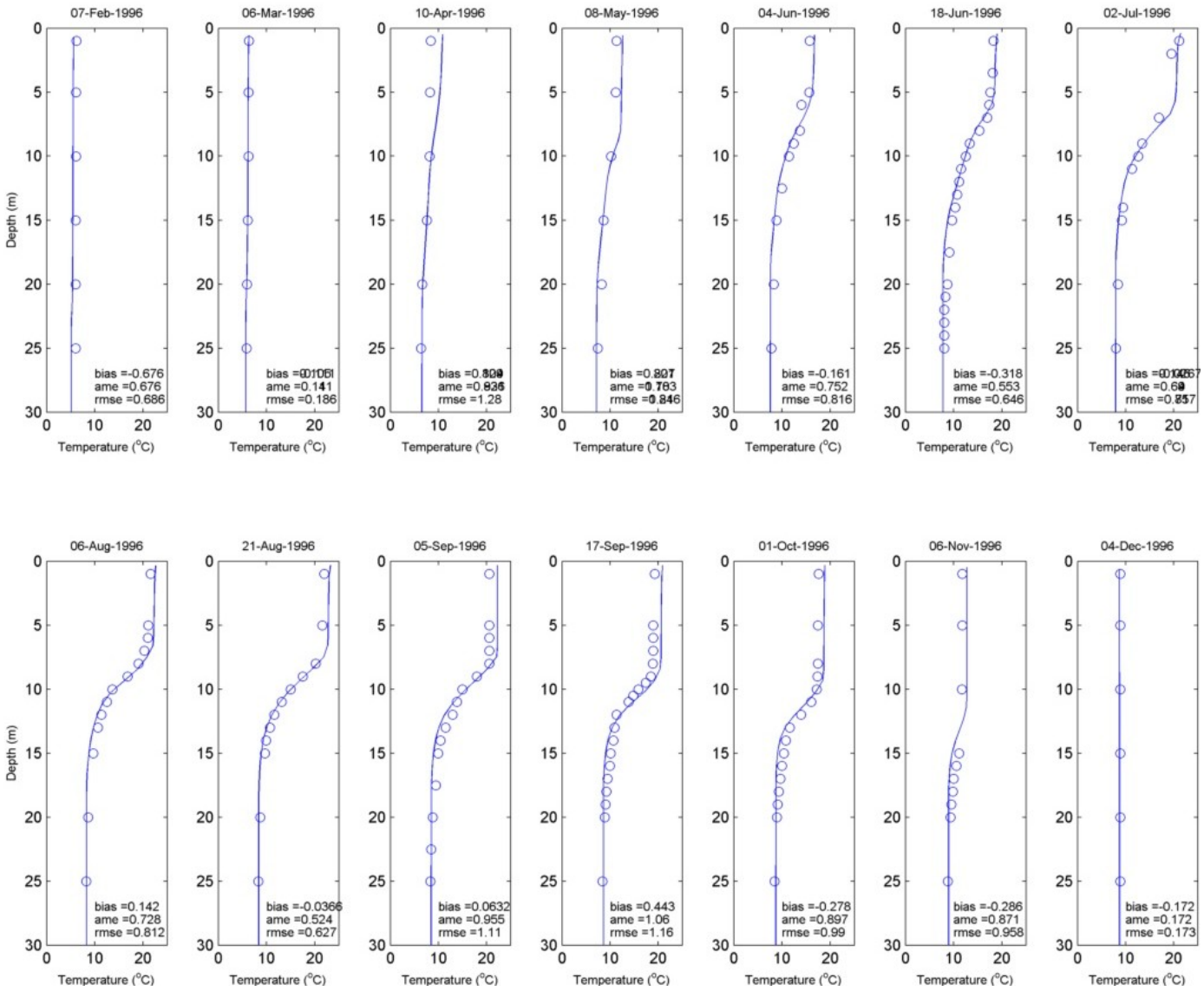

Figure 32. 2-D model (solid lines) vs. observed (open circles) temperature profiles – Station 0612, 1996.

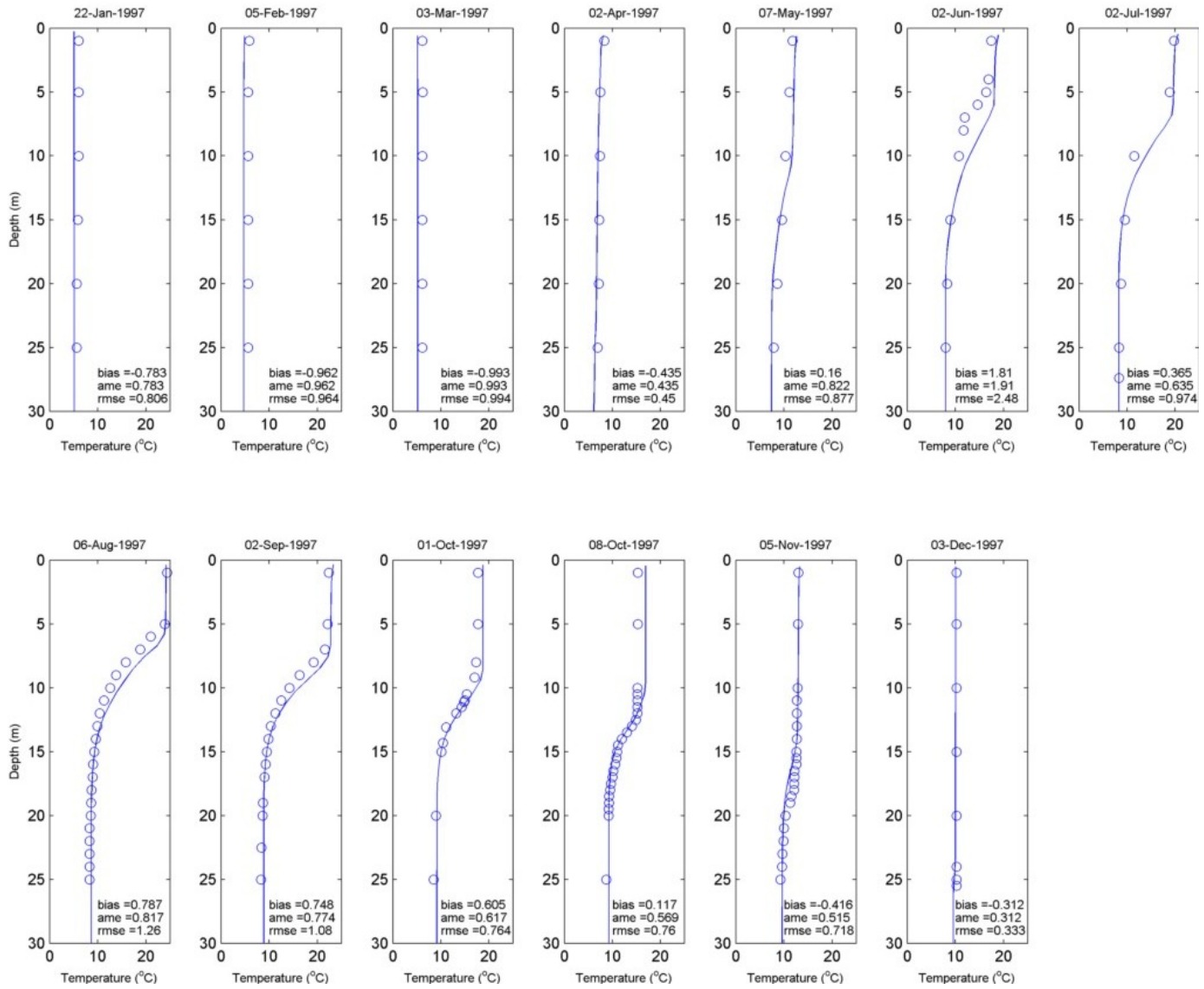

Figure 33. 2-D model (solid lines) vs. observed (open circles) temperature profiles – Station 0612, 1997.

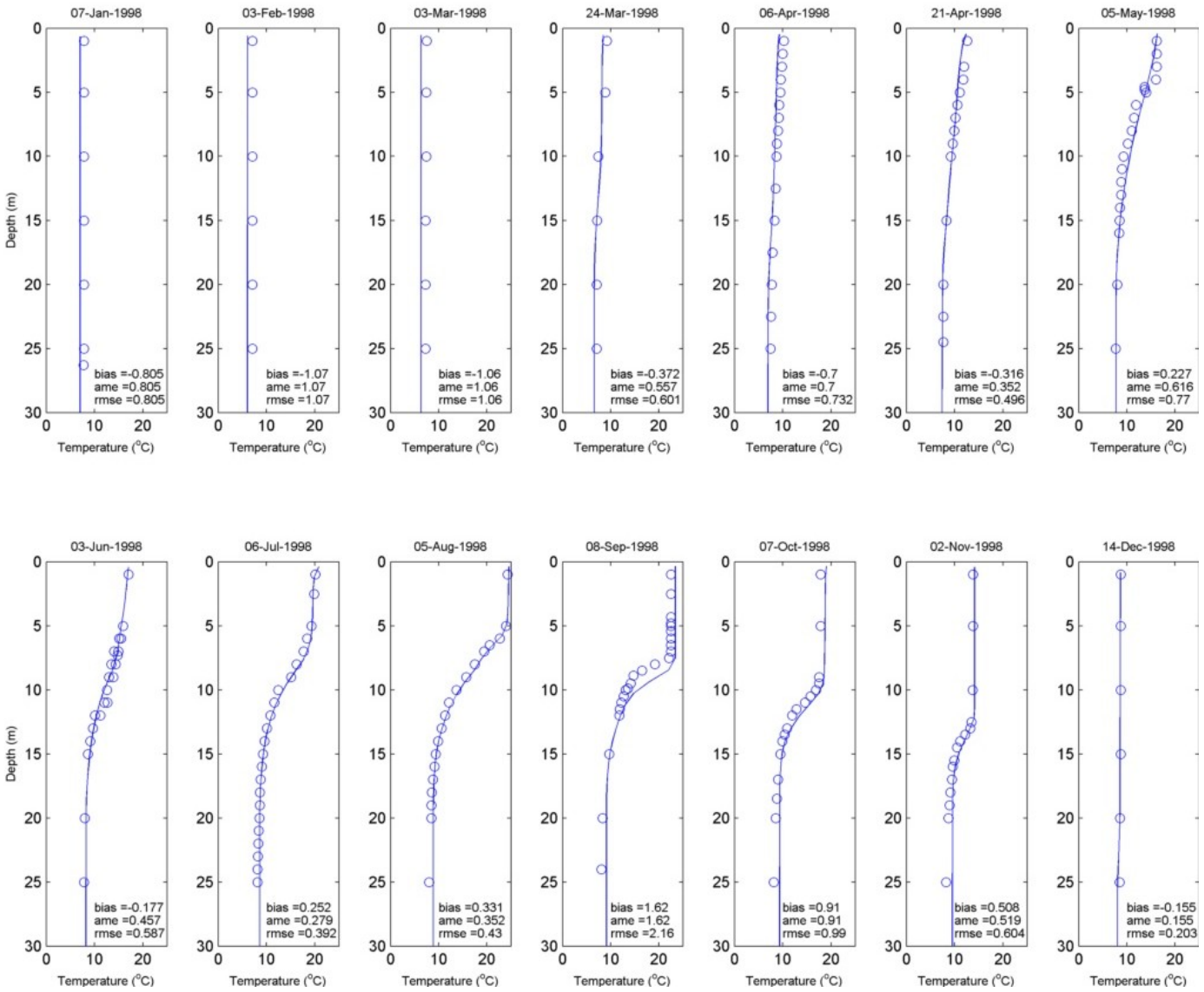

Figure 34. 2-D model (solid lines) vs. observed (open circles) temperature profiles – Station 0612, 1998.

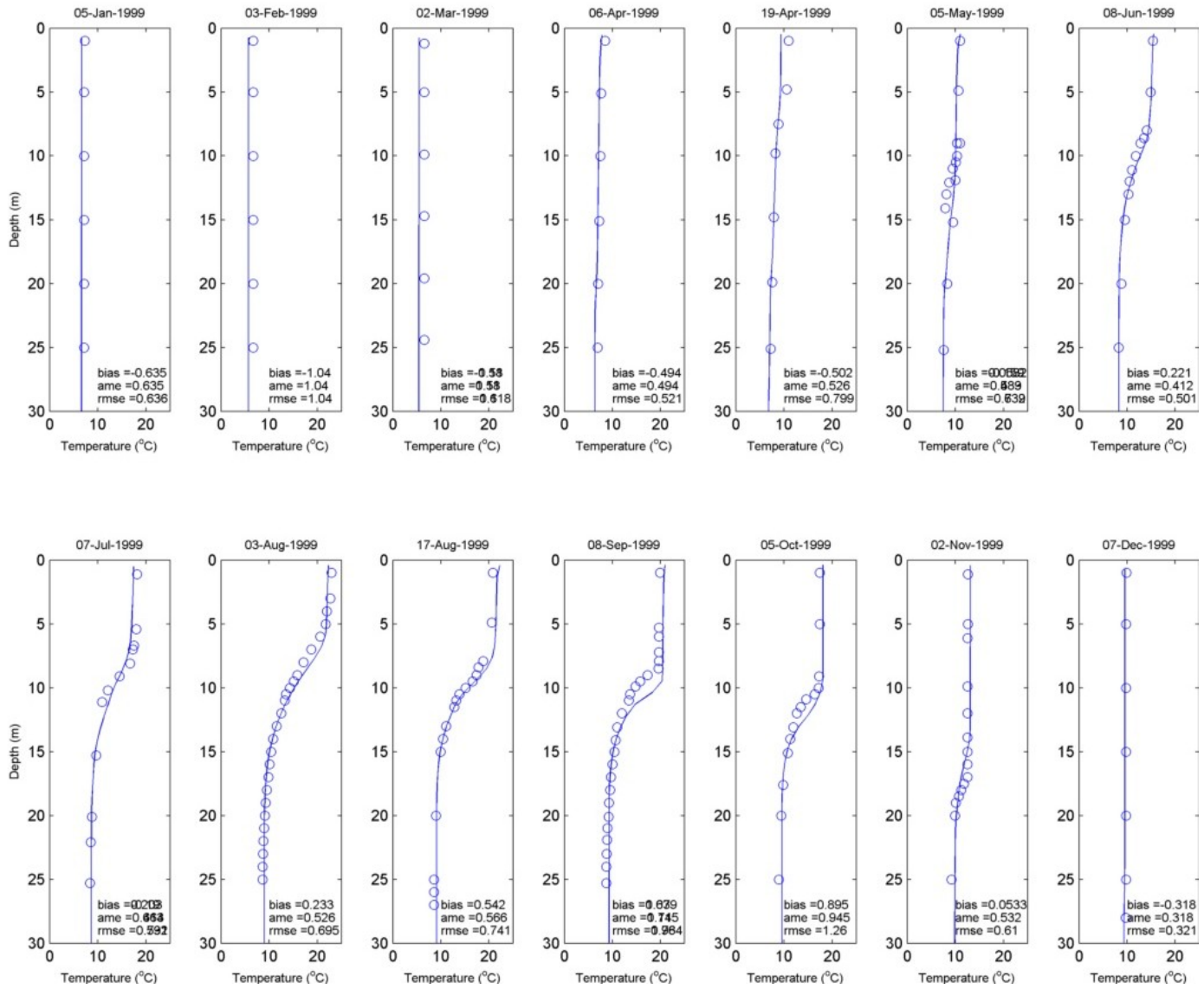

Figure 35. 2-D model (solid lines) vs. observed (open circles) temperature profiles – Station 0612, 1999.

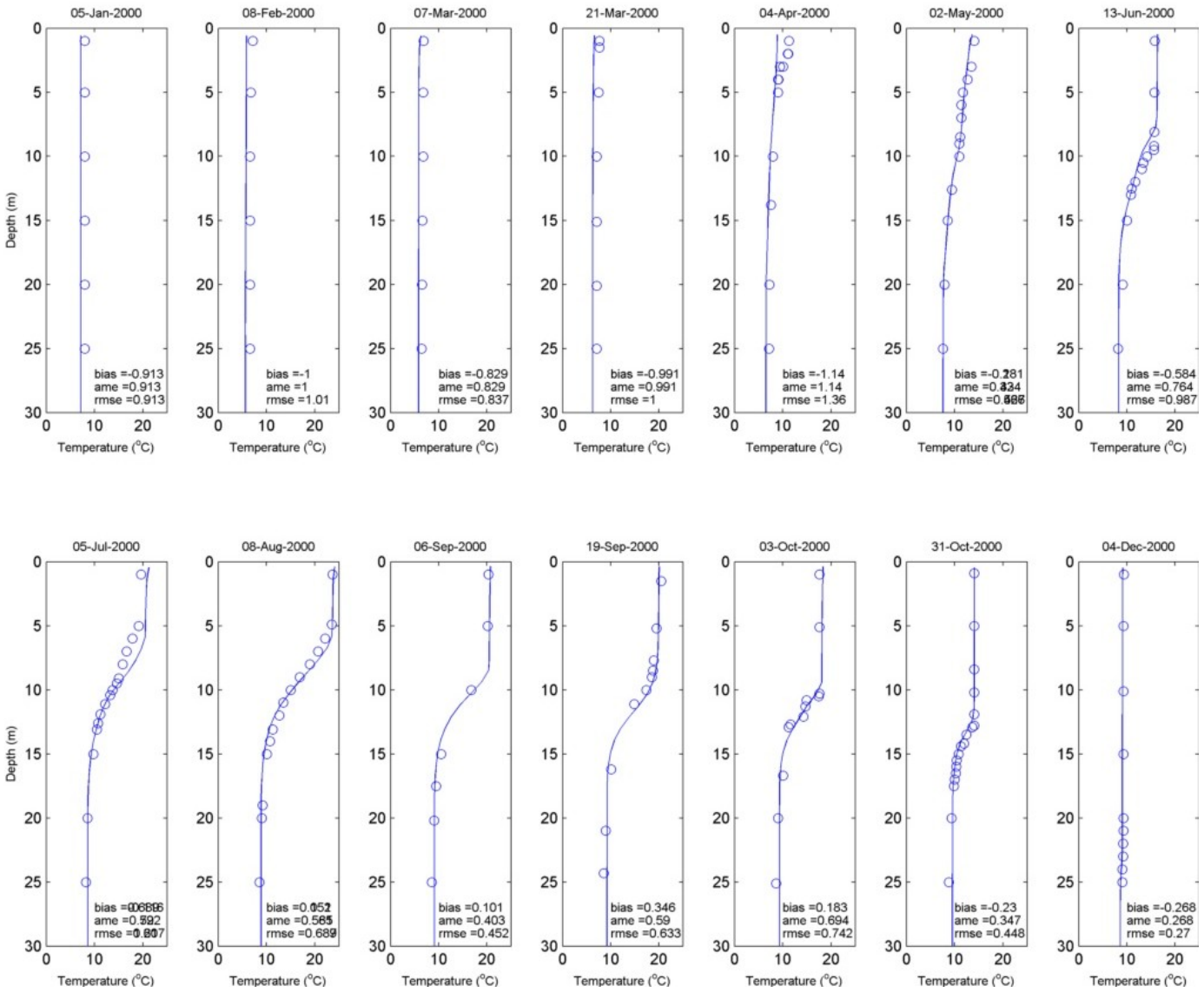

Figure 36. 2-D model (solid lines) vs. observed (open circles) temperature profiles – Station 0612, 2000.

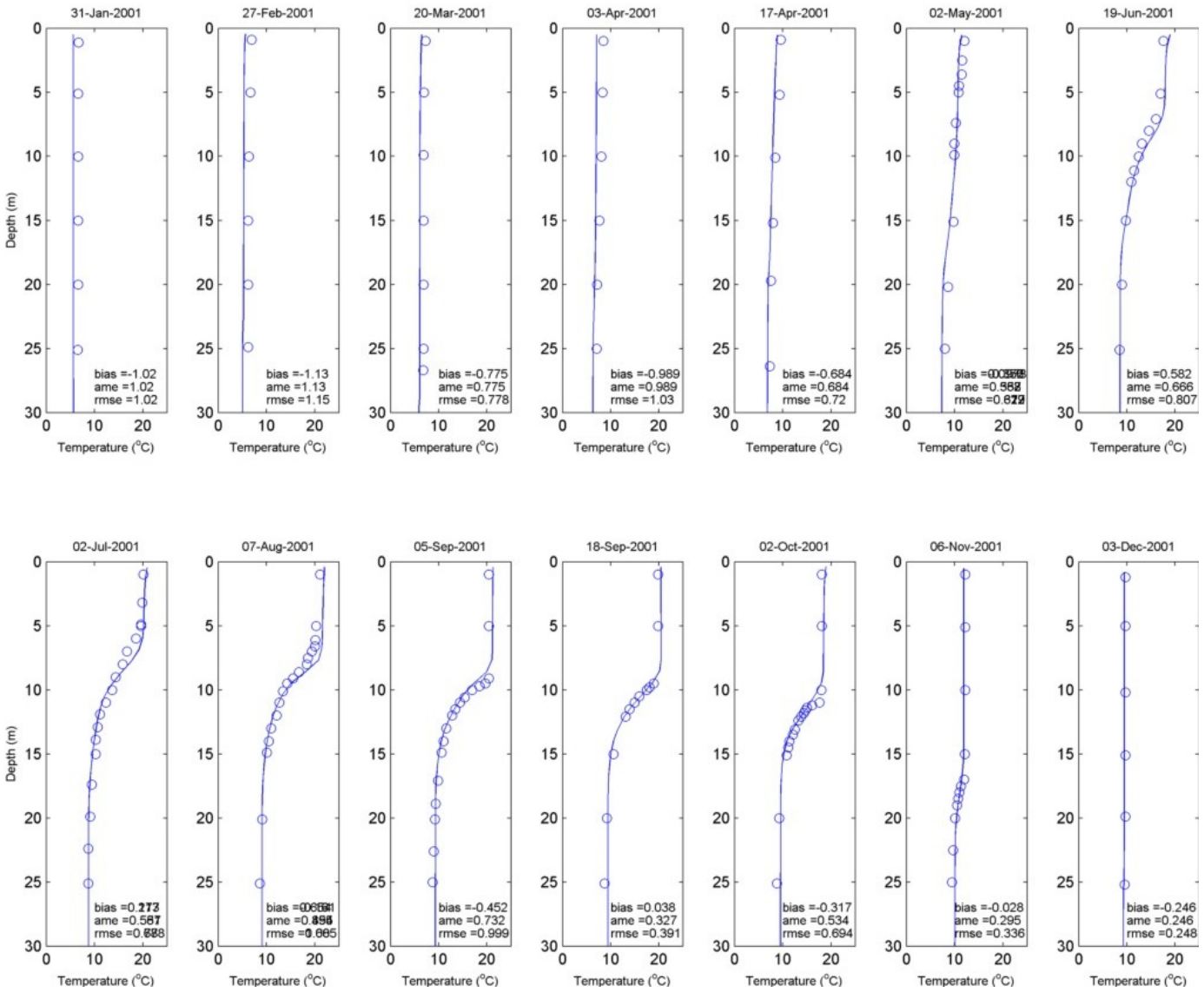

Figure 37. 2-D model (solid lines) vs. observed (open circles) temperature profiles – Station 0612, 2001.

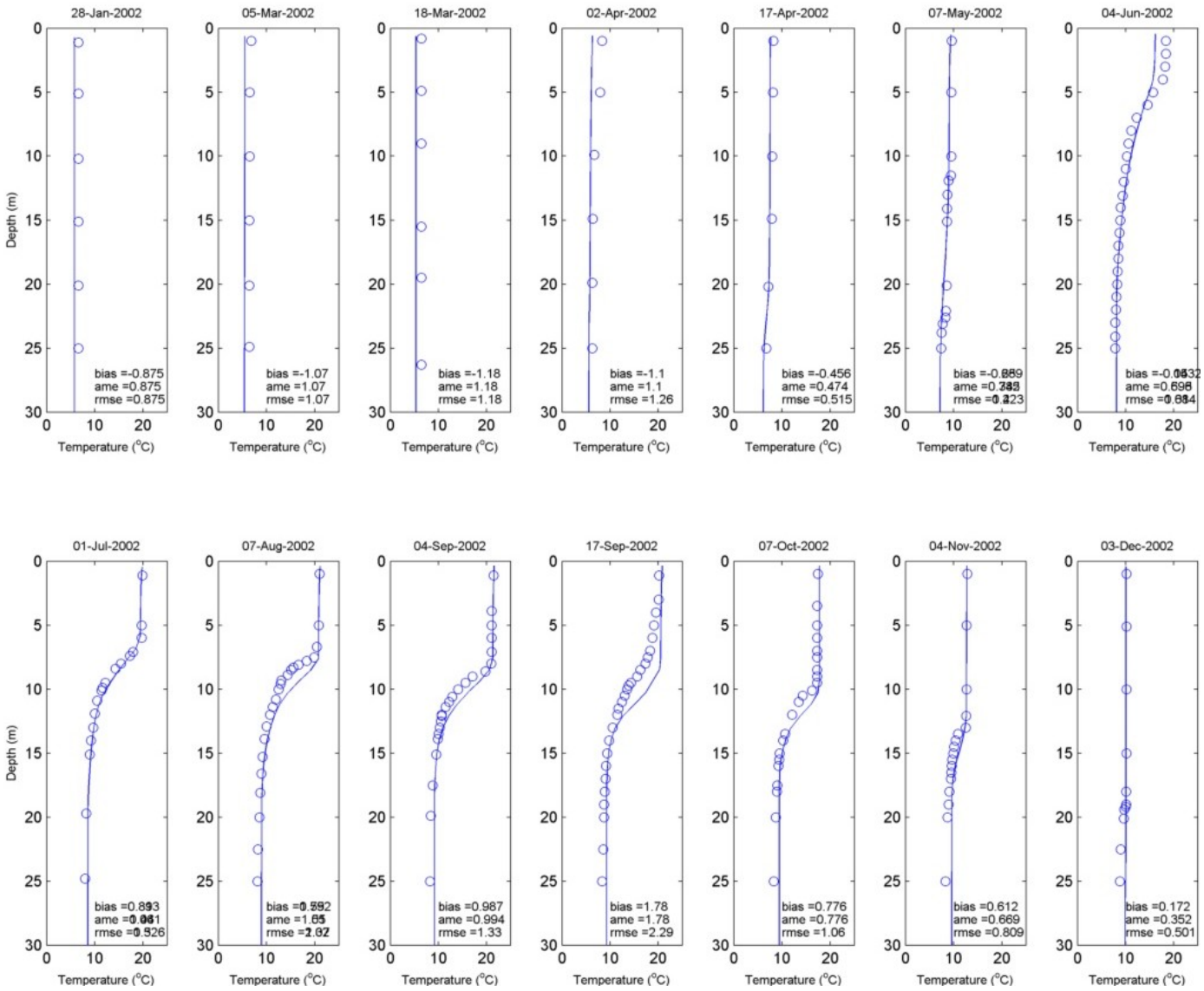

Figure 38. 2-D model (solid lines) vs. observed (open circles) temperature profiles – Station 0612, 2002.

Appendix B

3-D Model Calibration Figures for Station 0612

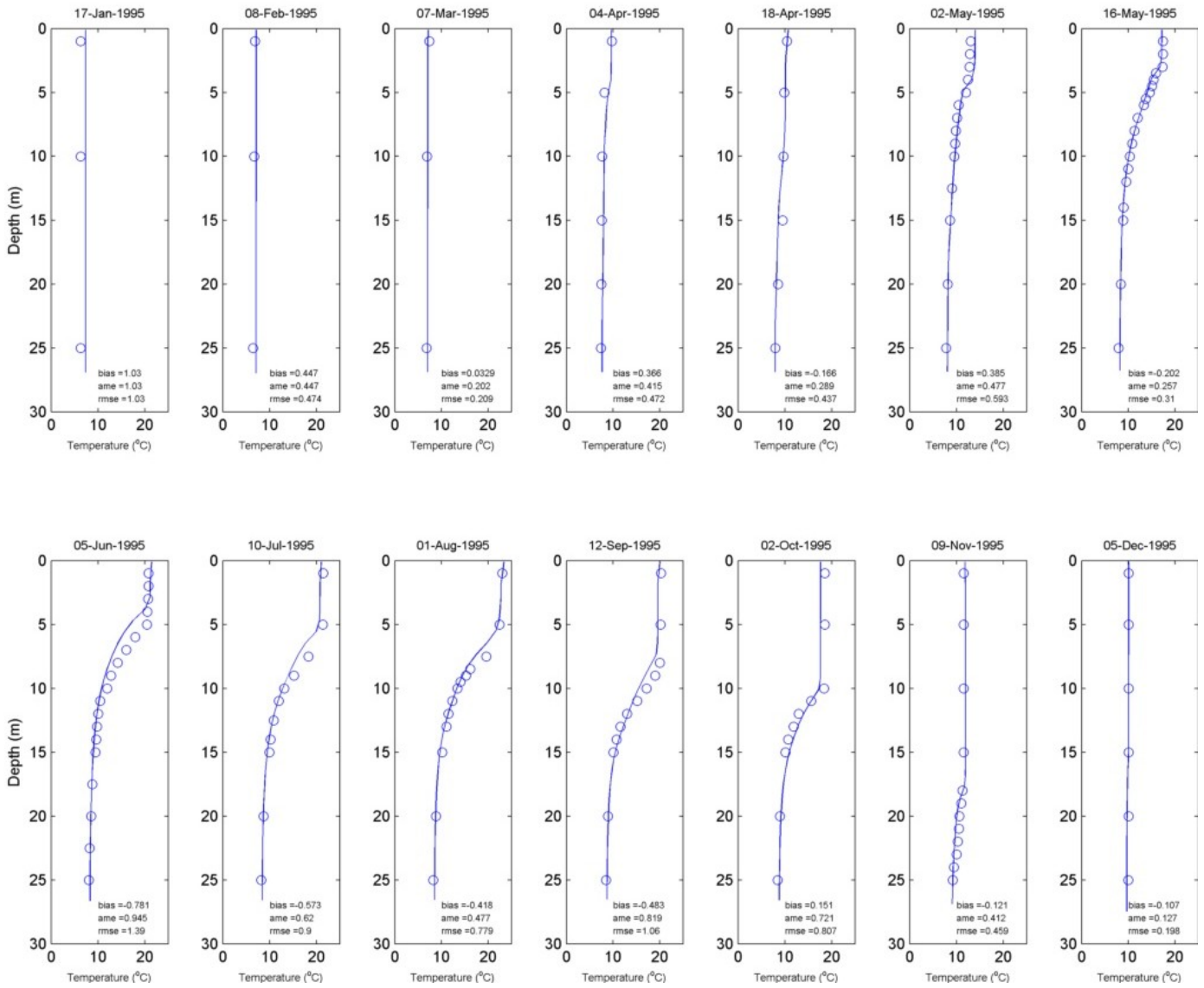

Figure 39. 3-D model (solid lines) vs. observed (open circles) temperature profiles – Station 0612, 1995.

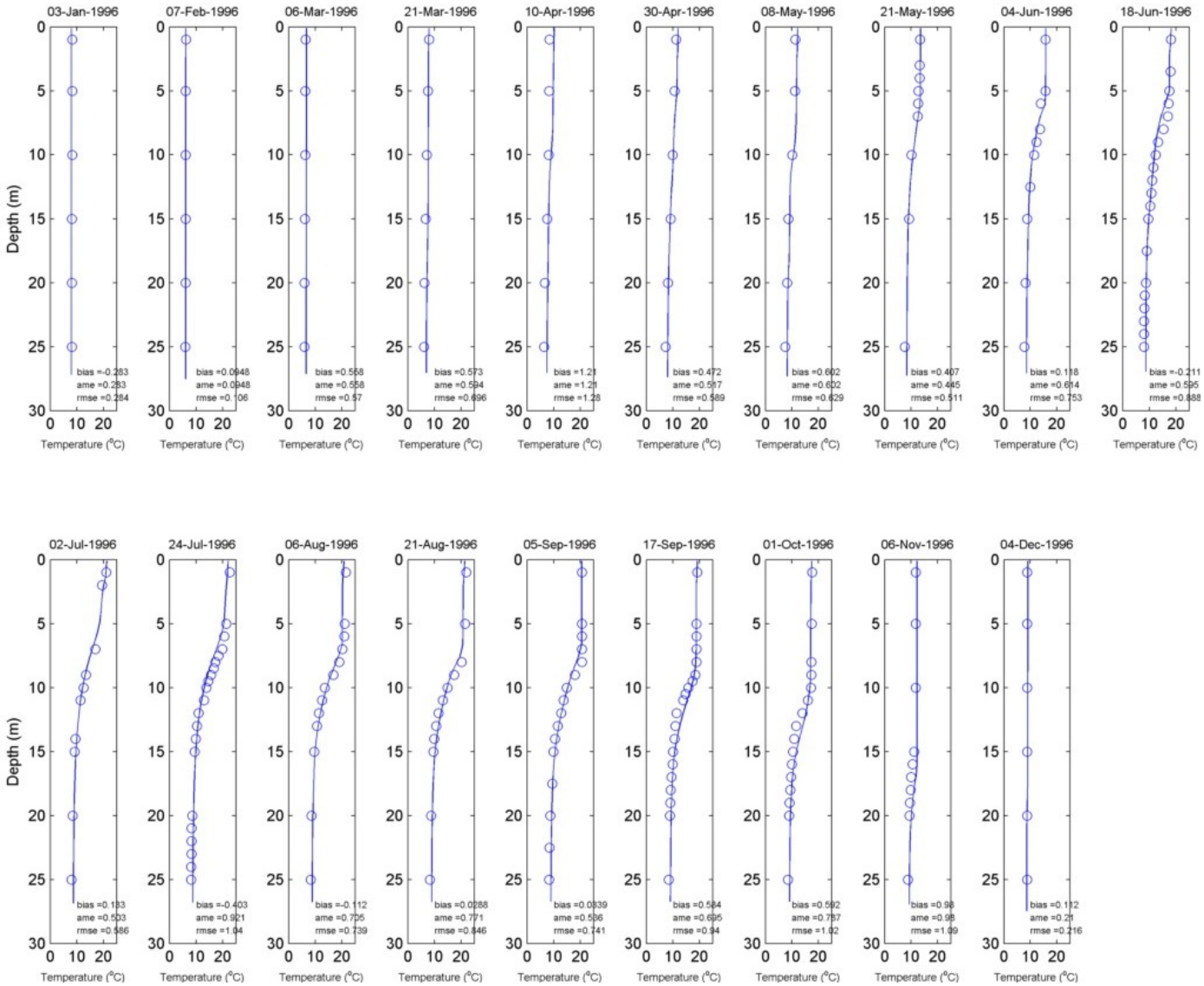

Figure 40. 3-D model (solid lines) vs. observed (open circles) temperature profiles – Station 0612, 1996.

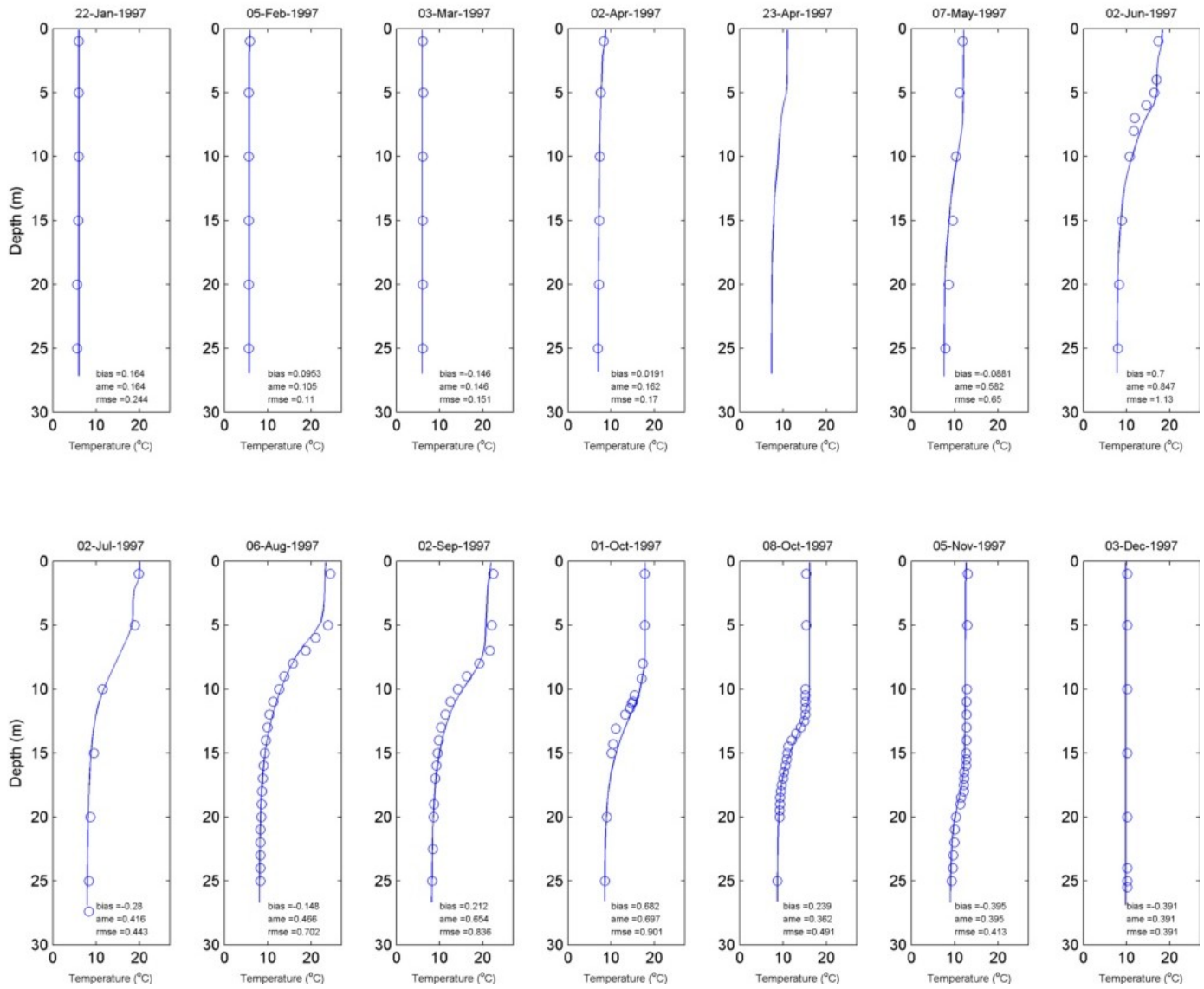

Figure Figure 41. 3-D model (solid lines) vs. observed (open circles) temperature profiles – Station 0612, 1997.

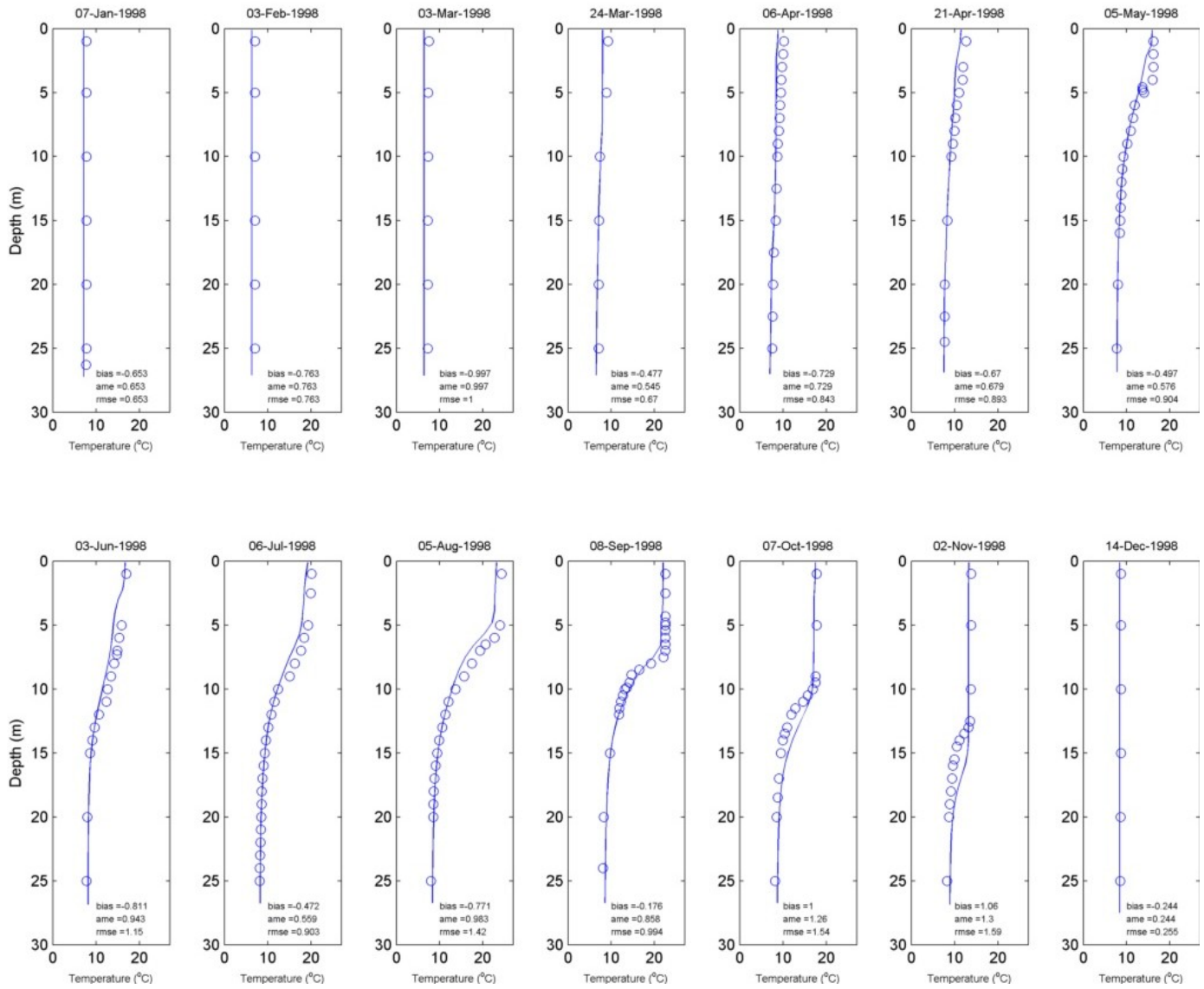

Figure 42. 3-D model (solid lines) vs. observed (open circles) temperature profiles – Station 0612, 1998.

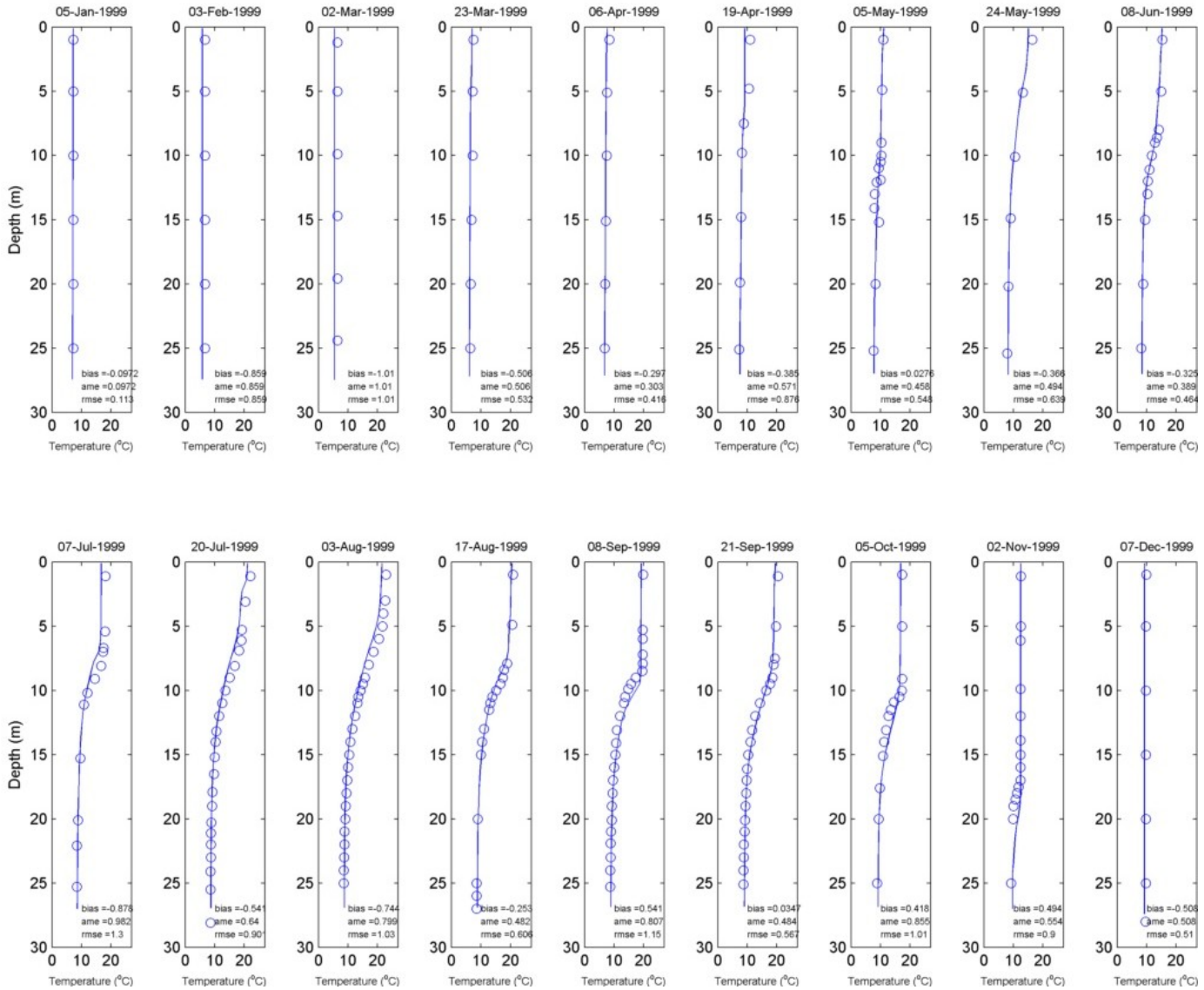

Figure 43. 3-D model (solid lines) vs. observed (open circles) temperature profiles – Station 0612, 1999

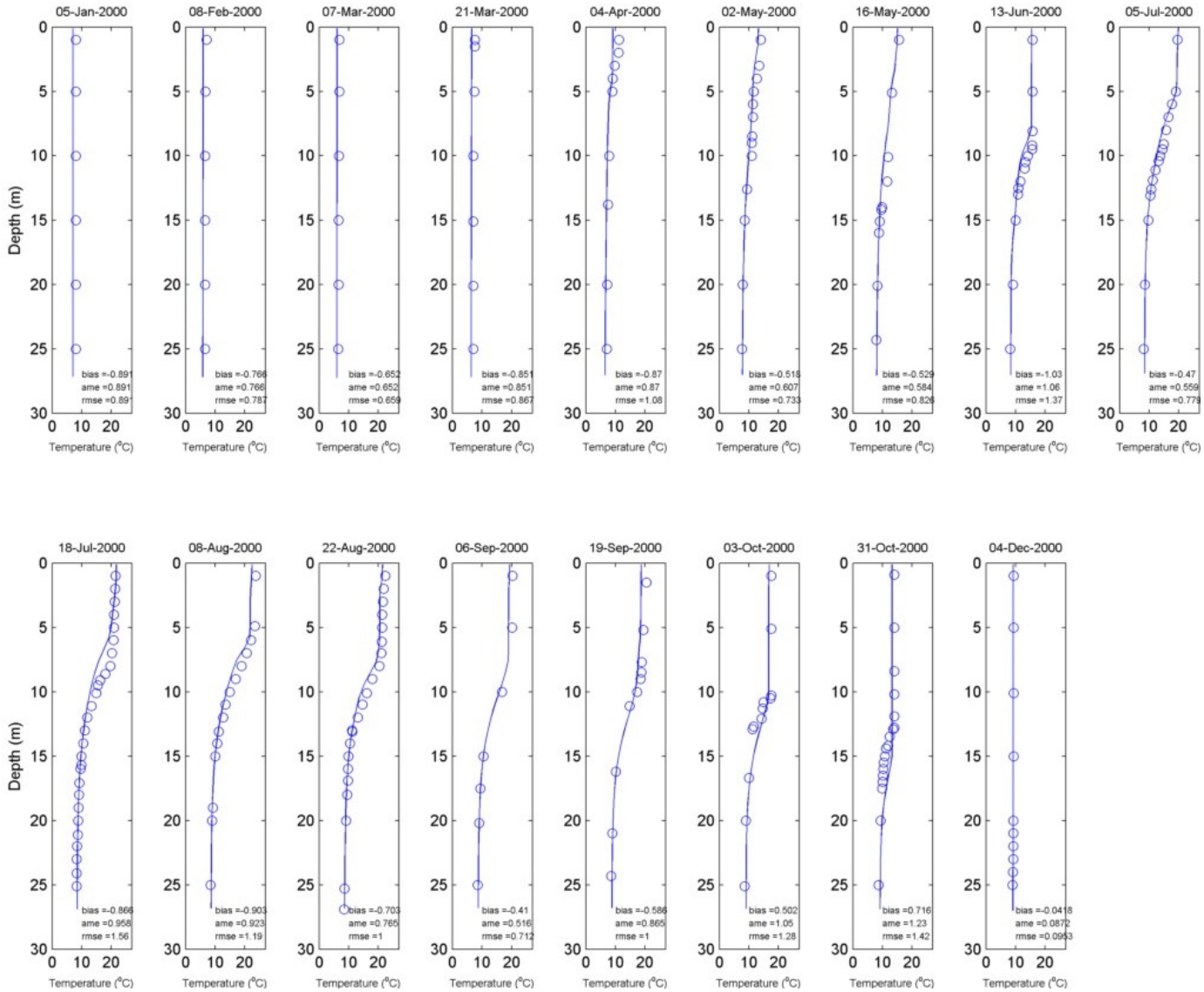

Figure Figure 44. 3-D model (solid lines) vs. observed (open circles) temperature profiles – Station 0612, 2000.

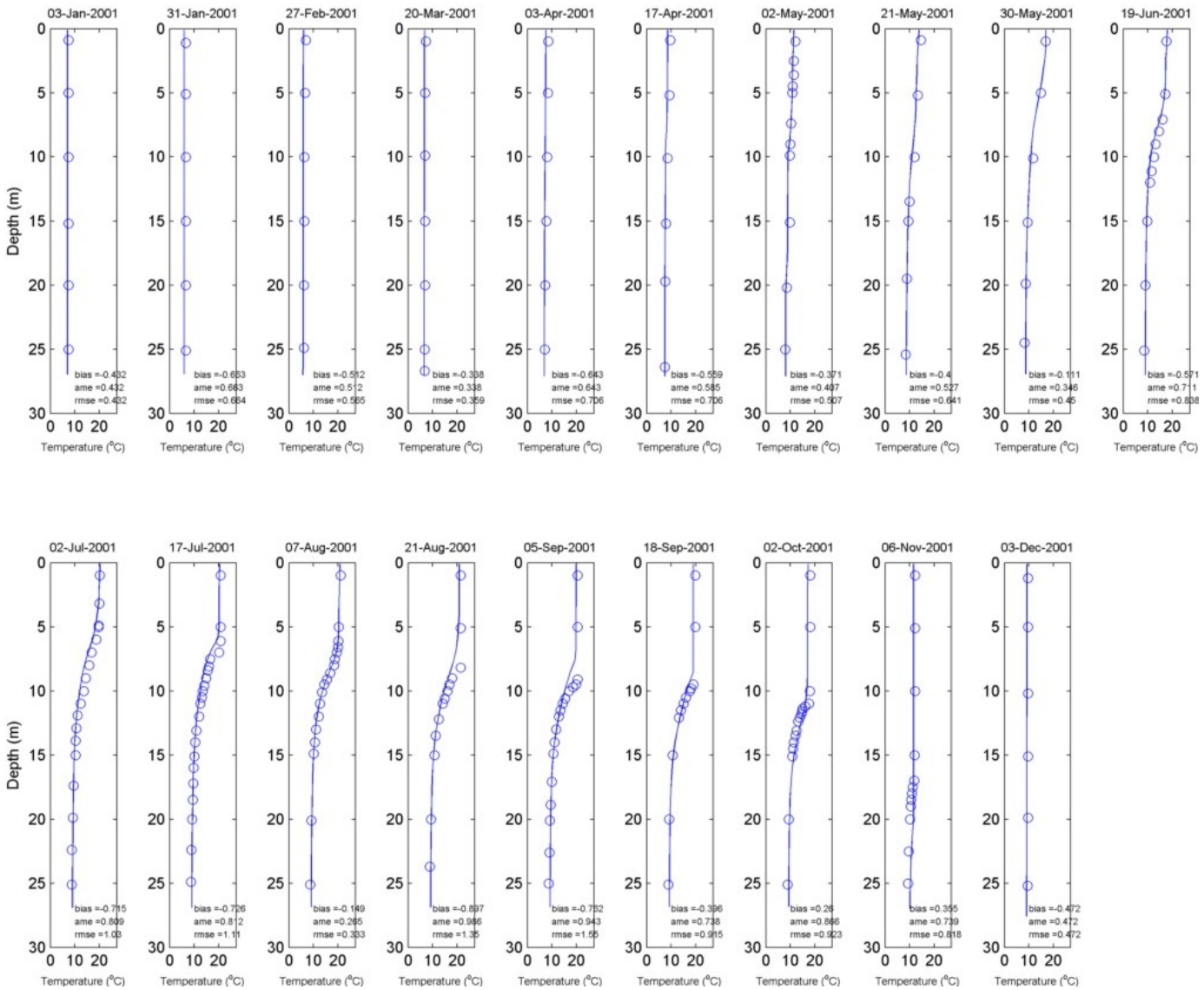

Figure 45. 3-D model (solid lines) vs. observed (open circles) temperature profiles – Station 0612, 2001.

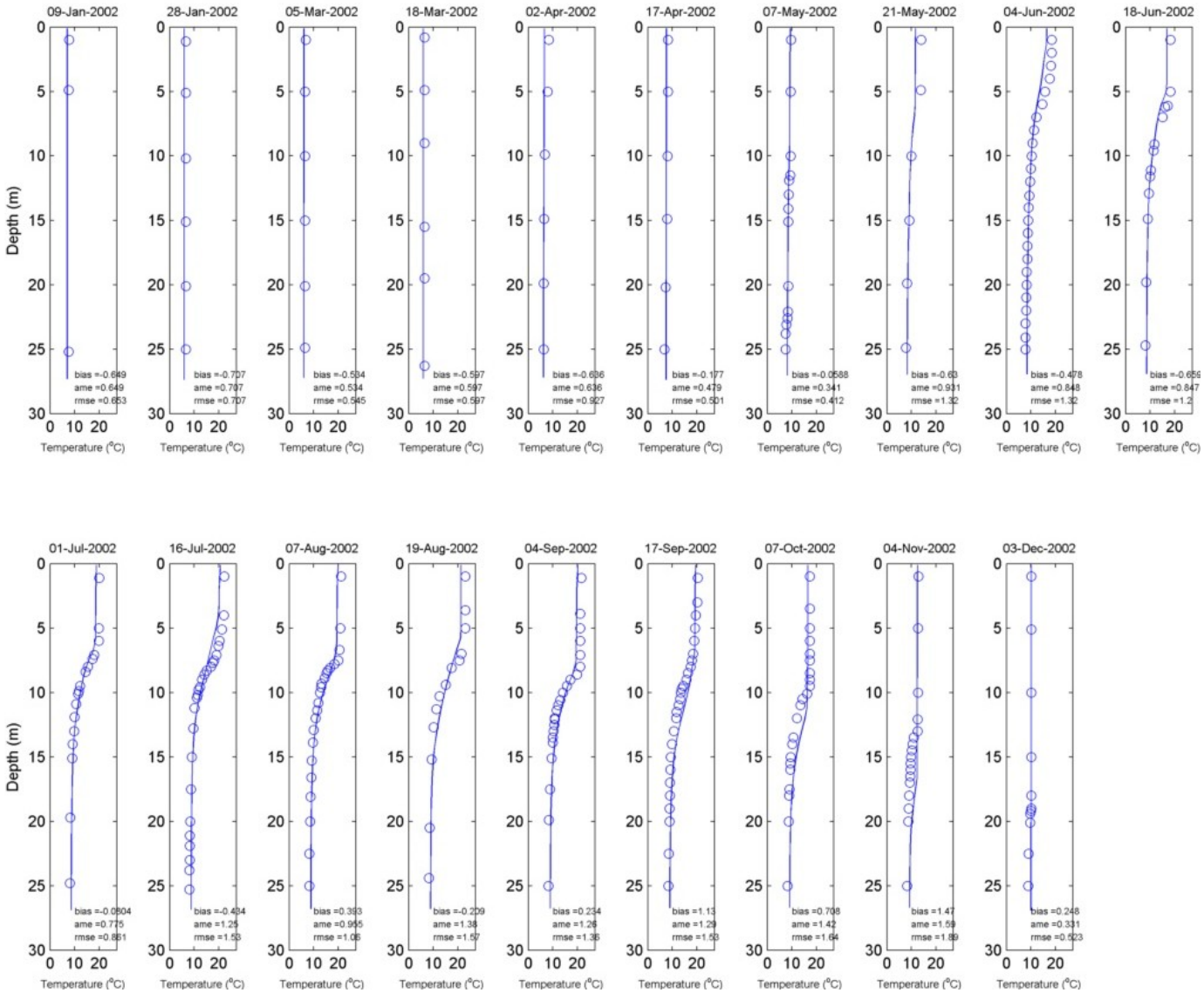

Figure 46. 3-D model (solid lines) vs. observed (open circles) temperature profiles – Station 0612, 2002.

Appendix C

Habitat Volume Figures

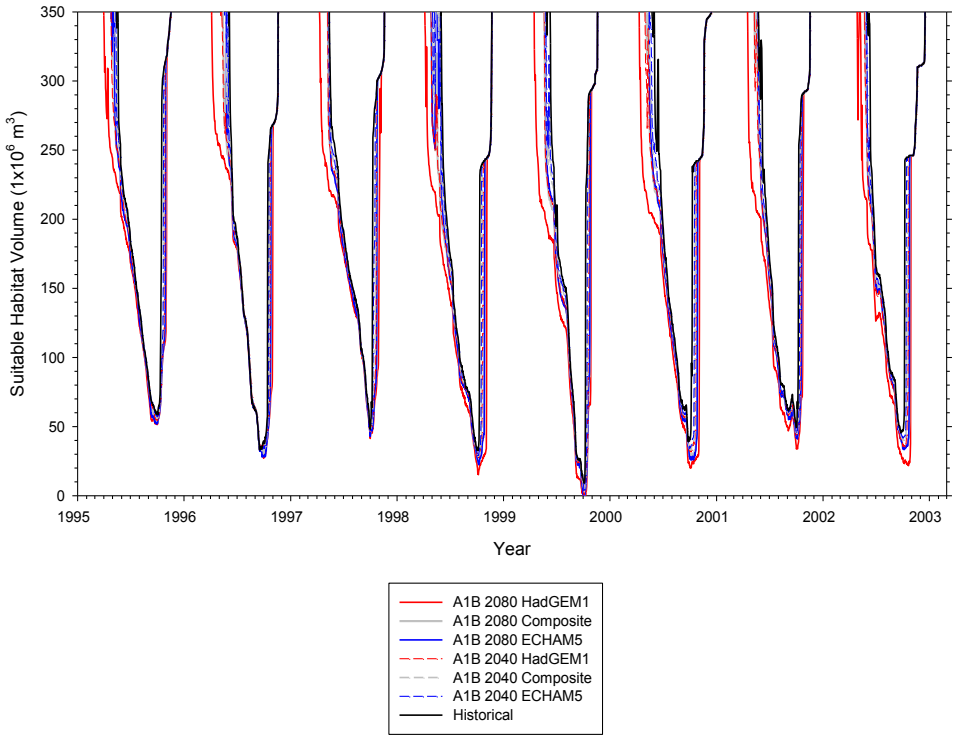

Note: Calculated habitat volume includes the subtraction of the estimated daily volume of the lake with dissolved oxygen concentrations less than 4 mg/L over the same period.

Figure 47. Salmonid habitat volume based on output from the 2-D Lake Sammamish model using a 17 °C temperature threshold, 1995-2002.

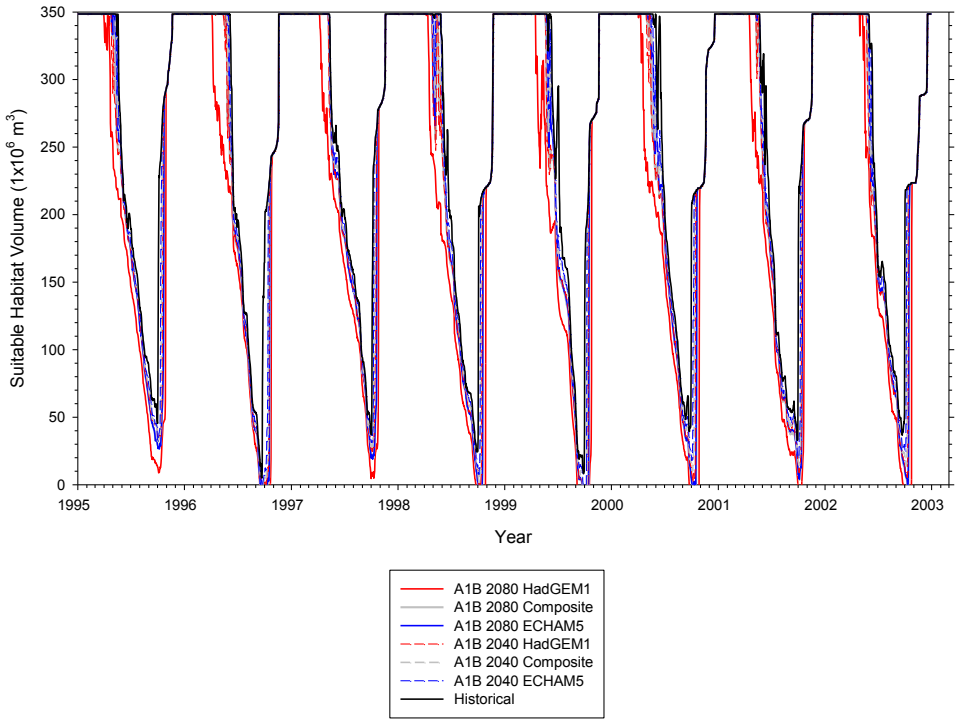

Note: Calculated habitat volume includes the subtraction of the estimated daily volume of the lake with dissolved oxygen concentrations less than 4 mg/L over the same period.

Figure 48. Salmonid habitat volume based on output from the 3-D Lake Sammamish model and a 17 °C temperature threshold, 1995-2002.

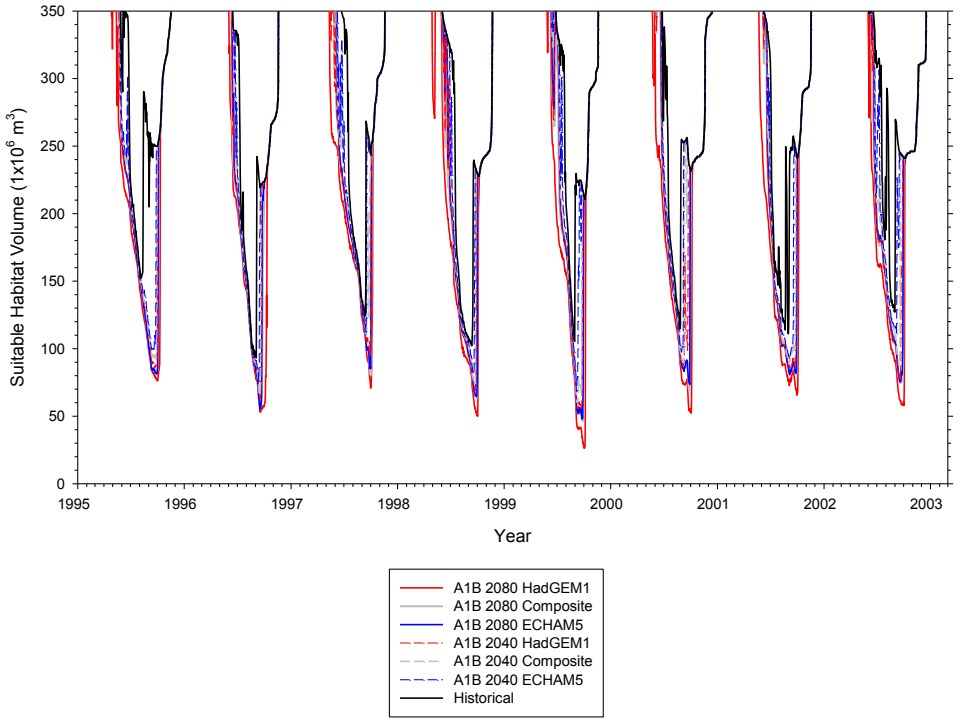

Note: Calculated habitat volume includes the subtraction of the estimated daily volume of the lake with dissolved oxygen concentrations less than 4 mg/L over the same period.

Figure 49. Salmonid habitat volume based on output from the 2-D Lake Sammamish model and a 21.5 °C temperature threshold, 1995-2002.

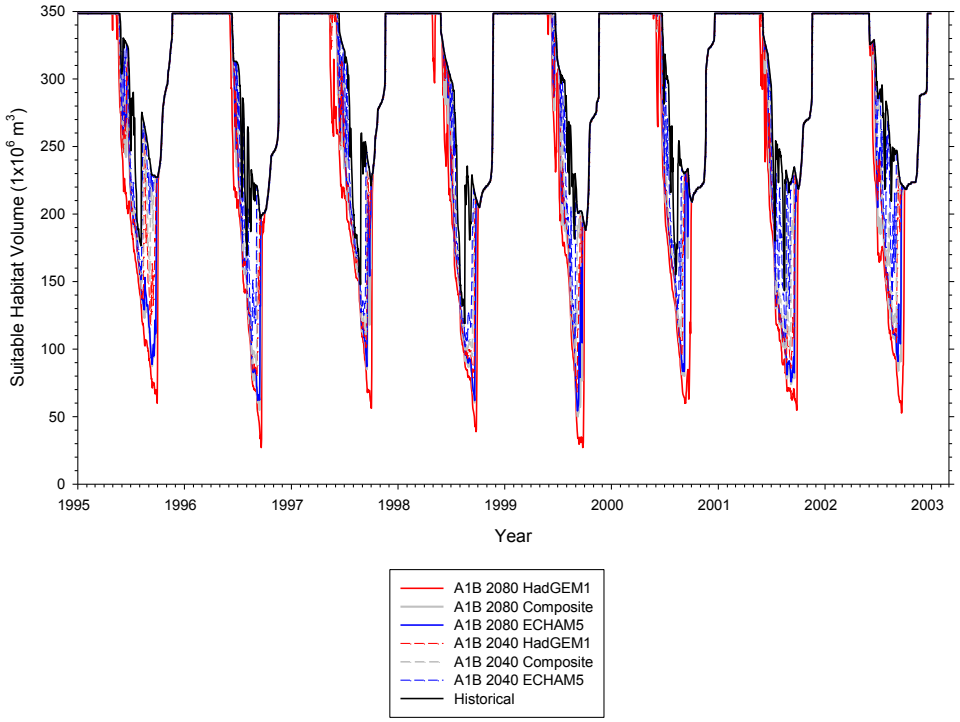

Note: Calculated habitat volume includes the subtraction of the estimated daily volume of the lake with dissolved oxygen concentrations less than 4 mg/L over the same period.

Figure 50. Salmonid habitat volume based on output from the 3-D Lake Sammamish model and a 21.5 °C temperature threshold, 1995-2002.

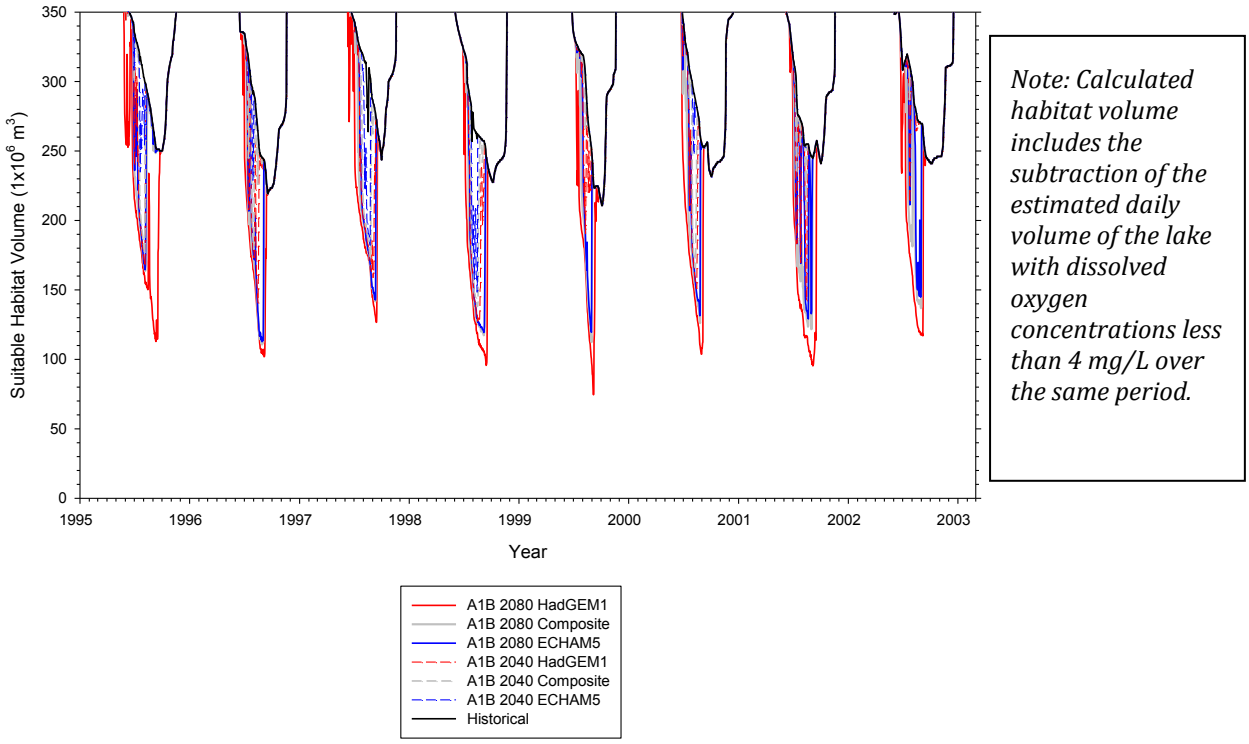

Figure 51. Salmonid habitat volume based on output from the 2-D Lake Sammamish model and a 25.1 °C temperature threshold, 1995-2002.

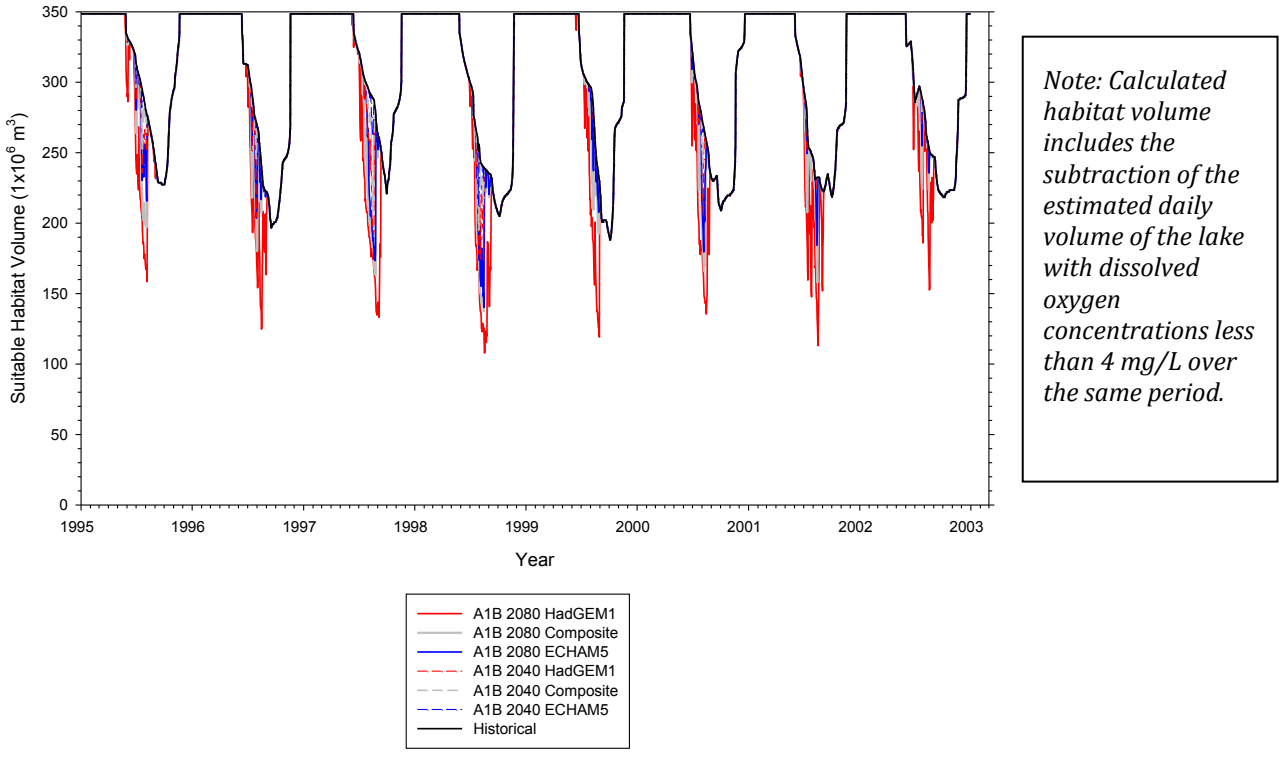

Figure 52. Salmonid habitat volume based on output from the 3-D Lake Sammamish model and a 25.1 °C temperature threshold, 1995-2002.

Appendix D

Isotherm Figures

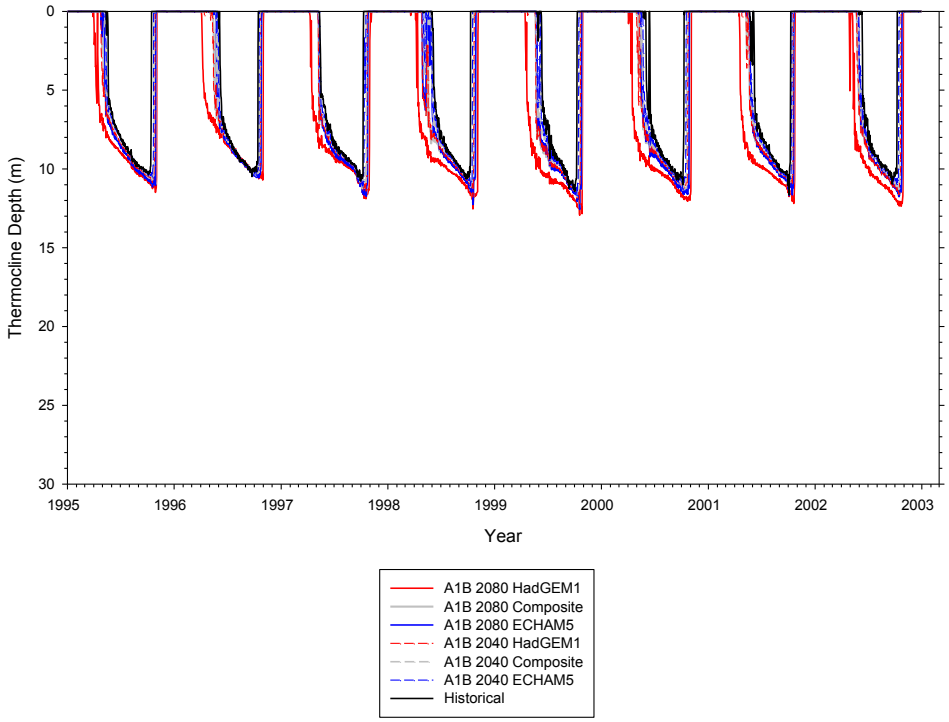

Figure 53. 17 °C isotherms based on output from the 2-D Lake Sammamish model, 1995-2002.

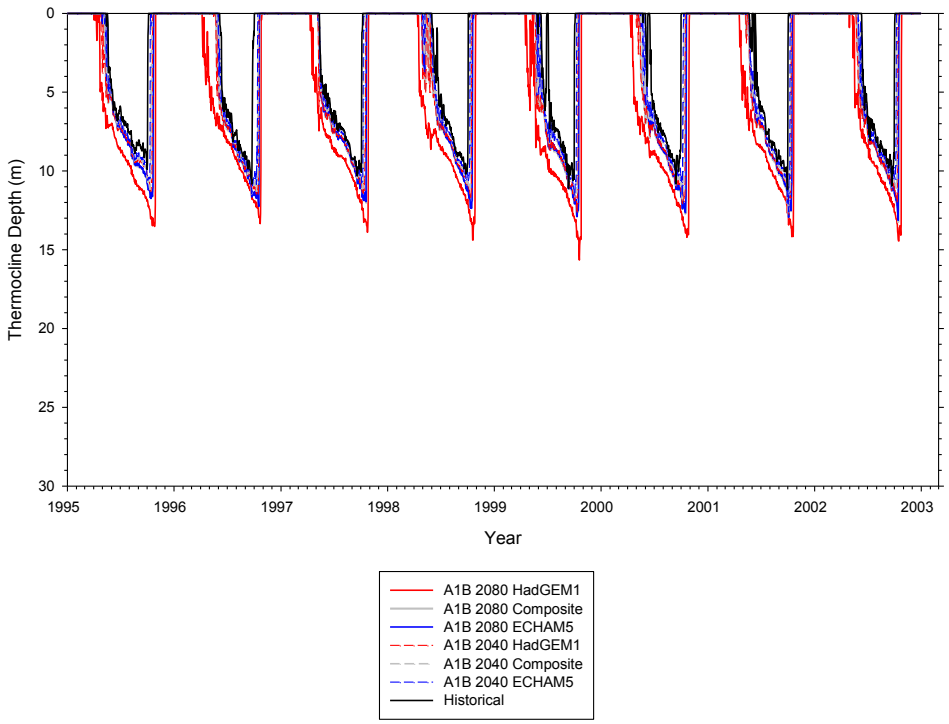

Figure 54. 17 °C isotherms based on output from the 3-D Lake Sammamish model, 1995-2002.

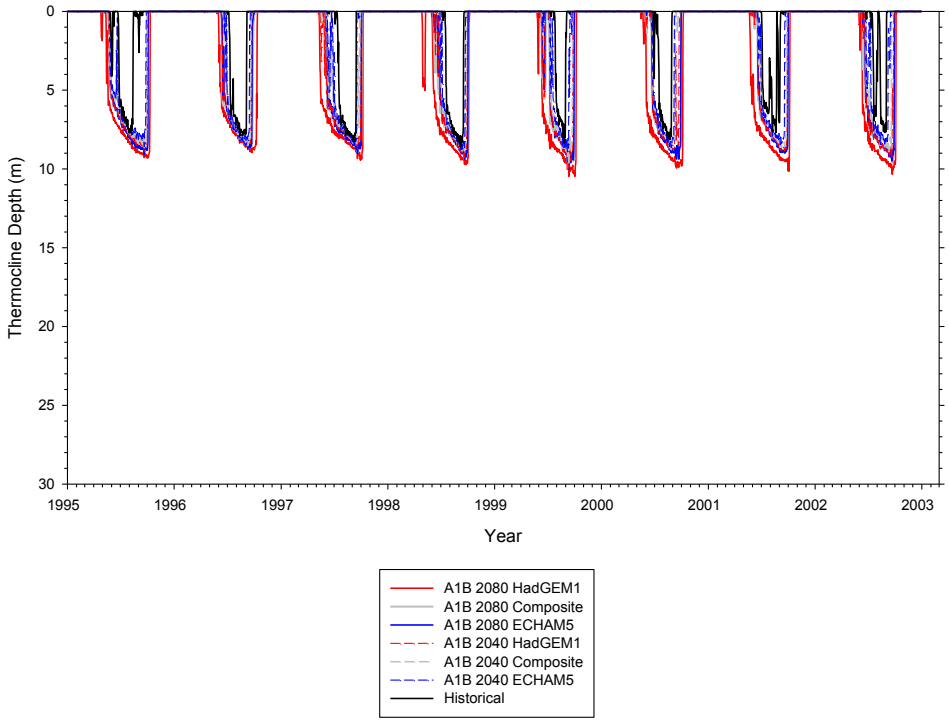

Figure 55. 21.5 °C isotherms based on output from the 2-D Lake Sammamish model, 1995-2002.

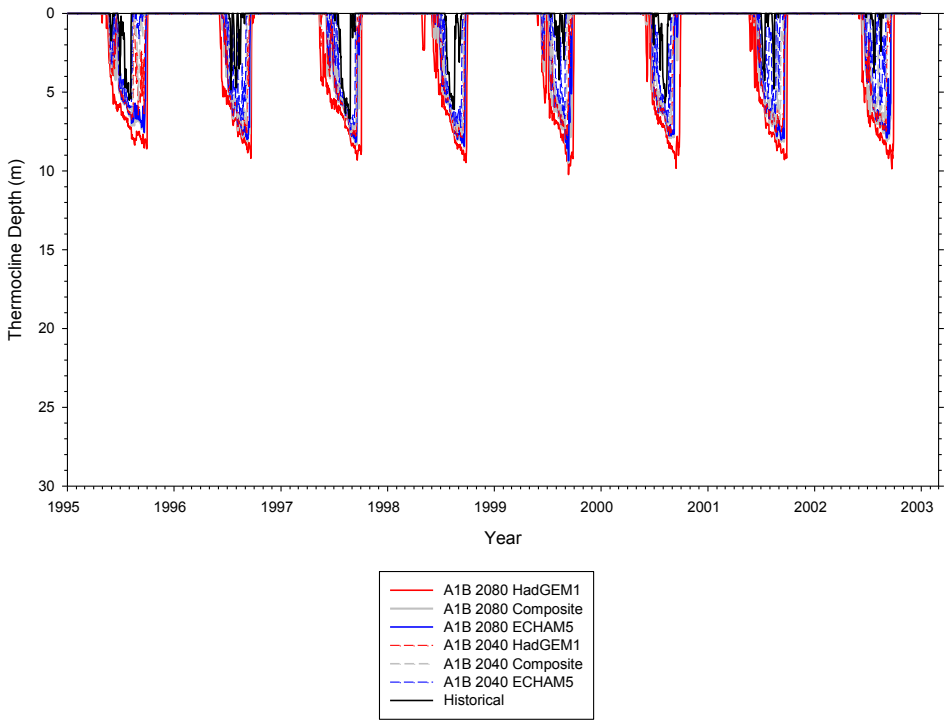

Figure 56. 21.5 °C isotherms based on output from the 3-D Lake Sammamish model, 1995-2002.

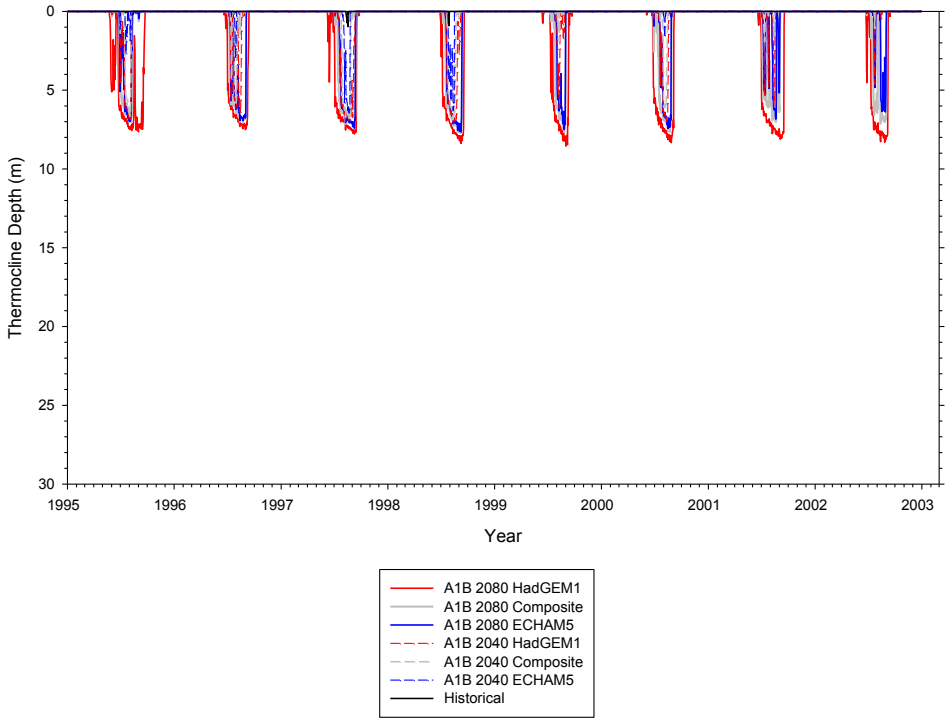

Figure 57. 25.1 °C isotherms based on output from the 2-D Lake Sammamish model, 1995-2002.

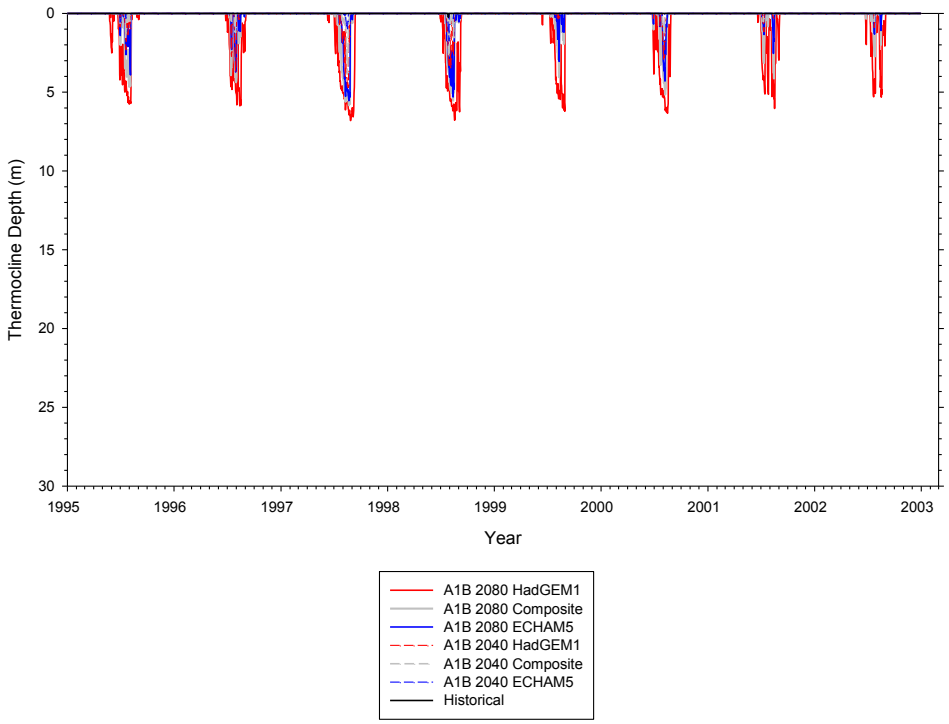

Figure 58. 25.1 °C isotherms based on output from the 3-D Lake Sammamish model, 1995-2002.

Appendix E

Thermocline Figures

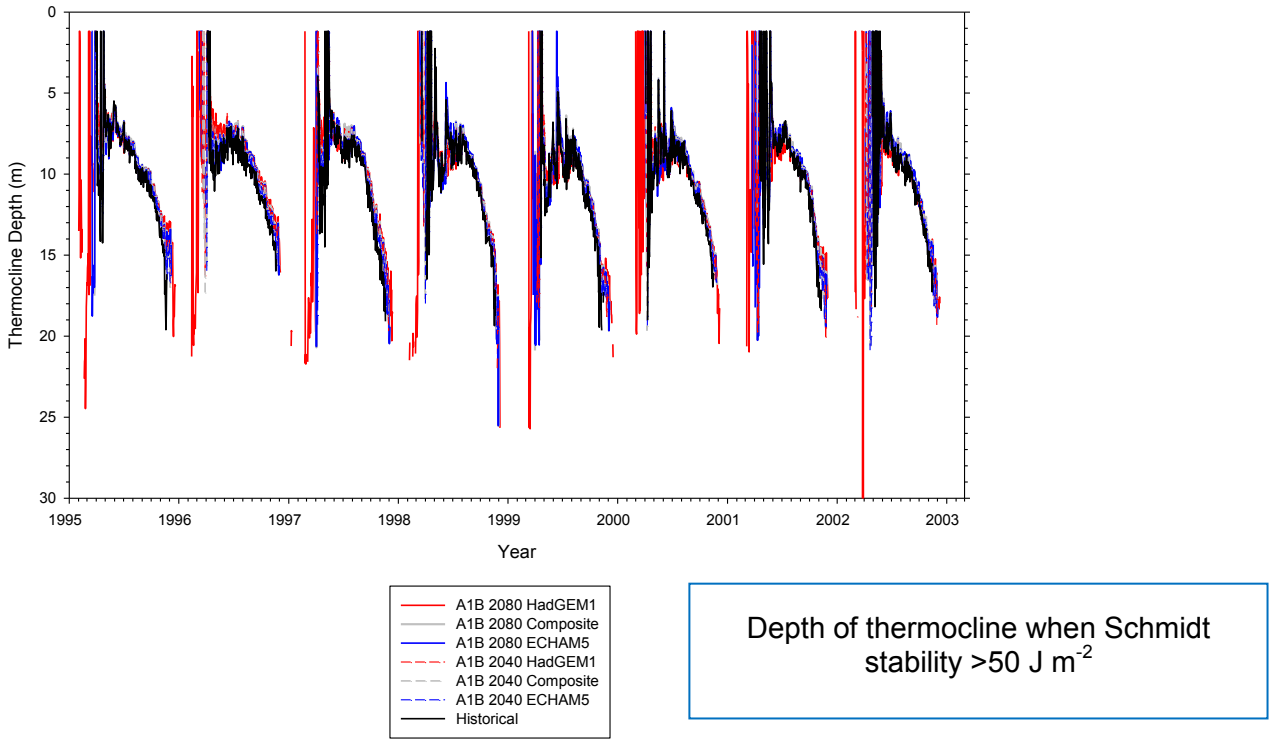

Figure 59. Thermocline depths based on output from the 2-D Lake Sammamish model, 1995-2002.

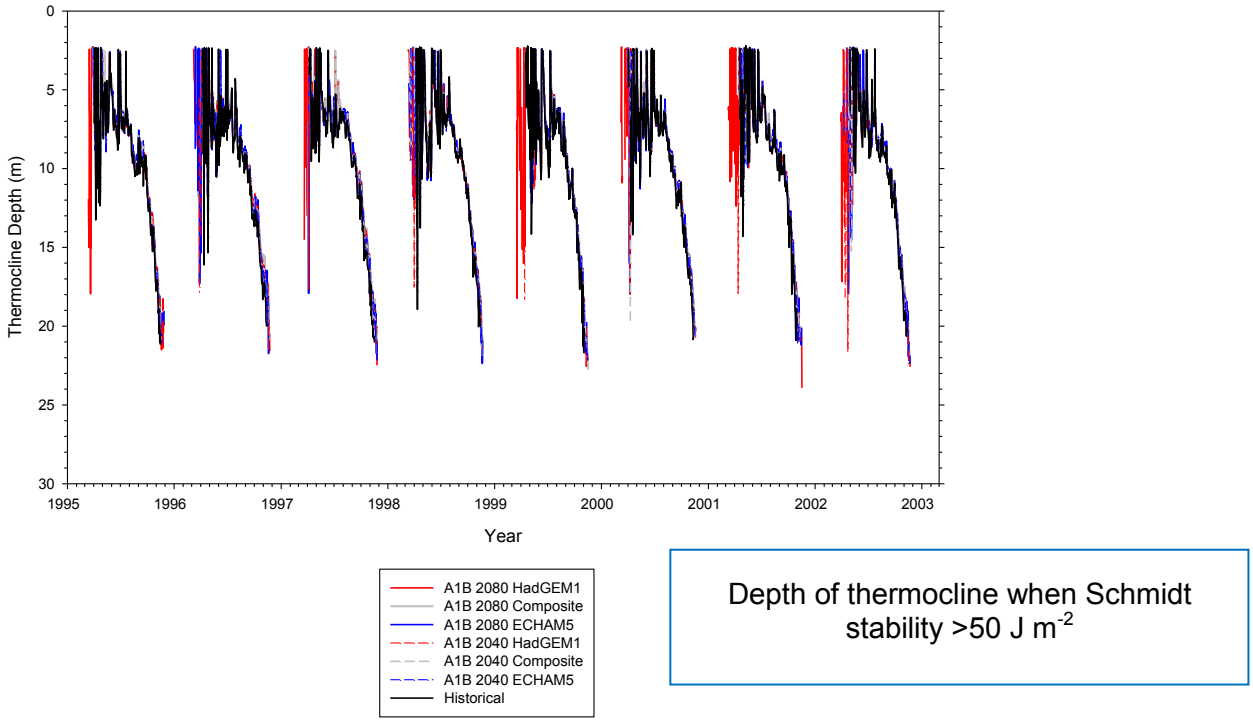

Figure 60. Thermocline depths based on output from the 3-D Lake Sammamish model, 1995-2002.

Appendix F

Schmidt Stability Figures

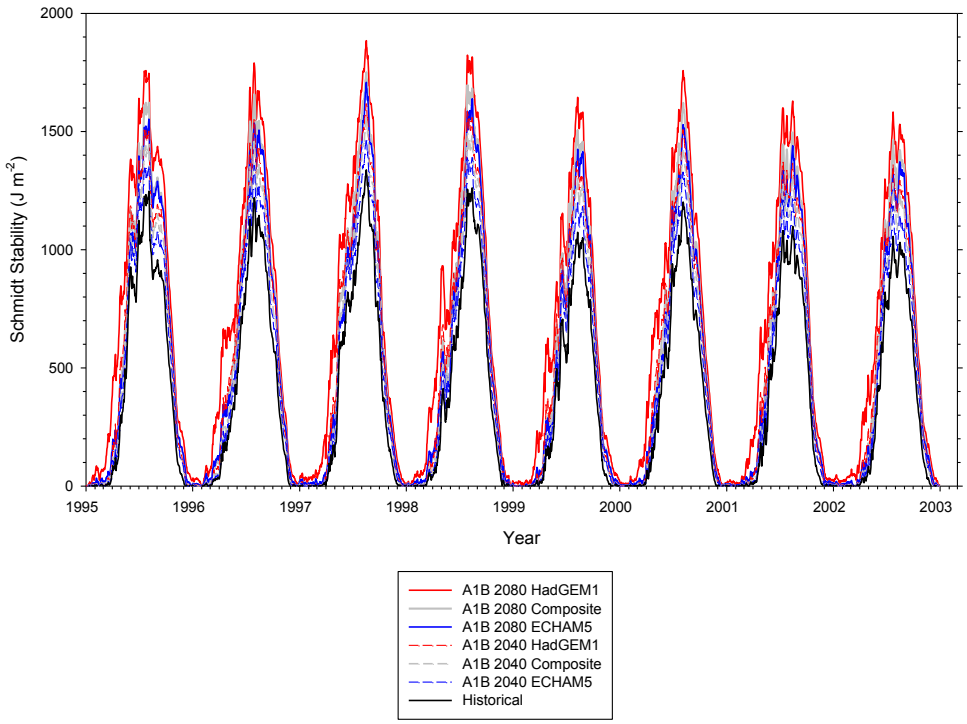

Figure 61. Schmidt stability based on output from the 2-D Lake Sammamish model, 1995-2002.

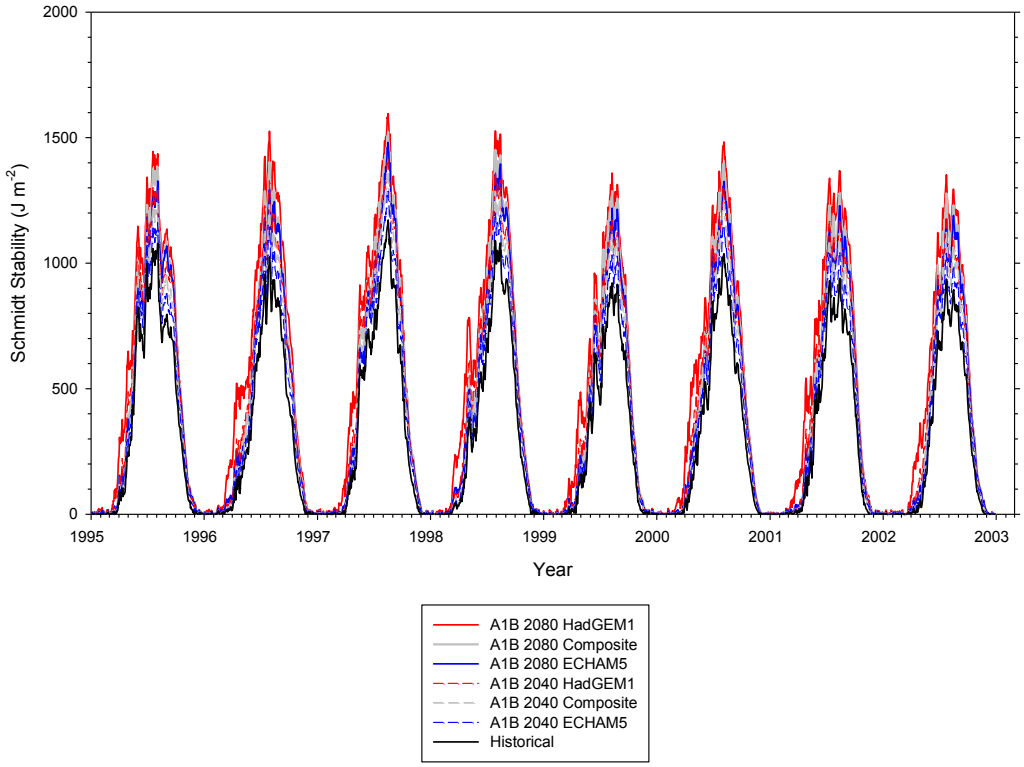

Figure 62. Schmidt stability based on output from the 3-D Lake Sammamish model, 1995-2002.